UNIVERSITY OF SOUTHAMPTON

Faculty of Environmental and Life Sciences
School of Ocean and Earth Science

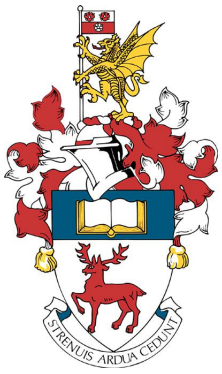

Changing Atlantic Influences on Northwest European Shelf Seas

by

Matthew Philip Clark

ORCiD: 0000-0002-5199-6632

A thesis for the degree of
Doctor of Philosophy

July 2023

University of Southampton

Abstract

Faculty of Environmental and Life Sciences
School of Ocean and Earth Science

Doctor of Philosophy

Changing Atlantic Influences on Northwest European Shelf Seas

by Matthew Philip Clark

The North Atlantic Ocean is highly dynamic. Its physical, biological, and chemical characteristics change across multiple timescales: from daily to inter-decadal and beyond. Surface oceanic flows in this region are dominated by the sub-polar and sub-tropical gyres, with the North Atlantic Current running between the two. Changes to these flows and the properties of conveyed North Atlantic water are not only felt in the ocean basin, but at the oceanic boundaries. The eastern boundary is adjacent to the northwest European shelf seas, and the location of a northward flowing shelf edge current commonly known as the European Slope Current. The shelf seas and this Slope Current are strongly affected by eastward geostrophic flows traced back to a combination of subtropical and subpolar sources. With the surface layers of the North Atlantic warming by nearly 2 °C over the past 4 decades, the density gradients that maintain these eastward flows have decreased, which has reduced the shelf edge flow on the order of 5 Sv. Atlantic inflow to the North Sea is directly related to the strength of the northward Slope Current transport. This inflow has reduced and acted to increase the residence time of Atlantic water in the North Sea by up to 100 days. Atlantic inflow provides the main nutrient flux to the North Sea. A reduction in this flux has implications for the productivity of the region, which remains an important fishery for the UK. In summary, basin-scale changes in physical properties reverberate at the shelf break flows and in the shelf seas, which in turn affect nutrient fluxes and primary production in the region.

Contents

List of Figures

List of Tables

Glossary and Abbreviations

Term	Definition
AMOC	Atlantic Meridional Overturning Circulation.
Ariane	A Lagrangian particle tracking software by Bruno Blanke and Nicolas Grima of Laboratoire d'Océanographie Physique et Spatiale, France.
Chl-α	Chlorophyll-α.
CPR	Continuous Plankton Recorder: a towed mechanical sampler to capture plankton samples. Managed by the Marine Biological Association.
DIN	Dissolved inorganic nitrogen.
DON	Dissolved organic nitrogen.
EN4	A Met Office Hadley Centre dataset containing quality controlled objective analysis of temperature and salinity profiles from the global ocean.
ESC	European Slope Current: A northward-flowing and bathymetrically constrained current at the European Shelf edge, characterised by a high salinity core above the 600m isobath.
GODAS	Global Ocean Data Assimilation System: A NOAA provided gridded global ocean dataset containing temperature, salinity and velocity component data.
NAC	North Atlantic Current. Sometimes referred to as the North Atlantic Drift.
NAO	North Atlantic Oscillation: the pressure difference between Iceland and the Azores Islands.
NPP	Net primary production.
SSH	Sea surface height.
SPG	Sub-polar gyre of the North Atlantic Ocean.
STG	Sub-tropical gyre of the North Atlantic Ocean.
Sverdrups	1 X 10^6 m^3 s^{-1}, a rate of volume water transport.
Subtropicalization	The process of warmer water species (from more tropical regions) arriving in waters that ordinarily would be too cold to support them.

TABLE 1: Commonly used terms or abbreviations/acronyms and their definitions

List of Additional Material

Code for Chapter 3: is published open-access and available via the Zenodo repository at https://doi.org/10.5281/zenodo.6415360. It can be cited as Clark et al. (2022a)

Code for Chapters 4 and 5 is available on request. It will be published open-access on journal publication of the research.

Declaration of Authorship

I declare that this thesis and the work presented in it is my own and has been generated by me as the result of my own original research.

I confirm that:

1. This work was done wholly or mainly while in candidature for a research degree at this University;
2. Where any part of this thesis has previously been submitted for a degree or any other qualification at this University or any other institution, this has been clearly stated;
3. Where I have consulted the published work of others, this is always clearly attributed;
4. Where I have quoted from the work of others, the source is always given. With the exception of such quotations, this thesis is entirely my own work;
5. I have acknowledged all main sources of help;
6. Where the thesis is based on work done by myself jointly with others, I have made clear exactly what was done by others and what I have contributed myself;
7. Parts of this work have been published as:
   M. Clark, R. Marsh, and J. Harle. Weakening and warming of the European Slope Current since the late 1990s attributed to basin-scale density changes. *Ocean Science*, 18(2):549–564, May 2022b. ISSN 1812-0784. doi: 10.5194/os-18-549-2022. URL https://os.copernicus.org/articles/18/549/2022/. Publisher: Copernicus GmbH

Signed:..... Date:.....

Acknowledgements

Firstly, I would like to thank my supervisors Prof. Robert (Bob) Marsh from the University of Southampton and Dr. James Harle from the National Oceanography Centre for their support throughout this PhD. They have always pushed me further and have invaluably helped me become a better researcher.

Thanks to the Natural Environment Research/UK Research and Innovation for funding my PhD through the SPITFIRE DTP (grant number: NE/L002531/1). I also thank the National Oceanography Centre for the use of their computer systems and allowing access to the ORCA12 model outputs. Thanks also to Science and Technology Facilities Council (STFC) and the Centre for Environmental Data Analysis (CEDA) for allowing access to the JASMIN computer systems.

In addition, I can't finish this thesis without thanking both my parents and sister who've supported me academically and emotionally from the very start. I'm eternally grateful to all that they have done for me.

I also need to thank my close friends for their support and their unwavering ability to put up with whatever I passed onto them over these years - they've always been there for me no matter what. I fully appreciate the tea and biscuit discussions and laps around Southampton Common, which helped me focus on what was important during the times when I couldn't see the wood from the trees. Of course, over the Covid lockdowns, their online support and encouragement kept me going. I can't finish this section without special recognition goes to my extremely supportive friends in (and the committee of) Southampton University Hillwalking Club (SUHC), which has always provided a welcome break from the near-endless screen time with some outdoor relief since I started my undergraduate degree at this very same University in 2013.

Chapter 1

Introduction to North Atlantic circulation and physical processes

Abstract: North Atlantic Ocean circulation is dominated by two large basin-scale gyres, with the Gulf Stream, becoming the North Atlantic Current (NAC), flowing between them. Changes to the circulation and other physical properties within the North Atlantic Basin have wide-ranging effects on the state of shelf edge and shelf sea physical processes. The North Atlantic Ocean has warmed by at least 1 °C since the 1990s, although there have been short-lived extreme cooling events such as the "Cold Blob" of 2013-15 which cooled the sub-polar gyre by 2 °C. In the shelf seas regions, salinity distribution changes have been extreme. Changes in temperature, and to a lesser degree the salinity, in the sub-polar North Atlantic have reduced the meridional density gradients, resulting in slowdowns in the geostrophic NAC and shelf-edge eastern boundary currents. This geostrophically-driven transport reduction is thought to have reduced inflow to the European shelf edge, and reduced the strength of the northward-flowing European Slope Current. Additionally, warming water temperatures have acted to alter the species distribution of the shelf seas. Most significantly, "subtropicalization" (where warmer water species replace native cooler-water species), has been observed in the North Sea which is still thought to be ongoing. This chapter presents an analysis of current research that addresses the changing Atlantic influences on the European shelf seas, both in terms of changing circulation and changing biogeochemistry, followed by an outline of this thesis and the main research aims.

1.1 The dynamics of the North Atlantic Ocean and the European shelf seas

Surface circulation within the North Atlantic Ocean is dominated by two gyre systems: the cyclonic sub-polar gyre (SPG) and the anticyclonic sub-tropical gyre (STG). The SPG controls circulation in several cooler and fresher areas, and helps export this water from regions such as the Labrador Sea to the North Atlantic basin (Fratantoni and McCartney, 2010). Likewise, the STG transports waters from along the eastern US seaboard. The Gulf Stream, that eventually becomes the North Atlantic Current (NAC, also known as the North Atlantic Drift) flows between the two gyres in a northeastward direction and gradually cools as it crosses the ocean basin (see Fig. 1.1). It passes the north coast of Scotland as it flows northeastward, splitting into several smaller traceable branches (Marzocchi et al., 2015). The majority continues to flow northward into the Norwegian Sea. In addition to this horizontal circulation is net sinking at higher latitudes (>60°N). This forms the components of North Atlantic Deep Water, which flows southward along the ocean's western boundary (Schmitz and McCartney, 1993; Gregory et al., 2005; Hátún et al., 2005). This process forms the northern part of the Atlantic Meridional Overturning Circulation (AMOC). The AMOC, combined with the gyre circulations, move heat, nutrients and plankton around the Atlantic and global ocean (Ortega et al., 2016; Johnson et al., 2013).

The AMOC is of key importance to both North Atlantic and global ocean circulation. It draws heat and nutrients from the South Atlantic and mid latitudes northwards. The state of the AMOC is measured through several mooring arrays in the Atlantic (Fig. 1.5). The RAPID project monitors the AMOC through a series of moorings at 26 °N, which have been in place since 2004 (McCarthy et al., 2020; Bryden et al., 2019; McCarthy et al., 2015). The OSNAP array measures the same physical parameters in the northern North Atlantic (at approximately 58 °N) (Lozier et al., 2019). Most recent analyses of the mooring data suggests the AMOC is slowing down by approximately 3.7 Sv since 2005 (Chen and Tung, 2018; Bryden et al., 2019), but the rate of slowdown may be decreasing (Bryden et al., 2019; Chen and Tung, 2018). A slowdown of the AMOC has implications for heat and nutrient distribution in the North Atlantic. Weakened AMOC in 2005 and 2010 has been associated with a period of rapid surface warming and saw positive sea surface temperature anomalies across the North Atlantic. (Chen and Tung, 2018; Hallam et al., 2019). Not only has this acted to alter surface density gradients that force circulation patterns (Marsh et al., 2017), it has also been associated with changes to weather patterns such as more frequent and intense tropical storms in the tropical North Atlantic (Hallam et al., 2019).

The European Slope Current (SC) is one pathway for Atlantic water entrained from the NAC to flow northward and in some cases get onto the shelf and into the North Sea. The SC is a northward-flowing bathymetry-constrained current, running parallel

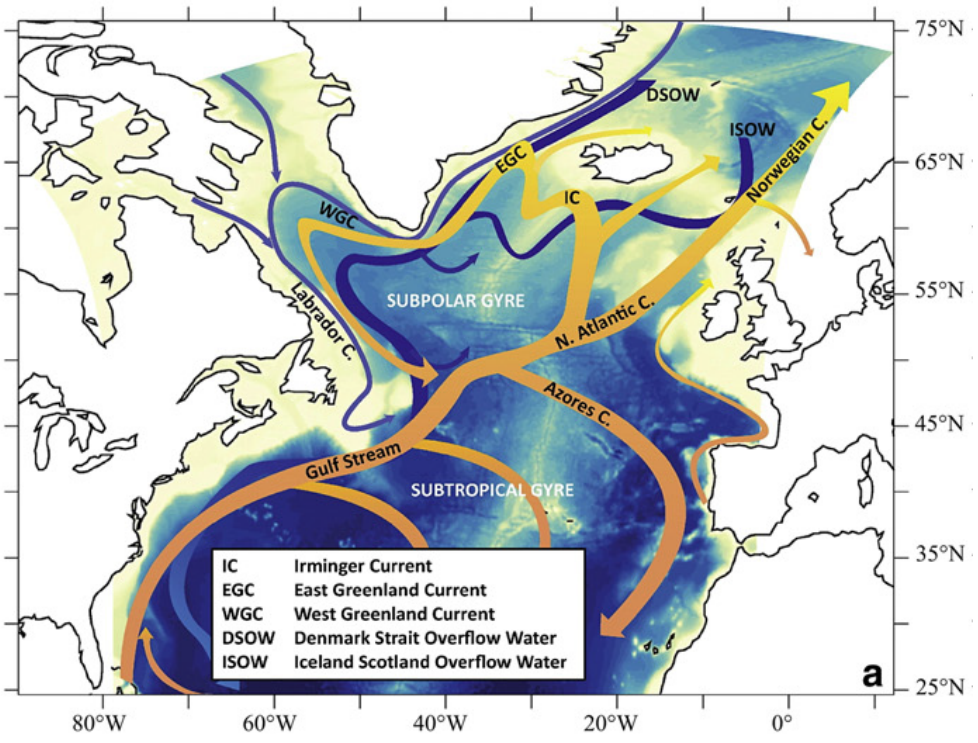

FIGURE 1.1: Schematic showing the main currents and circulation patterns in the North Atlantic Ocean. Orange arrows are near-surface (warm) currents, blue arrows are deeper (cool) currents. Background colour is bathymetry. Adapted from Marzocchi et al. (2015, Fig. 1).

to the European continental shelf edge. It is characterised by a high salinity core (>34.5) at 200 - 300m deep, flowing above the 300 - 600m bathymetry contour (Hill and Mitchelson-Jacob, 1993; Porter et al., 2018). It is primarily forced by a meridional density gradient in the sub-polar gyre region (Clark et al., 2022b; Marsh et al., 2017). However, on shorter (5 day to seasonal) timescales, the North Atlantic (basin scale heat and volume transport) and the SC is sensitive to surface wind forcing (Moat et al., 2016; Marsh et al., 2017). SC variability is also attributed to sea surface height (Marsh et al., 2017). Figure 1.2 is a schematic from Marsh et al. (2017) highlighting the main forcing of the SC. Weak phases of the Slope Current occur when the sub-polar North Atlantic density gradient is at a minimum, reducing geostrophic inflow. This is combined with weakened northward-blowing along-slope winds, reducing eastward Ekman flow. As a consequence, the along-slope sea surface slope is also at a minimum. During strong SC transport phases, the sub-polar density gradient is at a maximum, increasing eastward geostrophic inflow to the SC. The current understanding of basin-scale forcing of the SC is summarised in Fig. 1.3. Changes in the meridional density gradient within the sub-polar gyre alter the strength of the eastward geostrophic flow from this region. While some of the geostrophic transport will influence the Gulf Stream, it is thought that some can be entrained in the SC. This theory will be tested in Chapter 3. The characteristics of the temporal variability of the

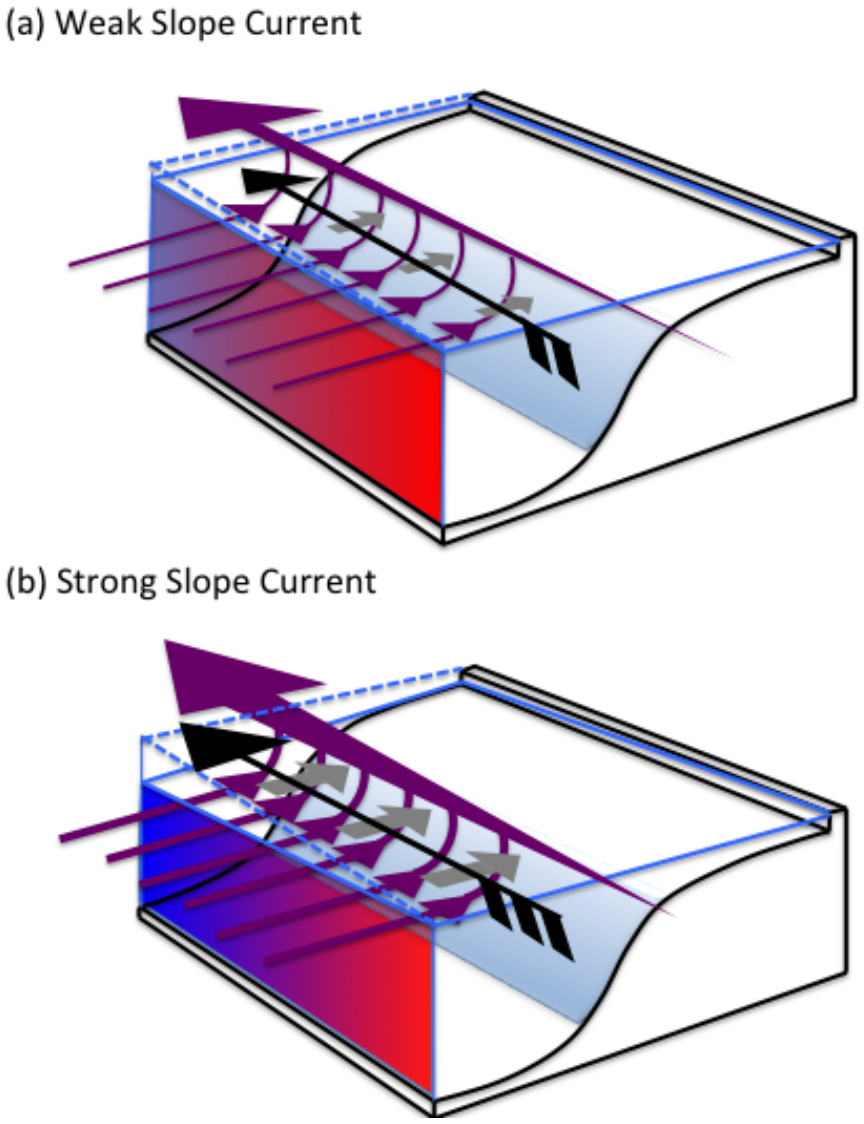

FIGURE 1.2: Schematic showing main forcing of the along-slope flowing European Slope Current. The red to blue gradient indicates the meridional gradient of density in the sub-polar North Atlantic. Purple arrows show the transport of water. The black arrow shows an along-slope wind, with the grey arrows showing the resultant Ekman flow. The dashed blue line indicates the sea surface slope. From: Marsh et al. (2017).

SC and other associated large and small scale flows (such as North Sea inflow) will be discussed later in Chapter 1.2.

The strength of the SC has implications on the North Sea as up to 40% of the flow enters the northern North Sea (Marsh et al., 2017). Inputs to the North Sea are highly variable, but the largest inputs are through the Norwegian Trench and then the Orkney-Shetland channel (Winther and Johannessen, 2006). These inflows are summarised in Fig. 1.4, with the Fair Isle Current and East Shetland Atlantic Inflow annotated. Once in the North Sea, Atlantic water flows southwards following the basin bathymetry and the coastline, gradually freshening with riverine inputs (Winther and Johannessen, 2006). Further Atlantic inflow enters through the English

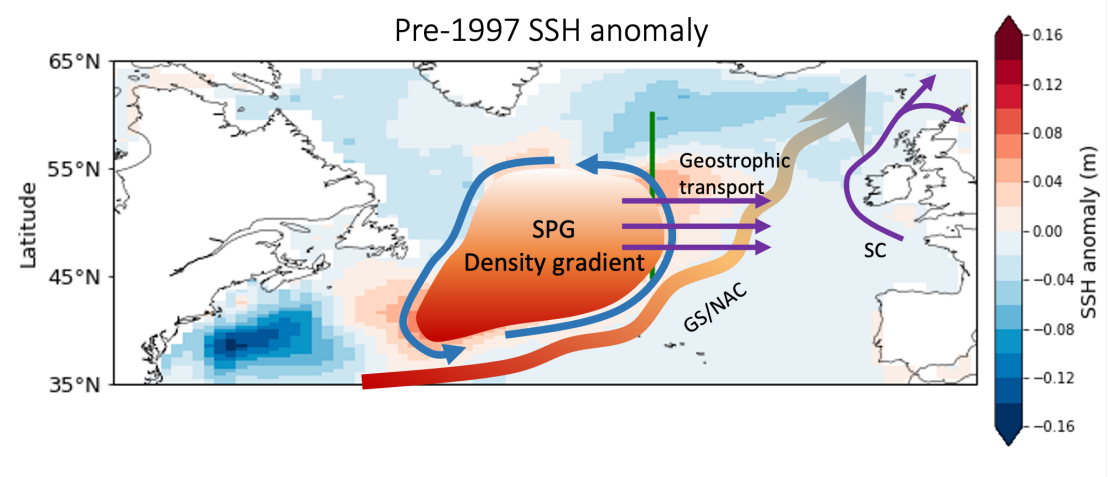

FIGURE 1.3: Schematic showing the sub-polar North Atlantic influence on the Slope Current (SC), based on the findings of Marsh et al. (2017). SPG is the sub-polar gyre, rotating anticlockwise. At the centre of the SPG is a density gradient: highest in the south, weakening northwards. This forces geostrophic eastward transport, indicated by the three purple parallel arrows. Some of this transport is thought to inflow into the SC, thus affecting the SC transport at different timescales. Background colour is pre-1997 SSH anomaly.

Channel as shown in Fig. 1.4, but this is small and on the order of 0.1 Sv (Marzocchi et al., 2015). Decreases to Atlantic inflow have already been observed in some models. A reduction of over 0.6-1 Sv in Atlantic inflow to the northern North Sea to a maximum of 0.6 Sv has been associated with the warming Atlantic and greater temperature and salinity stratification at the shelf edge (Holt et al., 2018). Such a slowdown of Atlantic inflow has potentially significant impacts for North Sea hydrography and ecology.

North Atlantic Ocean dynamics are intimately connected to atmospheric processes. Wind has a short to medium term influence on surface circulation as well as on nutrient up and downwelling. For the North Atlantic region, the North Atlantic Oscillation (NAO) is the main mode of atmospheric variability that affects circulation patterns in the region (Marshall et al., 2001). The NAO is defined as the pressure difference between Iceland and the Azores Islands, west of Portugal: relatively high pressure over the Azores and comparatively low pressure over Iceland. This pressure difference is stated as a positive or negative index. A negative phase is a weaker than usual pressure difference, bringing cooler air and less frequent storms. A positive phase brings warmer air and more frequent storms. The effect of the storm frequency has the most profound impacts on the North Atlantic Ocean: with the warming Atlantic, more frequent and severere autumn and winter storms are expected for Europe (Baatsen et al., 2015). In the intermediate to deep levels, winter NAO index has been shown to explain around two thirds of thermohaline dynamics (Sarafanov, 2009). Ocean circulation effects of the NAO can be observed at multiple (and often

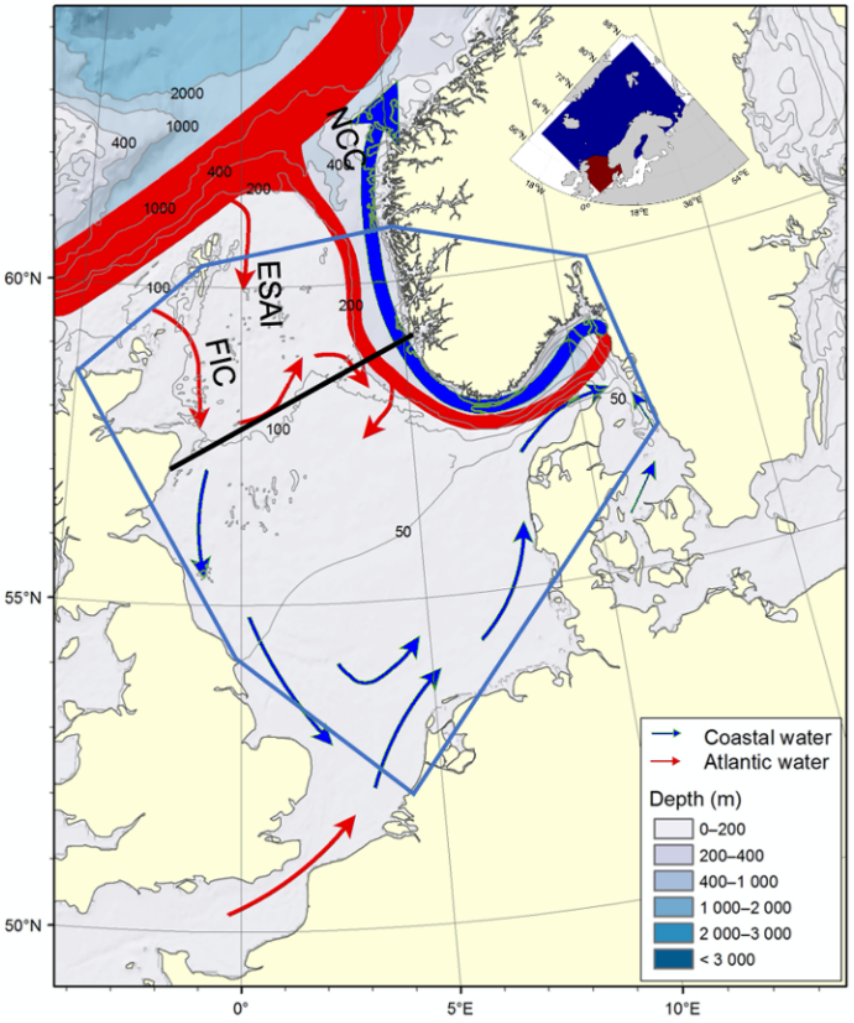

FIGURE 1.4: Schematic showing the Atlantic inflow to the North Sea and the main currents present. FIC = Fair Isle Current; ESAI = East Shetland Atlantic Inflow; NCC = Norwegian Coastal Current. From: Gao et al. (2021).

randomly distributed) time periods but the approximate spatial pattern (location of the pressure centres) reoccurs in the same regions each time (Marshall et al., 2001).

1.2 Changing North Atlantic hydrography over multiple timescales

Circulation and hydrography in the North Atlantic varies over multiple timescales: principally from annual, inter-annual to decadal. There are multiple factors determining the variability and trends, which are discussed in this section. Variability on shorter synoptic to seasonal timescales is notable in the surface layers that are subjected to the effects of direct solar and wind interaction. Over the longer term is a continuing well-documented surface warming trend over the past 40 years (Marsh

et al., 2017). This section breaks down the main periods of physical variability, and explains the mechanisms that lead to the observed patterns.

1.2.1 Synoptic to seasonal timescales

The European Slope Current is known to be highly seasonal, with strongest flows in December to January (Pingree et al., 1999). Although a predominantly northward flowing current, it can reverse in the summer months particularly in the upper layers at the Goban Spur, associated with seasonal surface warming and changes to the wind stress (Pingree et al., 1999; Porter et al., 2016b). Whilst these shorter timescales are important, especially in the coastal zones due to the potential for full-depth mixing of the water column and associated dissipation of nutrients and plankton, understanding the annual-onward timescales are more significant to assess the changing influence of North Atlantic Ocean circulation and hydrography. Changing wind patterns across the surface ocean can drive local and shelf-edge Ekman transport on short (5 day) timescales (Winther and Johannessen, 2006).

Both temperature and salinity of the sub-polar North Atlantic and surrounding shelf seas vary on synoptic to seasonal timescales. Such changes are observed via moorings such as RAPID and OSNAP, as well as during hydrographic surveys from research vessels, usually undertaken at the same time as servicing the moorings (Lozier et al., 2019). Autonomous systems, particularly the nearly 4000 active ARGO floats (as of 2017), also have recorded temperature and salinity profiles across the main ocean basins since the late 1900s (Jayne et al., 2017). Surface temperature and salinity have been recorded from various satellite systems, calibrated or quality controlled based on in-situ measurements (Hu and Zhao, 2022; Benazzouz et al., 2014). This has provided high spatial and temporal resolution observations (from 0.25° X 0.25°, daily output, depending on the satellite system used) (Hu and Zhao, 2022). Satellite SST/SSS observations have shown that coastal areas, particularly the Labrador Sea and other western Atlantic regions, are highly susceptible to seasonal freshwater input with ice melt water inflow (Hu and Zhao, 2022).

1.2.2 Abrupt changes and inter-annual timescale variability

The North Atlantic is also subject to other abrupt hydrographic phenomena which persist for up to a few years. For example, in 2013-15 there was a sudden cooling of the SPG. This cold water signature propagated 600m down, and lingered at depth in the warm summers. Termed by the media and some scientists as the North Atlantic "Cold Blob" (Ortega, 2017; Mooney, 2015), it was responsible for shifts in the circulation in the region. Weak NAO forcing has been attributed to the cooling of the SPG, as well as consecutive years of positive NAO index post-2015 leading to a

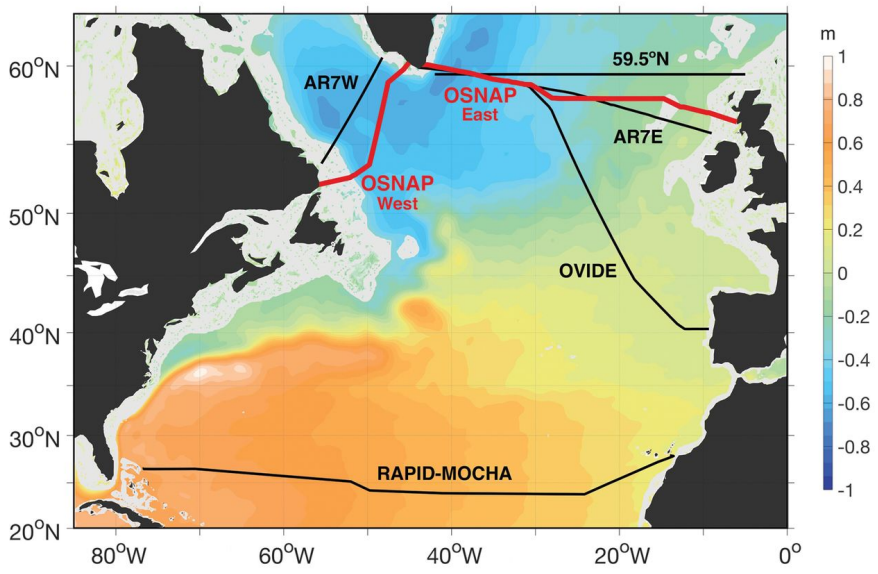

FIGURE 1.5: A schematic showing key observational arrays in the northern North Atlantic. RAPID and OSNAP are the two longest-running sections. CTD data has been provided here too. Background colour is absolute dynamic height. From: Lozier et al. (2019)

recovery to pre-anomaly temperature (Yeager et al., 2016; Josey et al., 2018). Although the cold anomaly was particularly strong, long lived and penetrating through the water column, it is not the only variation in SPG dynamics. The size of the SPG expands and contracts more periodically over time (Koul et al., 2019; Hátún et al., 2016). This in turn moves the position of the subpolar front. In 1996/1997, the SPG shrank in size, shifting the subpolar front westward (Bersch et al., 2007). The shrinking was associated with a negative phase of the NAO, with a 1 year lag Bersch et al. (2007). Conversely, expansion of the SPG correlates with high positive winter NAO index (Pätsch et al., 2020; Hátún et al., 2016). However, this relationship does not always materialise and others have developed gyre indicies based on temperature or sea surface height (Hátún and Chafik, 2018). Regardless of the index used, the size and strength of the SPG has implications for shelf edge and SC dynamics, inflow and productivity. An expanded SPG has been shown to increase plankton in some shelf seas such as those around Iceland (Hátún et al., 2016). In the Rockall Trough, Atlantic inflow from the NAC is has been directly related strength of the SPG (as tracked through a salinity signature) (Hátún et al., 2005). This raises the possibility of links between the SPG, NAC and the SC. Satellite altimetry has been used to track the SC over the past 20 years (Xu et al., 2015). Altimeter data as well as acoustic Doppler current profile (ADCP) data has suggested that the SC northward transport is decreasing by approximately 1% per year (Xu et al., 2015). However, the same study concluded that there is no apparent link between the SC strength and NAC/NAO variability.

1.2.3 Decadal variability and beyond

Most recent studies agree that the North Atlantic has warmed by approximately 1°C since the 1990s (Marzocchi et al., 2015). With anthropogenically forced global climate change and the prolonged (and ongoing) AMOC minimum, the warming trend is set to continue (Chen and Tung, 2018). A slowdown of the AMOC has also been attributed to helping maintain North Atlantic and global ocean surface warming due to a buffering effect (Chen and Tung, 2018). The strength (northward volume transport and heat transport) of the AMOC itself has been observed to be declining since 2008 (Bryden et al., 2019), leading to a cooling and freshening. However, a recent 30 year reconstruction of the AMOC using a model hindcast based on measurements at the RAPID array shows no long term decline in the volume transport (Worthington et al., 2021).

The NAO has already been discussed as an annual to interannual phenomena. While emphasised as influential at interannual timescales, part of the forcing of the NAO varies over a much longer timescale. The Atlantic Multidecadal Variability (AMV), also known as the Atlantic Multidecadal Oscillation (AMO), is a low-frequency North Atlantic sea surface temperature variability. It is identified by a relatively rapid increase or decrease, which occurs on a $\sim$60 year timescale (Zhang et al., 2019; Edwards et al., 2013; Ting et al., 2011). The AMV is often characterised by an Atlantic SST dipole with low-frequency variability (Zhang et al., 2019). The exact forcing mechanisms of the AMV remains under academic debate (Drews and Greatbatch, 2016). Some studies have linked the AMV to increases in atmospheric particulates, aerosols and volcanic eruptions altering the radiative forcing on the sea surface (Zhang et al., 2019; Drews and Greatbatch, 2016; Clement et al., 2015). Others, however, link the AMV to changes in northward heat transport through the Atlantic, predominantly driven by the AMOC (Buckley and Marshall, 2016; Knight et al., 2006). The strength of the North Atlantic Current (NAC) or Gulf Stream is closely related to the AMV. Without accurately resolving the NAC in models, the resultant AMV does not match up with observations (Drews and Greatbatch, 2016). Heat transported and stored in the subpolar gyre is also thought to help modulate the SST across the North Atlantic, and therefore directly linked to the multi-decadal AMV trends (McCarthy et al., 2018; Drews and Greatbatch, 2016). Whilst some authors show the AMOC helps determine the AMV, others argue that the AMV influences the AMOC over decadal to centennial timescales, again by adjusting basin-scale SST distribution (Buckley and Marshall, 2016; Knight et al., 2006). A lack of a reliable multidecadal sub-surface Atlantic temperature record makes it difficult to accurately reproduce AMV (Keenlyside et al., 2008; Knight et al., 2006), but clearly as warming trends are expected to continue, accounting for this variability will become important. However, as a multidecadal phenomena, it is thought that natural variability (from solar,

volcanic or other forcing) rather than anthropogenically-induced surface warming will continue to be the main driver of AMV (Ting et al., 2011).

Understanding the AMV, along with the NAO and AMOC, is necessary for understanding the forcing mechanisms for the European Slope Current. Changes in the SST distribution will strongly affect the strength of any meridional density gradient in the subpolar gyre. A stronger AMV signal (especially in collaboration with a positive winter NAO anomaly) has the potential to increase the SST gradients, and therefore density gradients. This would result in greater geostrophic transport towards the shelf edge, with the potential for greater entrainment into the Slope Current. The positive NAO anomaly would also allow the subpolar gyre expand more, based on typical observations discussed in Sect. 1.2.2. The Gulf Stream/North Atlantic Current could be shifted south in such conditions, further allowing for greater entrainment of Atlantic water into the Slope Current.

The future of North Atlantic circulation and associated physical and biological patterns will be evaluated later in this chapter, in section 1.4.

1.3 Subtropicalization and changing biogeochemistry of the shelf edge and shelf seas

This warming of the North Atlantic, shelf edge and shelf seas has lead to "subtropicalization" of the UK shelf seas - the process in which warmer water species more typically found in the subtropics are being recorded in greater numbers in areas which would usually be too cold to support them. This has been documented for several species of zooplankton as well as fish. This has knock-on effects for other marine life. Water temperature can also affect dissolved oxygen (O_2) concentrations: warmer waters hold less dissolved O_2, which means less is available for respiration of organisms (Beaugrand et al., 2008).

The changing temperature is not the only issue affecting the ecology. Anthropogenic CO_2 emissions have been lowering the surface ocean pH (increasing acidity), which can affect the growth of certain phytoplankton species, particularly species which produce calcite-based liths or exoskeletons (Hays et al., 2005). On the longer term, this could affect the ability for phytoplankton to sequester CO_2, increasing the potential for a feedback mechanism (Hays et al., 2005). There is also evidence to suggest nutrient upwelling and mixing has also been affected by the changes to the dynamics of the North Atlantic and European Slope Current (Hátún et al., 2021).

Ecological impacts of the changing North Atlantic circulation don't just include plankton. Fish, seabirds and marine mammals are all know to be affected. A strong statistically significant positive correlation has been observed between increases of

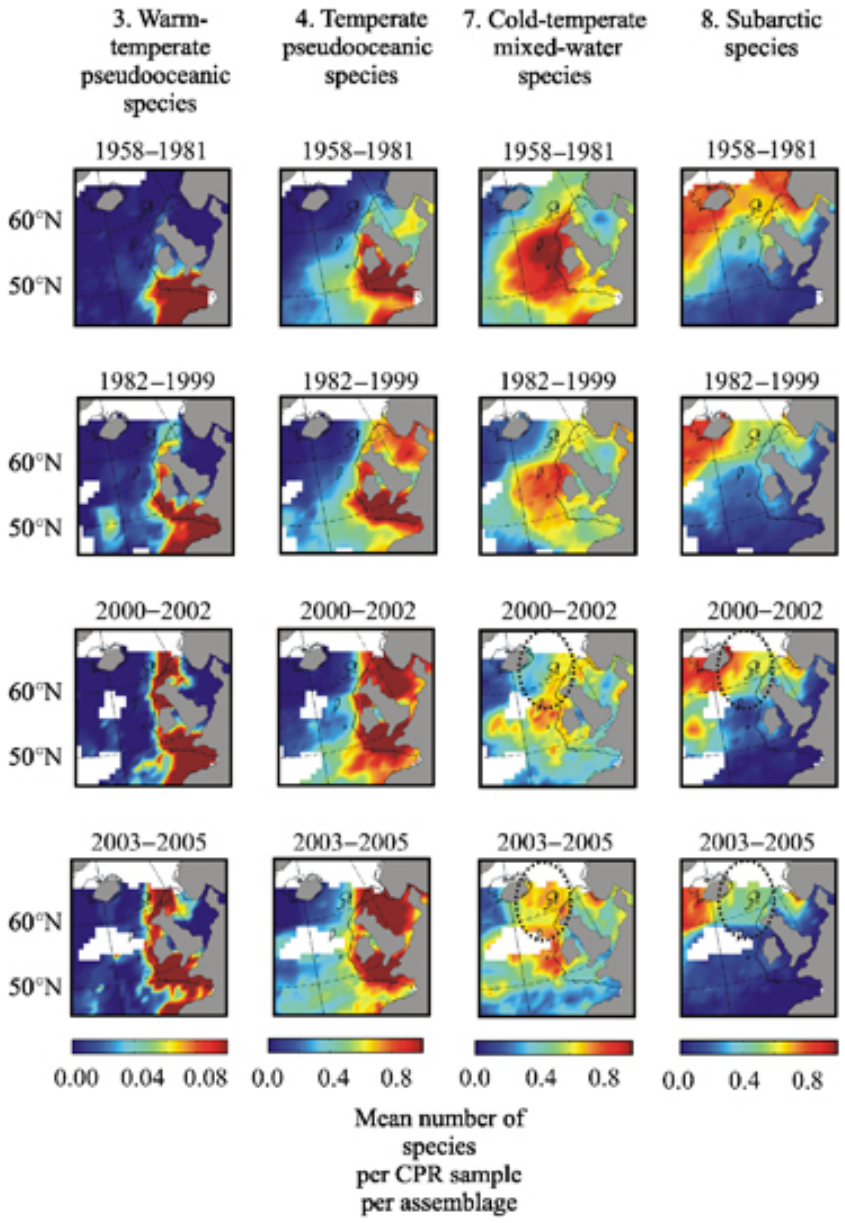

FIGURE 1.6: Redistribution of zooplankton species assemblage over time, showing an influx of more subtropical species into the UK shelf seas and North Sea since the mid to late . Adapted from Beaugrand et al. (2009, Fig. 4)

North Atlantic surface temperatures and an influx of southern fish species to south west UK shores (Stebbing et al., 2002). An expanded SPG in winter months increases zooplankton abundance southwest of Iceland (Hátún et al., 2017, 2016), which in turn feed sandeels (Hátún et al., 2017). Breeding success of black-legged kittiwakes was observed to be linked to this plankton and subsequent increase of sandeels as a direct result of the enlarged SPG (Hátún et al., 2017). The warming oceans is already having an effect on commercially exploited fish such as cod and haddock (Montero-Serra et al., 2015). The North Sea is the most important fishery for the UK, bringing much needed money and employment to many coastal communities (Kerby et al., 2012). Cod and herring are the main fish stocks, and these have seen long-term population

declines. Some of this has been attributed to over-fishing but the changing hydrography, nutrient distribution of and larval recruitment to the North Sea is also responsible (Porter et al., 2018; Reid et al., 2003). Salmon is another fish stock in the North Sea and estuaries that is influenced by changes in the sub-polar North Atlantic. Warming waters leading to a shift in plankton distribution is shifting salmon populations further north and limiting their southern extent (Beaugrand and Reid, 2003). North Sea warming is not the only driver of fish distribution changes. Analysis of historical fishing catch records show that fishing pressure on population has resulted in a decline of species numbers near the coast (Engelhard et al., 2014). However, these signals remain hard to disentangle.

1.4 Future changes to North Atlantic physical dynamics and biogeochemistry

The North Atlantic Ocean is likely to continue warming. This is likely to increase the amount of subtropicalization observed in the northwest European shelf seas. The North Sea, being an important fishery for the UK and European nations, could see greater shifts of fish stocks (Montero-Serra et al., 2015), therefore having a significant economic effect on those who depend on the productivity of the sea. If an increase of Atlantic and shelf edge surface temperatures does lead to a major shutdown of the northern North Sea Atlantic inflow pathways as described by Holt et al. (2018), this could lead to a reduction of productivity in the North Sea basin as well as create an ecosystem controlled by estuary inflow. This may lead to increased eutrophication at the North Sea coastline (Vermaat et al., 2008; Holt et al., 2018).

The AMOC has been subject of intense study due to it's implications for Atlantic-wide circulatory impacts and subsequent impacts on ecosystems. Further warming could cause the AMOC to slow down. Modelling studies have suggested that a slowdown of the AMOC as a result of ocean warming could reduce North Atlantic plankton stocks by over 50 percent (Schmittner, 2005). This could lead to a reduction in the overall food chain, further reducing the potential fisheries in the North Sea. The ecological impacts of longer-term forcing such as the AMO remain unclear, predominantly due to the lack of long-term (60+ years) ecological data (Edwards et al., 2013). A current warming phase of the AMO has already been attributed to be a significant factor of temperature-related ecosystem shifts in the North Atlantic and shelf seas (Edwards et al., 2013)

If the warming trend does indeed continue, then it would be likely that the trend of subtropicalization would also continue. However, it is important to note that natural population dynamics is almost impossible to separate from anthropogenically-forced climate change (Perry et al., 2005; Beaugrand et al., 2008; Hofstede et al., 2010), making

it extremely difficult to confirm what happens in response to natural variability (Schmittner, 2005) and what changes are being accelerated by human activities.

1.5 Research aims and outline of the Thesis

This thesis collates nearly 4 years of research. My research aimed to obtain evidence of any direct link between sub-polar North Atlantic physical processes with circulation, physical and biochemical properties observed at the European shelf edge and surrounding shelf seas. This overarching theme was focused into 3 research questions, which were developed as new findings were made:

1. Do physical (hydrographic) changes in the subpolar North Atlantic significantly influence flow and cross shelf exchange at the European shelf edge?
2. Does the slowdown of shelfward geostrophic transport effect the fate of European Slope Current waters?
3. What are the potential impacts on shelf sea and North Sea biogeochemistry from the past 4 decades of changes to the subpolar North Atlantic and reduction in associated shelf edge transport?

These research questions were then further split into the following working objectives:

A. Identify datasets and assess their suitability for analysing hydrographic changes in the subpolar North Atlantic over the past few decades (this is discussed briefly Ch. 2, and further discussed in each of the relevant chapters).
B. Use temperature and salinity data to quantify changes to density gradients in the sub-polar gyre region of the North Atlantic and calculate the shelfward (zonal) geostrophic volume transport.
C. Identify and quantify the changing provenance of European Slope Current waters through the use of Ariane Lagrangian particle tracking experiments, forced with ORCA12 5-daily mean output.
D. Quantify the declining transport of the European Slope Current, using ORCA12 northward velocity output.
E. Obtain a measure of the changing destination of the northward-flowing component of the European Slope Current using Ariane Lagrangian particle tracking experiments, forced with ORCA12 5-daily mean output, as well as using salinity as a tracer for Atlantic water arriving in the North Sea.

F. Using a 1D shelf sea coupled physics-biology model forced with nutrient flux proxies (from changing Atlantic inflow), attempt to quantify potential changes to the primary production of the Northern North Sea.

The thesis is structured to enable a clear "story": presenting evidence of how the sub-polar North Atlantic has warmed over the past 4 decades, leading to a decrease of geostrophic transport feeding into the European shelf seas, which is reducing shelf edge flow and cross-shelf exchange. I begin by summarising the main methods and datasets used. More detailed accounts of the specific analysis performed is provided within each research chapter. There are 3 research chapters, which sequentially follow on from each other. The first (Chapter 3) addresses the mechanisms and conditions in the sub-polar North Atlantic that force the European Slope Current since 1980. By using a combination of ocean "observations" and two Ariane particle tracking hindcast simulations, evidence is presented for a weakening and warming of this along-slope northward flow since the late 1990s caused by shifting meridional density gradients in the sub-polar gyre. The second (Chapter 4) further uses 22 Ariane particle tracking forecast simulations to determine the changing destination of Slope Current waters over the same 4 decade period. I show how the warming of the North Atlantic has slowed the Slope Current and altered the on-shelf transport and destination of the Slope Current waters. The third (Chapter 5) examines the links between the changing physical and biological environment in the Slope Current and surrounding shelf seas. This chapter aimed to determine the effects on primary production in the northern North Sea of variable Atlantic water and nutrient inflow. A coupled physics and ecosystem model was used to analyse the ecosystem response of the changing Slope Current transport and inflow as seen in the previous chapters. In the final Chapter (6), the results from all areas of the research are are discussed in relation to existing literature, further developing the key links between the changing dynamics of the North Atlantic and the changing physical and ecological state of the Slope Current and North Sea. Finally, a summary of the main conclusions of my research is presented before highlighting possible directions for future investigations by myself or other researchers in the field.

Chapter 2

Datasets and Methodology Summary

Abstract: This work has been completed by using several observational (including assimilated and gridded) and model datasets. GODAS, EN4, ORCA12 and CPR survey, have all been utilised. Here I introduce and summarise these different datasets used in each chapter of work and describe the utility, resolution, and analysis of them. A combination of Python, Matlab and Fortran code was used to manipulate the data and obtain the research outputs presented here in the chapters and published works. Where possible, the code is published via the Zenodo open access code publishing platform using a CC-BY licence. More details of each analysis are provided in the chapter specific methods sections. Please see the relevant chapters for details on how to access any datasets or code.

2.1 Observational and gridded datasets

2.1.1 Global Ocean Data Assimilation System (GODAS)

GODAS, the "Global Ocean Data Assimilation System", is a gridded reanalysis data product provided by NOAA, USA (NOAA, 2019). It is freely accessible on the NOAA website. GODAS is used to analyse the North Atlantic, particularly the sub-polar gyre region, to assess the changing hydrography of the region and obtain estimates of the eastward geostrophic transport from 30 °W, 46-60 °N, towards the shelf edge. Further details of this analysis are available in Chapters 3.2.1 and 3.2.2. GODAS has been chosen to calculate geostrophic transports in the subpolar gyre region as it is a relatively high resolution dataset that provides a long time series: providing temperature, salinity and u/v components of velocity gridded on a 1 by 1/3 degree grid, as monthly means for over 4 decades. This was determined to be the best dataset

to fulfil the research aims as set out in Chapter 1.5. Whilst not a pure observational dataset, it does provides a standardised, quality controlled and gridded set of hydrographic-based data. Similar datasets such as the Met Office's EN4 product was considered but was determined to be of too low spatial resolution (1 degree regular grid) to resolve finer flow structure which may influence the European Slope Current. Additionally, EN4 data older than the 1980's were potentially unreliable in all but the surface layers due to the lack of available data sources.

2.1.2 EN4

EN4 is a gridded data product provided by the Met Office, UK (Good et al., 2013). Data is available from 1900 to present. It provides monthly global temperature and salinity data from four different quality controlled sources, presented on a 1 by 1 degree grid with 42 depth levels. Version EN4.2.1 has been used in Ch. 4/5 only to attempt to create a salinity-based proxy for Slope Current transport at the shelf edge and associated DIN flux rates into the North Sea. EN4 salinity data, although at a lower spatial resolution than GODAS, is considered more reliable due to the methods used to obtain and grid the data. Generally, for the 1980s onwards, the salinity values show good resemblance to those of GODAS (analysis not shown here). Please see each respective Chapter for the full methodology used in each analysis of EN4 salinity.

2.2 Model analysis

Outputs from two different models were used in this work: a global ocean general circulation model and a shelf seas model for simulating vertical physics and biological processes at selected locations.

2.2.1 ORCA12

ORCA12 here refers to a 1/12th degree resolution ocean general circulation climate model, developed as part of the NEMO family of models by the National Oceanography Centre and partners (Madec, 2015). A concatenated North Atlantic Ocean sector dataset from an ORCA12 hindcast was used for computational efficiency of direct analysis and subsequent particle tracking experiments (described in Chapter 2.3) in the absence of reliable access to more extensive ORCA12 output. The ORCA12 dataset was provided by the National Oceanography Centre as 5 day mean output and was limited to the year range January 1988 to December 2010 (inclusive). Sadly, it was not possible to access more recent ORCA12 output for the North Atlantic, therefore limiting the analysis of shelf edge processes to this time scale (including the running

of Lagrangian particle tracking experiments, as described in section 2.3. The spatial and temporal resolution is high enough to resolve the relatively narrow European Slope Current and any subsequent monthly, seasonal and interannual variability. To test if the Slope Current is adequately resolved, Figure 3.1 plots the northward velocity and resultant current vectors in the shelf region. This is plotted at the 245m depth level to obtain the highest velocity 'core' of the Slope Current. The figure shows the strong along-shelf predominantly northward flowing Slope Current presented both as quivers proportional to the overall transport, and magnitude of the northward velocity vector presented on the colour scale, adequately satisfying the need to resolve the current. Comparing the different months also confirms seasonal variability of the Slope Current is also resolved. However, one caveat of utilising ORCA12 is that the model does lacks tides, therefore potentially limiting any cross-shelf exchange seen, particularly as a result of internal tides. Yet, by being a part of the global domain model, this means that using ORCA12 to determine the basin-scale influence on the shelf edge and shelf seas is appropriate as confirmed/validated by Marsh et al. (2017). We conclude that ORCA12 is appropriate for observing the general long-term trends of Slope Current flow and Atlantic inflow to the North Sea. It was used in calculating northward volume transport at the shelf edge in Chapter 3.2.3. ORCA12 data and the northward transport was used in seeding the Ariane Lagrangian particle tracking experiments in Ch. 4, summarised below in section 2.3.2.

2.2.2 1D coupled shelf seas ocean-ecosystem model

A 1-dimensional shelf seas coupled physics and primary production "S2P3" model was used in Ch. 5 to quantify the biological implications of changing Atlantic inflow to the North Sea. It uses user-selected dissolved inorganic nitrogen flux rates (from the surface and from the seabed) to simulate plankton growth over a year in the water column at any selected co-ordinates. The model is forced with tides and meteorological variables, as well as a phytoplankton grazing rate and nutrient recycling. Details of the selection of DIN rates and model run location are available in Ch. 5.2.2. The model was developed by (Sharples, 1999) and later improved and adapted in (Simpson and Sharples, 2012). In the current implementation, the model outputs temperature, dissolved inorganic nitrogen, chlorophyll-α, net growth and gross and net primary production through the water column. In this work, the S2P3 model output has not been validated against any observational data.

2.3 Lagrangian particle tracking experiments

Multiple virtual particle tracking experiments were performed using the Ariane Lagrangian analysis software package (Blanke and Raynaud, 1997). Ariane is freely

available from: http://stockage.univ-brest.fr/~grima/Ariane/ariane.html. Please see the software website and documentation for minimum operating requirements, installation instructions and how to use the package. The software allows the user to seed particles at any x-y-z co-ordinate at any timestep, and track them in time and space. Ariane was operated in both the backward (hindcast) and forward (forecast) modes. In all cases, Ariane was run in the "qualitative mode". The "quantitative mode" provides transport streamfunctions for selected water masses, not considered here. The ORCA12 model 5 day mean output (Madec, 2015) was used in particle tracking experiments in hindcast mode to explore subpolar and subtropical provenance of water in the Slope Current. Additionally, it was run in forecast mode to explore subsequent shelf edge exchange and residence time.

2.3.1 Particle hindcasts

Virtual water particles were seeded at the shelf edge and tracked backward for a maximum of 4 years. Two release years were considered: 1992 and 2010. In each case, particles were seeded in proportion to the northward velocity at the shelf edge in each grid coordinate, in the upper 300m of the water column. Full details of the releases are available in Chapter 3.2.4. The aim of these two experiments was to determine the changing provenance of Atlantic water to the shelf edge and Slope Current. Statistical analysis of the outputs were performed for each Ariane run, focusing on particles crossing at 30 °W, 40-60 °N. This region was chosen to compliment the earlier analysis of the GODAS gridded reanalysis product, and highlights the region with the strongest meridional temperature and density gradients. On doing so, we obtained metrics of the warming and southward shift of Atlantic flow to the shelf edge.

2.3.2 Particle forecasts

Chapter 4.2.2 explains how particles were seeded at the shelf edge and tracked forward for a maximum of 365 days. This work follows on from Ch. 3 by looking at the changing destination of Slope Current waters, with respect to the observed changing hydrography of the sub-polar North Atlantic. To summarise here, 22 qualitative forecast experiments each sampling releases over 12 months and so spanning two years were run (1988-89 to 2009-10). Once again, the same proportional seeding system was used to obtain virtual particle initial positions. Using the ORCA12 bathymetry, a binary mask was used indicate regions of the model domain that were on-shelf: classed as all areas with 200m of water or shallower. The mask ignores non-mask shallower areas such as the Rockall Bank. The number and proportion of particles that were released that made it onto the shelf was counted. Linear regression was performed on the mean residence time of particles on shelf, against Slope Current

northward transport and eastward Ekman flow to determine their relative importance to cross-shelf exchange.

Chapter 3

Weakening and warming of the European Slope Current since the late 1990s attributed to basin-scale density changes.

Abstract: Oceanic influences on shelf seas are mediated by flow along and across continental slopes, with consequences for regional hydrography and ecosystems. Here we present evidence for the variable North Atlantic influence on European shelf seas over the last 4 decades, using ocean analysis and reanalysis products, as well as an eddy-resolving ocean model hindcast. To first order, flows oriented along isobaths at the continental slope are related to the poleward increase of density in the adjacent deep ocean that supports a geostrophic inflow towards the slope. In the North Atlantic, this density gradient and associated inflow has undergone substantial, sometimes abrupt, changes in recent decades. Inflow in the range 10-15 Sv is identified with eastward transport in temperature classes at 30 °W, in the latitude range 45-60 °N. Associated with major subpolar warming around 1997, a cool and fresh branch of the Atlantic inflow was substantially reduced, while a warm and more saline inflow branch strengthened, with respective changes of the order 5 Sv. Total inflow fell from 15 Sv pre-1997 to 10 Sv post-1997. In the model hindcast, particle tracking is used to trace the origins of poleward flows along the continental slope to the west of Ireland and Scotland before and after 1997. Backtracking particles up to 4 years, a range of subtropical and subpolar pathways is identified from a statistical perspective. In broad terms, cold, fresh waters of subpolar provenance were replaced by warm, saline waters, of subtropical provenance. These changes have major implications for the downstream shelf regions that are strongly influenced by Atlantic

inflow, the northern North Sea in particular, where “subtropicalization” of ecosystems has already been observed since the late 1990s.

This work has been submitted to and published in the journal "Ocean Science". It was published as a pre-print on the 13th July 2021 and was published as Clark et al. (2022b) in final peer-reviewed form on the 2nd May 2022. This paper was co-authored by Prof. Robert Marsh and Dr. James Harle.

3.1 Introduction

Over recent decades, the European shelf seas have undergone profound changes in hydrography, biogeochemistry and ecosystems. Major ecosystem changes are most notable in the North Sea. Continuous Plankton Recorder (CPR) data indicate that North Sea ecosystems underwent a regime shift over 1982-1988, from a “cold dynamic equilibrium” of 1962-1983 to a “warm dynamic equilibrium” of 1984-1999 (Beaugrand, 2004). At species level, impacts have been profound: northward shifts in copepod populations (Beaugrand, 2004); steady increase in squid catch since 1980 (van der Kooij et al., 2016), “subtropicalization” of pelagic fish communities (Montero-Serra et al., 2015), and evidence that cod recruitment and herring spawning stocks are highly responsive to temperature in the northern North Sea (Akimova et al., 2016).

While these poleward range shifts have been directly attributed to local warming (Beaugrand, 2004), a natural conduit for range expansion is the European Slope Current (henceforth, ‘Slope Current’), conveying warm-affinity species from equatorward latitudes to the North Sea. Furthermore, Slope Current water and flow is highly variable. Observations at the “Extended Ellett Line” (EEL) repeat hydrographic section off western Scotland indicate background warming and declining nutrient concentrations in upstream flows, from 1996 to the mid-2000s (Johnson et al., 2013). Meanwhile, peak inflows of warm, salty Atlantic Water coincide with chlorophyll α increases, despite declines in nutrient concentration (McQuatters-Gollop et al., 2007). CPR data indicate that periodic changes in zooplankton in the North Sea are directly related to variations of Atlantic inflow (Reid et al., 2001b, 2003). In conclusion, local warming alone may not explain the rapid, sometimes abrupt, and ongoing changes in community structure and ecosystem functioning in the North Sea. It is likely that the Slope Current provides the connectivity necessary for bottom-up (food supply) and/or top-down (predator) drivers of change.

Variability of the Slope Current related to ecosystem change (Reid et al., 2001b, 2003) may be related to basin-scale events (Marsh et al., 2017). The North Atlantic is a highly dynamic ocean basin, dominated by two gyre systems: the Subpolar Gyre (SPG) and the Subtropical Gyre (STG). The Gulf Stream flows between these two and eventually becomes the North Atlantic Current (NAC), also referred to as the North Atlantic

Drift. The NAC brings warmer Atlantic waters from the subtropics across to the eastern boundary and continues north-eastwards: taking a multi-route path including branches flowing through the Rockall Trough (Holliday et al., 2018). The NAC eventually flows beyond the UK and into the Norwegian Sea. Here, the water cools and sinks, forming the cold, deep return flow which completes the North Atlantic Overturning Circulation (AMOC). However, not all of the water follows this pathway. Some of the NAC, which has multiple branches, is entrained into the European Slope Current which flows around the European Shelf (Marsh et al., 2017). Flowing northward along the shelf break and through the Rockall Trough, the current at times is deflected onto the shelf (Porter et al., 2018). However, the majority continues past the north of Scotland. Some of this water follows the path of the Norwegian Current but some follows the northeast Scottish coastline, onto the shelf and into the North Sea. Some of the Slope Current water that travels further north is eventually deflected into the northern North Sea via East Shetland Inflow and Norwegian Trench inflow (Holliday and Reid, 2001). Previous estimates suggest that up to 40 percent of Slope Current water ends up in the North Sea (Marsh et al., 2017).

Gradients of sea surface height are also a factor in toward-shelf and along-shelf transport. Empirical orthogonal function analysis of sea surface height variability across the North Atlantic subpolar gyre has previously been used as a proxy for a "subpolar gyre index" (Hátún and Chafik, 2018; Hátún et al., 2005). Changes to the subpolar gyre index correlate strongly with pulses of salinity observed in the northern North Sea (Pätsch et al., 2020). Satellite altimetry data has been used to produce a gyre index, which is significantly correlated with the North Atlantic Oscillation (NAO) index (Pingree, 2002). Extreme low winter NAO index conditions (weaker than usual air pressure differences between Iceland and the Azores) are found to enhance poleward flow along the European shelf edge (Pingree, 2002). The NAO has also been shown to affect surface temperatures along the eastern boundary: strong negative NAO in the months leading to January has been shown to enhance shelf-edge winter warming and current strength along the Iberian Poleward Current, also called the "Navidad years" (Garcia-Soto et al., 2002).

The Slope Current is a narrow bathymetry-constrained, northward-flowing shelf edge current. It is primarily driven by geostrophic inflow in proportion to the poleward density gradient in the North Atlantic basin (Marsh et al., 2017). It is therefore likely that changes to the density distribution of the North Atlantic could have profound effects on the Slope Current transport and composition, and the wider shelf edge and shelf sea environment. The Slope Current is also partially driven by onshore Ekman flow associated with poleward winds parallel to the coastline and shelf edge (Xu et al., 2015). Associated vertical mixing and flow instabilities at the shelf break provide an important mechanism for drawing essential nutrients to the shelf seas (Holt et al., 2009; Huthnance et al., 2009; Mathis et al., 2019). The Slope Current is often

characterised in literature as having a high salinity and velocity core at approximately 200 – 300 m above the 600 m bathymetry contour (Porter et al., 2018). The subpolar North Atlantic underwent extensive warming in the second half of the 1990s (Marsh et al., 2017), which was sustained well into the 2010s. Superimposed on this warming has been more recent short-term (interannual) variability: temperatures of up to 2 °C less than the mean were observed in the SPG from 2013, peaking in 2015 (Duchez et al., 2016; Josey et al., 2018). Coupled with this cooling was a sharp and record-breaking decline in salinity of the subpolar North Atlantic and shelf edge after 2015, associated with a strong positive NAO index over the SPG (Holliday et al., 2020). The NAC is influential in conveying material such as pollutants, nutrients and organisms including their larvae into changing shelf sea environments (Huthnance et al., 2009; Reid et al., 2003), which are becoming more or less conducive to any given species, and potentially more conducive (and more favourable) to invasive species (Holt et al., 2018; Porter et al., 2018). The SPG and NAC are also known to have significant effects on the geographical shifts of plankton, fish, and whales in the ocean basin and shelf seas. Stronger phases of the SPG have been shown to reduce the amount of plankton and fish observed at the shelf edge and in the Rockall-Hatton Plateau (Hátún et al., 2009). Changes to certain seabird populations such as kittiwakes, terns and auks have been strongly correlated to the SPG index: more specifically, high breeding success coincided with an expanded SPG, increasing zooplankton availability for the fish they feed on (Hátún et al., 2017). Conversely, a reduction of the AMOC and contraction of the SPG has previously been suggested in coupled climate-ecosystem models as a mechanism for a suppressed ecosystem in the North Atlantic (Schmittner, 2005). In summary, the Atlantic influence on European shelf seas is spatially and temporally variable. The strongest and most variable influence of Atlantic Water is felt along the shelf break and in the northern North Sea (Koul et al., 2019). The Slope Current is a major pathway for bringing waters of sub-polar and sub-tropical origin to the shelf edge and shelf seas. Warmer water arriving from the North Atlantic into the European shelf seas has already been attributed to changes in the ecology and nutrients of UK waters (Holliday and Reid, 2001; Stebbing et al., 2002; Reid et al., 2003; Mathis et al., 2019). Given these changes, it is therefore timely to determine the effects of the changing North Atlantic on Slope Current provenance.

This study has been split into three main aims: (1) to identify the geostrophic inflow to the Slope Current; (2) to examine and where possible quantify the effects of changes of this inflow on the Slope Current; (3) to assess and quantify the changing provenance of the Slope Current waters. The rest of the paper is outlined as follows. In Sect. 3.2, we outline datasets and diagnostics. In Sect. 3.3, we first examine sub-surface hydrographic variability across the mid-latitudes of the North Atlantic along the eastern shelf break over 1980-2019, followed by analysis of zonal transport variability across mid-latitudes; we then focus on shelf edge transport and establish Lagrangian evidence for the changing provenance of Slope Current water before and after 1997. In

Sect. 3.4, we synthesize these findings in the context of previous studies of large-scale and regional change in the northeast Atlantic and shelf seas.

3.2 Datasets and Methods

We use several data sources and resources: an ocean reanalysis product and an eddy-resolving global ocean model hindcast. Lagrangian computational particle tracking experiments have been conducted to determine the provenance of shelf edge and Slope Current waters. These datasets and diagnostics are outlined in the following sub-sections. The code used for the data analysis mentioned below and plotting is available separately via Zenodo, see Clark et al. (2022a).

3.2.1 Gridded reanalysis datasets

For a consistent physical and dynamical description of the North Atlantic, the NOAA gridded dataset known as "GODAS: Global Ocean Data Assimilation System" (NOAA, 2019; Nishida et al., 2011) has been used here. The dataset provides monthly values of temperature, salinity, and zonal/meridional components of velocity for 1980 – 2019 inclusive. The dataset assimilates measurements from a suite of observational tools, including XBTs, Argo floats, moorings and satellite altimeters (Nishida et al., 2011). Resolution for all parameters is 1/3° latitude by 1° longitude, at 40 depth levels. GODAS data is an assimilation of multiple measurement techniques and data sources. We acknowledge that, because of the small scale of the Slope Current, the current itself is not resolved in this dataset. However, it does provide data in sufficient resolution to assess the state and changes in the North Atlantic basin, particularly the changes within the subpolar gyre. As an assimilated and gridded dataset, GODAS uses a 3DVAR assimilation scheme to plug gaps in the data, especially at depth (NOAA, 2019). GODAS salinity is mostly "synthetic": it uses a computed salinity profile using the annual T-S relationship of a region (NOAA, 2019; Behringer and Xue, 2004). Despite the fact that GODAS "seriously underestimates salinity variability" (NOAA, 2019), since the density and hence the geostrophic velocity is mainly influenced by temperature variability in the North Atlantic region (based on the analysis presented in the results), it is appropriate for looking at longer term (decadal scale) North Atlantic variability, where density anomalies are predominantly associated with temperature variability. Eastward and northward velocity field is also included in the analysis. For this work, we created a climatology of mean temperature, salinity and density at each chosen depth level, for the entire time series.

Monthly climatologies of temperature and salinity were constructed for the entire time series by taking the mean average temperature and salinity per month. Using the

calculated climatologies, we have produced anomaly maps (for any selected depth) and meridional profiles, in the form of Hovmöller diagrams, along the shelf edge to capture the greatest density gradient of temperature and salinity. The shelf edge was defined as the first grid cell, reading from east to west, containing data at a grid depth of at least 600 m.

3.2.2 Transport calculations and metrics

Using the Python "Gibbs Sea Water" package, hosting the full Equation of State of Seawater TEOS10 (IOC et al., 2015), density was calculated from the temperature and salinity. The density was then used to calculate the geostrophic eastward volume transport of water through sections, using the (eastward) Thermal Wind Equation (Equation 3.1):

$$\frac{\partial u}{\partial z} = -\frac{g}{\rho_0 f}\frac{\partial \rho}{\partial y} \tag{3.1}$$

where $\partial u/\partial z$ = eastward velocity change over depth, g = gravitational acceleration, ρ_0 = reference density, f = Coriolis parameter, $\partial\rho/\partial$y = change of density over latitude. Integrating within the upper 1000m of water between 45 – 60 °N to obtain geostrophic volume transport (U_{geo}) through the section:

$$\int_{-1000m}^{0m}\int_{45^\circ N}^{60^\circ N}\frac{\partial u}{\partial z}dz = ((\sum(u \times \Delta z) \times \Delta y)/1 \times 10^6 \tag{3.2}$$

where Δz is the depth step, Δy is the change in latitude, and dividing by 1×10^6 provides the transport in Sverdrups (Sv, where 1 Sv = $1 \times 10^6 m^3 s^{-1}$).

We further use the eastward component of currents (part of the absolute velocity) in the GODAS dataset to calculate Utot, the total transport in the upper 1000 m. We also calculate two other different transport types, to help determine the changing provenance of Slope Current waters: large-scale Sverdrup transport, calculated from NCEP wind field (gridded atmospheric wind on a 2.5 degree regular latitude/longitude grid, updated to 2020 (Kalnay et al., 1996)), which is used as a proxy of subpolar gyre circulation; and Ekman transport at the shelf edge (15 °W, 50 – 58 °N), based on the GODAS wind stresses. Please note that transport in our results and discussion is assumed to be volumetric water transport unless otherwise stated.

Sverdrup balance:

$$\beta V = \frac{1}{\rho}\left(\frac{\partial \tau_{sy}}{\partial x} - \frac{\partial \tau_{sx}}{\partial y}\right) = \frac{curl\tau_s}{\rho} \tag{3.3}$$

where β is the meridional derivative of the Coriolis parameter (units $m^2 s^{-1}$), V is meridional transport, ρ is mean density (1025 kg m^{-3}), τ_{sy} and τ_{sx} are surface wind stress in the northward and eastward directions respectively. For a given latitude, we integrate V westward to obtain the total northward Sverdrup transport ($m^3 s^{-1}$) and select the maximum value in the subpolar range of latitudes as an index of the wind-driven subpolar gyre.

Ekman volume transport (eastward):

$$U_{Ekman} = \sum_{50^\circ N}^{58^\circ N} ((\frac{\tau_{ys}}{\rho f})\Delta y)/(1 \times 10^6) \tag{3.4}$$

where τ_{ys} is northward wind stress, ρ is mean density (1025 kg m^{-3}) and f is the local Coriolis parameter.

We also calculate monthly SSH gradients (from GODAS sea surface height relative to the geoid (SSHG) data) along the same meridional transect (30 °W, 45 – 60 °N), to provide a proxy for SSH gradient associated eastward barotropic transport.

3.2.3 Eddy-resolving model output analysis

The GODAS assimilated values have been compared against and complimented with a 1/12° resolution eddy-resolving global ocean model: ORCA12, part of the NEMO family of models (Madec, 2015). In previous studies, the model has been confirmed to be a good representation of North Atlantic subpolar circulation (Marzocchi et al., 2015). Quiver plots of velocity (fig. 3.1) have been produced for the ORCA12 250 m depth level to visually represent the currents at the shelf edge. This provided the evidence showing that shelf-edge flows, including the Slope Current, are resolved in this model. The northward velocity component of the model output has been integrated to produce an estimate of total northward volume transport at the shelf edge. A similar calculation was used to calculate eastward transports in the subpolar North Atlantic. The transport calculation was limited to the upper 1000 m of the water column. This acts as an indicator for Slope Current transport.

3.2.4 Particle trajectory calculations

We use virtual particles to represent water parcels recruited to the Slope Current. To examine the origin of Slope Current waters, two particle tracking simulations were performed using ARIANE particle modelling software (Blanke and Raynaud, 1997), calculating trajectories backwards through time in the 'qualitative mode' of ARIANE. The ORCA12 model 5-day means (Madec, 2015) were used to provide the state of the

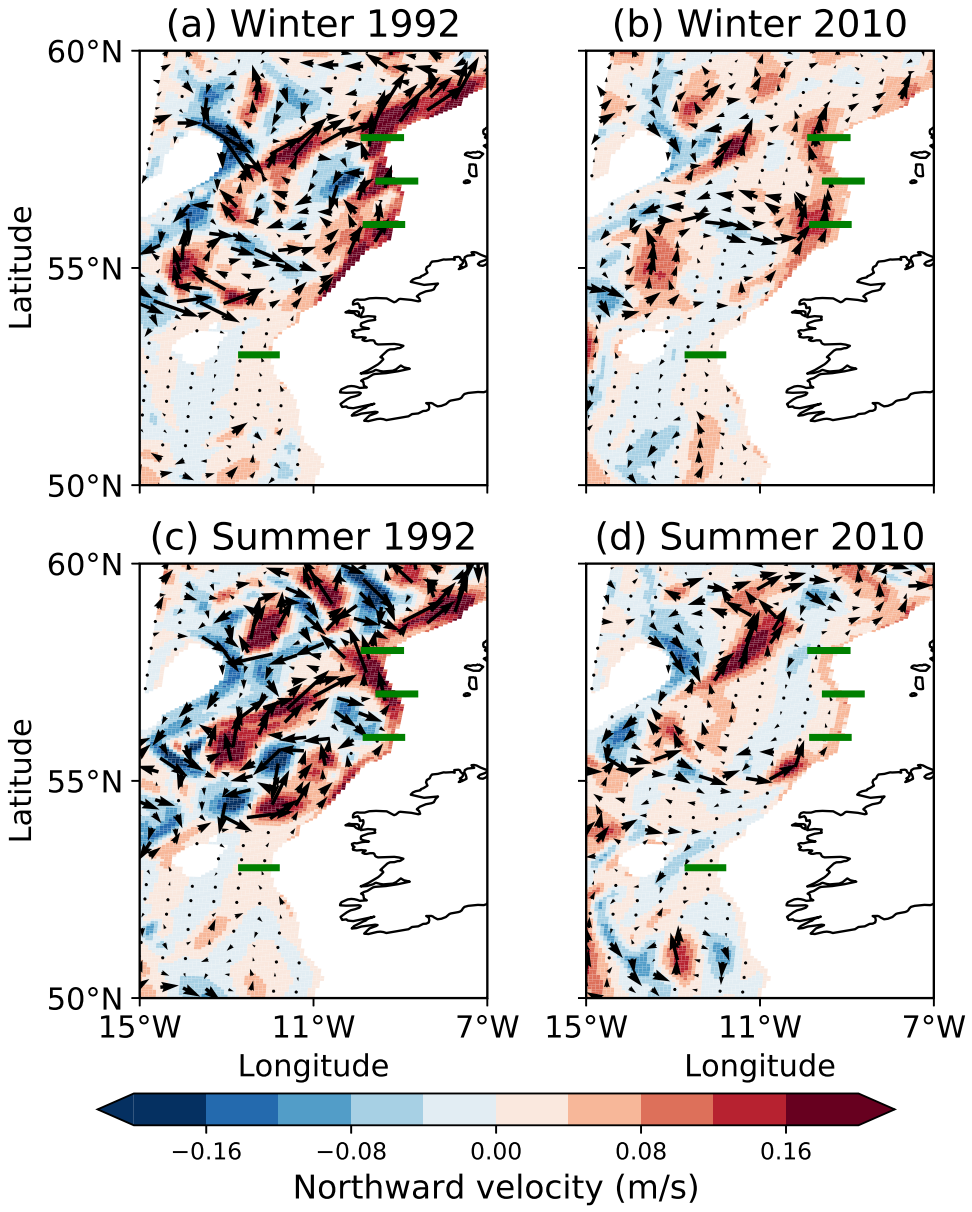

FIGURE 3.1: Quiver plot, using ORCA12 data, indicating subsurface (245 m) relative velocity magnitude and direction of the water, comparing winter and summer releases: (a) winter 1992; (b) winter 2010; (c) summer 1992; (d) summer 2010. Background colour highlights the magnitude of the v component of velocity, positive northwards. Green lines indicate the profiles used.

ocean for the simulated years, in a sub-domain of the global ocean (constrained by computational demands), with a southern limit at 34.5°N and a northern limit ranging – due to the tripolar mesh of ORCA12 – from 64°N (around 85°W) to 72.5°N (around 30°W). A number of particles were back-tracked in proportion to the northwards transport at the NW European shelf edge between 54.2 – 58.4 °N, a latitude range over which the Slope Current recruits Atlantic inflow; as such, the number of back-tracked particles varied with each experiment. Releases were designed to target the "core" of

the Slope Current: ORCA12 gridcells in the upper 300 m were defined as a release location if there was northward transport present within 50 km of the 300 m isobath. The model co-ordinates of these gridcells provide the initial positions for particles, which were distributed evenly across the vertical dimension of each gridcell, in proportion to the northward component of flow, with 1 particle allocated per 5 cm s^{-1}. As such, our 1992 ARIANE hindcast had 16470 releases, and our 2010 hindcast had 3626 releases, reflecting the reduction of northward transport within the stated latitude, longitude and depth limits.

Particles were released monthly, at the start of each month, for each chosen release year, and back-trajectories were calculated for a maximum of 4 years from the time of release; many particles reached the domain limit within 4 years, in which case their trajectories were terminated. The calculations provided daily particle location (latitude, longitude, and depth) as well as in-situ temperature, salinity and potential density (relative to the surface). Subsequent to these calculations, particle data are statistically analysed at selected on a grid of resolution 0.5º x 0.5º for areal fraction (percent cover of sea surface) and particle mean age (days adrift, prior to arrival in the Slope Current), depth and potential temperature. We further record particles crossing 30 ºW in the latitude range 40-60 ºN, binned per 0.5º of latitude to obtain the corresponding percentages, along with mean age (days before arrival in the Slope Current), temperature and depth. Back-trajectories and associated statistics were thus calculated for the periods 1992 – 1988 and 2010 – 2006, addressing changes observed in the earlier dataset analysis, in particular the shift to a warmer subpolar North Atlantic.

3.3 Results

In the following section, we first examine sub-surface hydrographic variability in the northern subtropical and subpolar North Atlantic, and along the eastern shelf break, from the GODAS dataset. We then examine the variability of zonal transport across mid-latitudes. Finally, we examine shelf edge meridional transport and present Lagrangian evidence for changing provenance of the Slope Current over the last 40 years.

3.3.1 Sub-surface hydrographic variability across mid-latitude North Atlantic and along the eastern shelf break over 1980-2019

Since the Slope Current is defined as being a sub-surface feature with a core of 200 – 300m (Porter et al., 2018), we focus on changes to the mean decadal density (Figure 3.2) anomalies at the GODAS depth layer of 205 m, calculated from the temperature and salinity data using the equation of state of seawater (Equation 3.2.1). Other depth

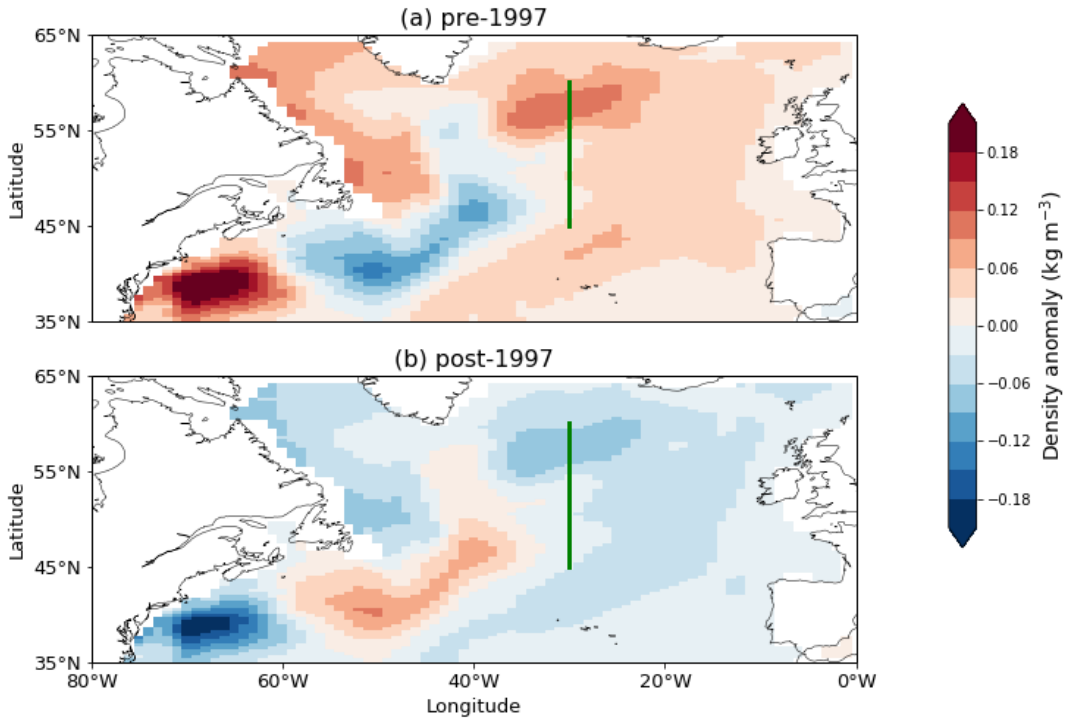

FIGURE 3.2: Mean anomaly maps of density at 205 m below the surface: (a) pre-1997; (b) post-1997. Data from GODAS. Anomalies calculated with respect to the 1980 – 2020 climatology. Green line at 30°W shows the meridional profile used for eastward transport calculations, between 45 °N and 60 °N

levels were tested (not shown) but 205m gave the strongest gradients in density at a depth likely to influence the Slope Current. Salinity and temperature are closely related throughout the sub-surface North Atlantic Ocean. Where temperature is higher (lower) than the decadal mean, the water is typically more saline (fresher). This pattern is observed in all decades (not presented here). The trend in temperature anomaly is from a cool subpolar gyre to a warm subpolar gyre, although periods of intense (2 °C) cold temperature anomalies were observed in the subpolar region, particularly around 2011 - 15. Density shows an inverse relationship with temperature and the patterns of variability match almost exactly. This is not always true when we compare the salinity to the density anomalies, especially nearer the Labrador Sea, where salinity anomalies are particularly large. Over the study period, there have been notable 'regime shifts' in temperature and density (and to a lesser extent, salinity) of the North Atlantic. The patterns of temperature and density anomalies have changed considerably over time, to the point at which the 2010s patterns are an approximate inverse of the 1980s patterns. Figure 3.2 compares the mean density anomaly (with respect to the 1980 – 2020 climatology) pre and post-1997, to assess the impact of the warming of the subpolar North Atlantic on density patterns in the region. The subpolar region transitioned from a positive density anomaly of approximately 0.13 kg m^3 to a negative anomaly of approximately 0.11 kg m^{-}3. The subtropical regions, especially just south of Cape Hatteras showed an even larger

swing of density anomaly, exceeding ±0.18 kg m^{-}3. These changes will have profoundly affected the density gradients. SSH anomalies (Figure 3.3) show large changes too. Where positive density anomalies are present, there are negative SSH anomalies (and vice-versa), with an overall anomaly switch of ±0.11 m from pre to post 1997, in the subpolar gyre region: with anomalies of ±5 cm along 30 °W; in particular, the gradient of SSH (down-slope) from the central northern subtropical gyre to the eastern subpolar gyre reduces by 20 cm from pre-1997 to post-1997, primarily associated with subpolar warming and reduced densities.

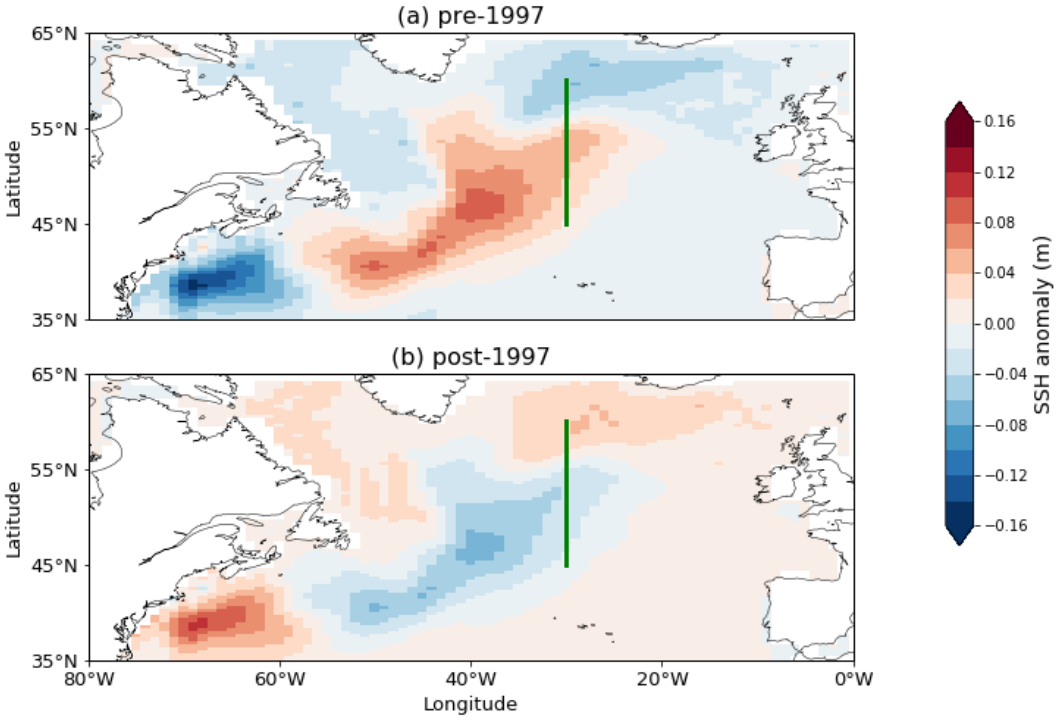

FIGURE 3.3: Mean anomaly maps of sea surface height (SSH): (a) pre-1997; (b) post-1997. Data from GODAS. Anomalies calculated with respect to the 1980 – 2020 climatology. Green line at 30 °W shows the meridional profile used for eastward transport calculations, between 45 °N and 60 °N.

When examining temperature and salinity as meridional profile time series along-slope, the same strong temperature-density relationship is observed. Hence, depth-averaged (0 to the nearest 600m depth bin) along-slope density anomaly for GODAS (Figure 3.4) have been plotted. The horizontal bands seen at 48 – 49 °N and 55 °N in Figure 4 are an artefact of jumping between grid cells to trace the shelf edge. From 1980 to 1987, the GODAS time series is dominated by a positive density anomaly. A short-lived switch to a negative anomaly is observed at 1990 before a more sustained positive density anomaly to 1997. From 1997 onwards, the profile is dominated by negative anomalies, peaking just after the year 2000 at lower latitudes (< 48 °N). This negative density anomaly persists at most of the shelf edge until 2010. From 2010 onwards, anomalies vary between positive and negative values. The density anomalies in Fig. 3.4, dominated by temperature anomalies, are indicative of

variable properties of water circulating in the Slope Current system, in turn related to changing provenance – a theme we return to in Sect. 3.3.3.

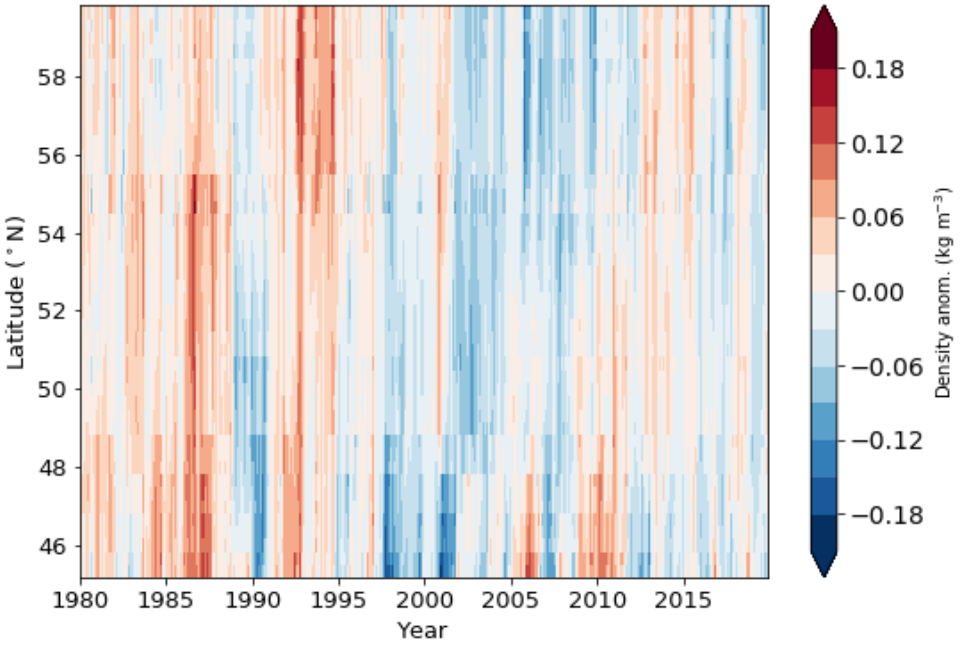

FIGURE 3.4: Time series Hovmöller plot of GODAS mean density anomaly, averaged over depth levels 0 – 600 m, at the shelf edge between 45 – 60 °N.

3.3.2 Zonal transport variability across North Atlantic mid-latitudes over 1980 - 2019

Geostrophic eastward volume transport (Figure 3.5a), calculated via the "thermal wind" equation as detailed in section 2.1, and absolute eastward volume transport (Figure 5b) has been calculated at 30 °W, between 45 – 60 °N. Transport was calculated monthly and then annual means taken to remove the large seasonal variability (not shown). A "temperature separation" threshold of 11°C was determined as appropriate for the chosen meridional profile by testing different temperatures (in the upper 200m) in the range 10 – 12 °C, based on the mean decadal temperature variation and anomalies in the subpolar North Atlantic (subpolar gyre region, not shown). 11°C was eventually chosen to best highlight the changes in transport and mean temperature after the Atlantic warming event in the mid 1990's. It is also the temperature separation point that resulted in the transport of both the warm and cool classes being the most similar/comparable before the warming event in this region.

From 1995, the transport begins to switch to a warmer regime ($\geq$ 11 °C). By 1999, the cool geostrophic transport decreased to between 0 – 1 Sv, with some very brief periods

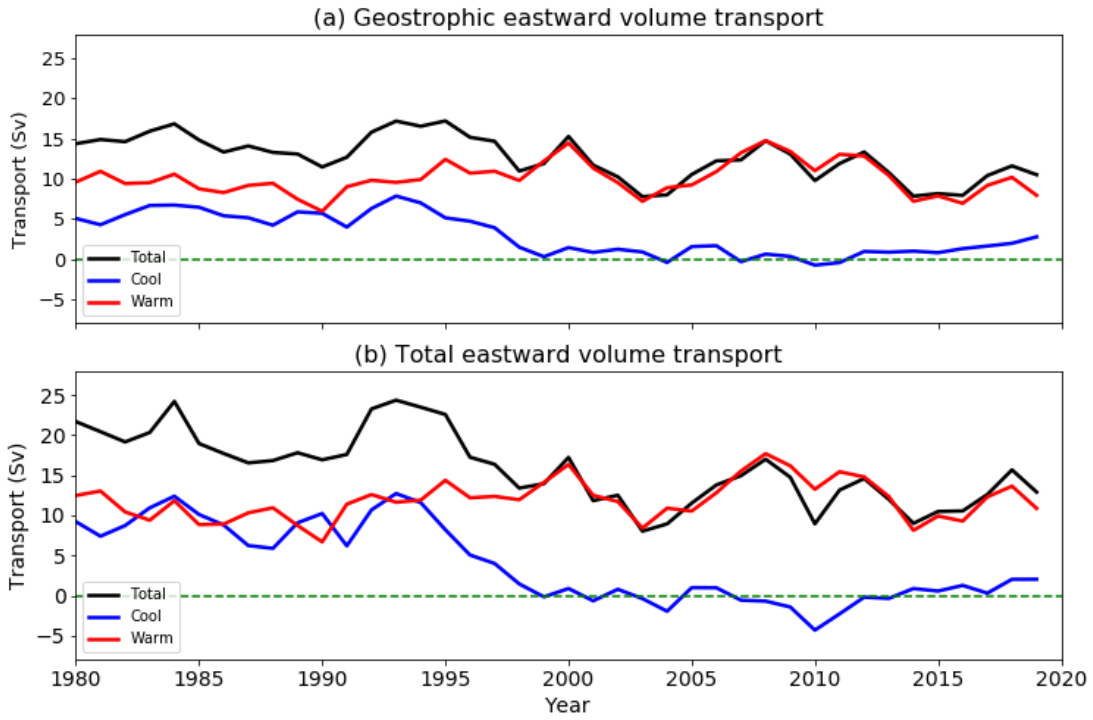

FIGURE 3.5: Eastward volume transport time series (annual means) from the GODAS dataset, (a) Geostrophic; (b) Total; at 30 °W between 45.2 °N - 60.2 °N and in the upper 1000 m. "Cool" is defined here as temperatures <11 °C, "warm" is ≥ 11 °C.

of negative (westward) transport of magnitude <1 Sv. In both the geostrophic transport and the total transport (Figure 5), the cold pathway does begin to grow once again from 2012 in. However, total transport does not show any sign of increasing to pre-1997 levels.

The GODAS geostrophic component (Figure 3.5a) of transport strongly relates to the peaks shown in the total transport time series in Fig.3.5b. Total absolute velocity through the same section also shows the same general trends and peaks, but the magnitude of the transports is approximately 5 to 6 Sv more. The total transport decrease after the 1995 – 97 regime shift is evident in both the geostrophic and total eastward transport estimates, with an observed decrease of approximately 10 Sv. The geostrophic transport estimates equate to the baroclinic, temperature and density-driven part of transport, which is slowly changing in relation to the changing density distribution as shown in Figs. 3.2 and 3.4. The total transport therefore includes additional contributions to transport below 1000 m, including any deep flows that may be identified with barotropic transport.

To provide further metrics of the regional and boundary circulation, we calculate the basin-scale Sverdrup transport (Fig. 3.6a), wind-driven Ekman eastward transport in the vicinity of the Slope Current (Fig. 3.6b), and a mid-basin sea-level slope anomaly as an index of geostrophic surface flow (Fig. 3.6c). All three indices reveal a range of

monthly and interannual variability. The annual amplitude of Sverdrup transport is on the order of 60 Sv, although annual-mean transport in the approximate range 25-35 Sv is much more stable. Ekman transport can vary annually by up to 2 Sv. There is no observed trend in Sverdrup or Ekman transports. As considered in previous studies (e.g., (Marsh et al., 2017)), eastward Ekman transport at the shelf break makes only a minor contribution to Slope Current transport, being most substantial during strong southwesterlies in winter. The sea surface slope indicative of surface geostrophic flow at 30 °W (Fig. 3.6c) varies in synchrony with the geostrophic and total transport (Fig. 3.5), dominated by decadal variability superimposed on long-term decline.

Figure 3.7 shows the same GODAS absolute transports respectively, binned in temperature and salinity space (in intervals of 0.5°C and 0.05 respectively) and shown on a Temperature-Salinity (T-S) diagram for (a) pre-1997 and (b) 1997 onwards, to further understand the observed shift to warmer transport from a water mass perspective. Transport is spread across temperatures in the range 5 - 22 °C and salinities in the range 34.25 – 36 pre-1997 (Fig. 3.7a). Post-1997 (Fig. 3.7b) shows a similar temperature distribution but is more constrained in salinity, with a range of 34.7 – 36.2. The corresponding potential density range is 26.8 – 27.0 kg m-3 (GODAS), with higher values corresponding to Subpolar Mode Water (McCartney and Talley, 1982). The cold, fresh transport at temperatures around 5 °C, 35 PSU have all but disappeared or reversed: a small amount of negative (westward) transport is observed at temperatures below 7.5 °C in both analyses. This flow reversal in the transport of the cold temperature classes was previously observed in the transport time series in Fig. Fig. 3.5. The strongest transports occur at temperatures of 7.5 – 10 °C and 35.25 – 35.50 in GODAS: this T-S class transport strengthens by at least 0.02 Sv, but overall transport determined by the sum of the gridcells has decreased. Differences in pre-1997 and post-1997 transport distributions in T-S space are consistent with the declining total transport and increase in the significance of the warmer flow observed in Fig. 3.5. An overall regime shift of higher salinities and temperatures is observed in the post-1997 period, with a decrease of total transport. Once again, this is consistent with the time series shown previously. There is a greater spread of temperature from 1997, however a narrower salinity range is apparent. The changes in transport salinity and temperature observed here are indicative of a warming North Atlantic, and an apparent salinification of the sub-polar gyre. The warming of the North Atlantic as a whole (and slight cooling of the sub-polar gyre) with increased salinification trend has previously been attributed to AMOC slowdown and a different provenance of sub-polar gyre waters (Winton et al., 2013; Bryden et al., 2019). Viewed with the other transport estimates, particularly the eastward geostrophic and total transport from the GODAS dataset (Fig. 3.5), it may suggest the origin of the subpolar waters may be changing, favouring a warmer and saltier water mass. This theme will be revisited when examining the Lagrangian experiment outputs. Another explanation for the changing temperature and salinity signature of the transport is localised changes in

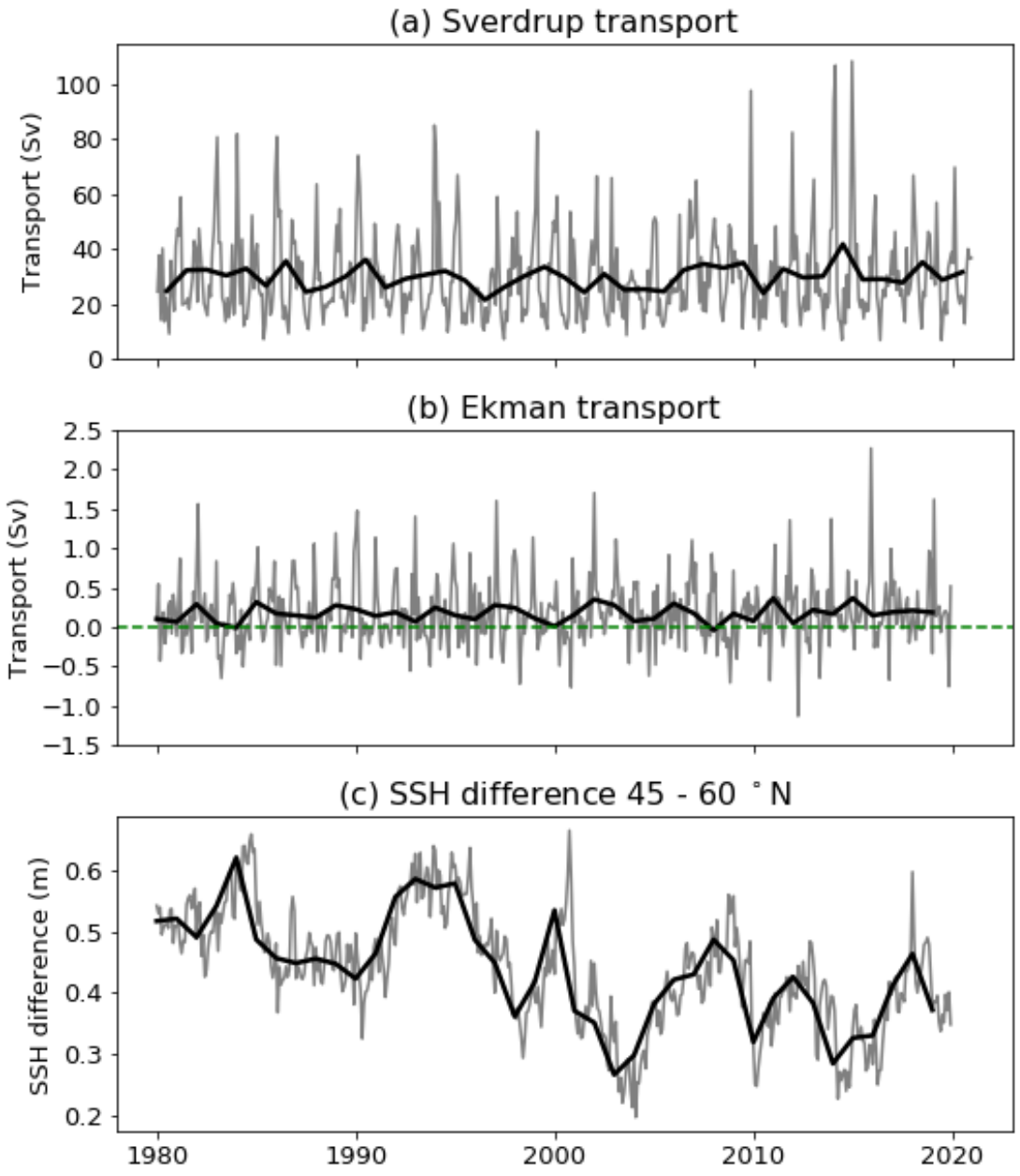

FIGURE 3.6: Annual and monthly mean eastward volume transport time series: (a) Sverdrup transport, calculated from NCEP winds; (b) Ekman transport, calculated from GODAS northward momentum (wind) flux, for the shelf edge region (15 °W, 50 – 58 °N); (c) SSH difference between 45 °N and 60 °N, at 30 °W

ocean heat convergence and 'poorly understood' air-sea fluxes (Williams et al., 2014), but this is not examined in our work.

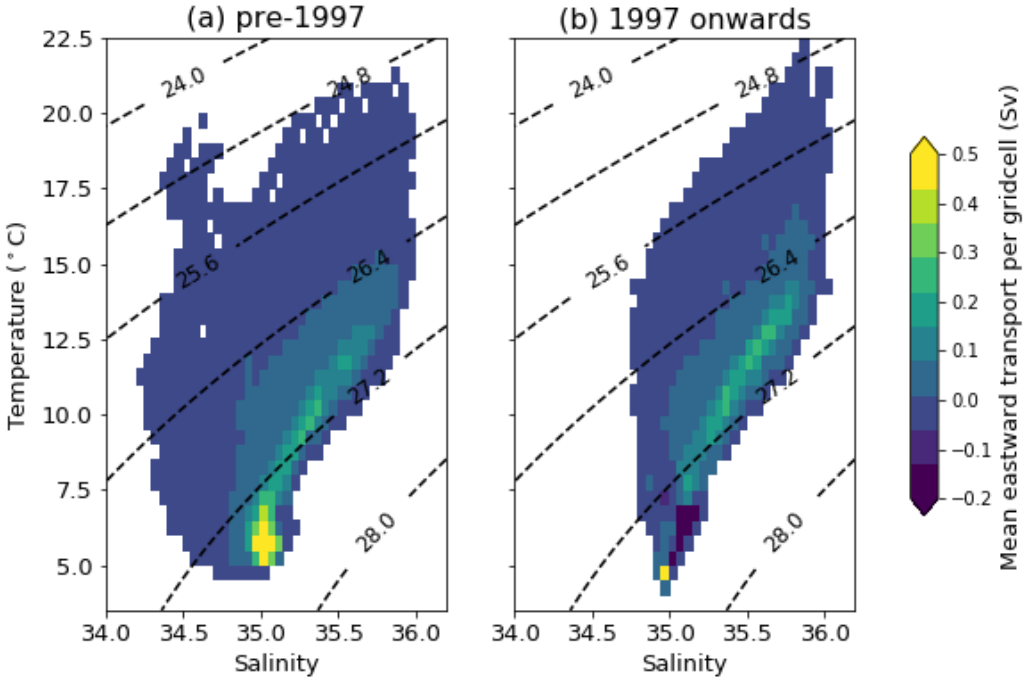

FIGURE 3.7: GODAS Temperature-Salinity binned eastward transport at 30°W between 45 – 60 °N, in the upper 1000 m for (a) pre 1997 and (b) 1997 onwards. Dashed lines are isopycnals. The sum of the gridcells in (a) is 17.2 Sv and (b) 11.1 Sv.

3.3.3 Shelf edge transport and Lagrangian evidence for changing provenance of Slope Current water

Shelf edge current velocity from the ORCA12 model hindcast was plotted in Fig. 3.1, with quivers showing the magnitude and direction, and the background colour indicating the northward velocity component. 245m was the chosen model depth level to target the high-velocity Slope Current core and negate the effects of large flows at the sea surface caused by surface heating and winds. This depth level also resides within the accepted range of the Slope Current core ((Porter et al., 2018)). Northward velocity has clearly decreased between 1992 (Fig. 3.1 panels a, winter; and c, summer) and 2010 (Fig. 3.1 panels b, winter; and d, summer). Winter flows appear stronger in both years. To examine how eastward transport in the SPG region of the North Atlantic translates to northward volume transport at the shelf edge (unresolved in GODAS), four approximately cross-slope (zonal) transects were identified in the ORCA12 hindcast, at 53, 56, 57 and 58 °N (Fig. 3.8, with the transects annotated on Fig. 3.1). At each transect, transport was calculated from 5-day averages of the northward component of velocity, in 0.5 °C temperature bins. As for the zonal transports at 30 °W presented earlier, we partition shelf-edge meridional transports above and below 11 °C. These transports and corresponding annual means are presented in Figure 8. Transports across 56-58 °N (Fig. 3.8a-c) are up to 5 times greater than the transports at

53 °N (Fig. 3.8d), consistent with recruitment of zonal inflow to the Slope Current along the Hebridean shelf (Porter et al., 2018). Given considerable shelf edge exchange poleward of 56 °N, and the choice of transects that may more or less capture the Slope Current flow, transports across 56-58 °N are consistent with progressive inflow from the west: the shelf edge transport time series show similar variability, peaks and troughs to the GODAS-derived geostrophic and total eastward transports in Fig. 3.5. Notable in these time series is considerable variability, on timescale from synoptic to decadal. In particular, transport at 56 - 58 °N declines from the mid-1990s onwards, contemporaneous with the declines in zonal transport evident in Fig. 3.5. Prior to 1997, annual-mean transports at 56-58 °N remain above 3 Sv. Post-2001, annual-mean transport at 58 °N does not exceed 2 Sv and falls below 1.5 Sv at 56-58 °N during most years over 2007-10. Transports across 53 °N reveal a more distinct seasonal cycle, with peak transport each winter, but little of the long-term decline seen further to the north.

The temperature partitioning emphasises a sharp contrast between 53 and 56 °N. Almost all transport at 53 °N is in temperature classes exceeding 11 °C at all times of the year, interrupted by occasional cold pulses. Transports across 56-58 °N is dominated by temperature classes below 11 °C, with transports of water warmer than 11 °C restricted to late summer and early autumn in most years, when this water can briefly account for the majority of transport. On the longer timescale, this fractional contribution of warm water to Slope Current transport across 56-58 °N is relatively steady, in spite of the decline in total transport. We can therefore deduce that the weaker transport in later years is warmer. This is the same as we observed in the eastward transports from the subpolar North Atlantic in Figure 3.5.

To trace inflows to the Slope Current, Lagrangian 4-year hindcast experiments were run: releasing virtual water “particles” in 1992 and 2010 at the core of the Slope Current (see Sect. 3.2.4 for details). These dates were chosen to obtain the flow pathway of water towards the shelf edge before and after the 1997 regime shift as observed in the analysis of the GODAS data (as shown in Sect. 3.3.2) and noting the model trends in shelf-edge transport that were previously highlighted. Figure 3.11 shows the differences between the two ARIANE particle tracking 4-year hindcast experiments (Figs. 3.9 and 3.10): the ensemble mean output for 1992 was subtracted from the 2010 ensemble means. The output, specifically the fractional presence of particles (panel a in Figs. 3.9 to 3.11) shows a shift – comparing later to earlier backtracking – to a more south-westerly origin of particles ending up at the shelf edge. The vast majority of particles originate off the eastern coast of the United States, with the most followed pathway corresponding with the Gulf Stream and North Atlantic Current. This is also the fastest pathway, with particles off the US east seaboard having a mean age of 600 days (Table 3.1). A smaller fraction of particles can be traced back to the subpolar gyre. The later experiment also shows more influence of water traced to the Bay of Biscay. The mean particle depth subplots (panel c in figs. 3.9 to

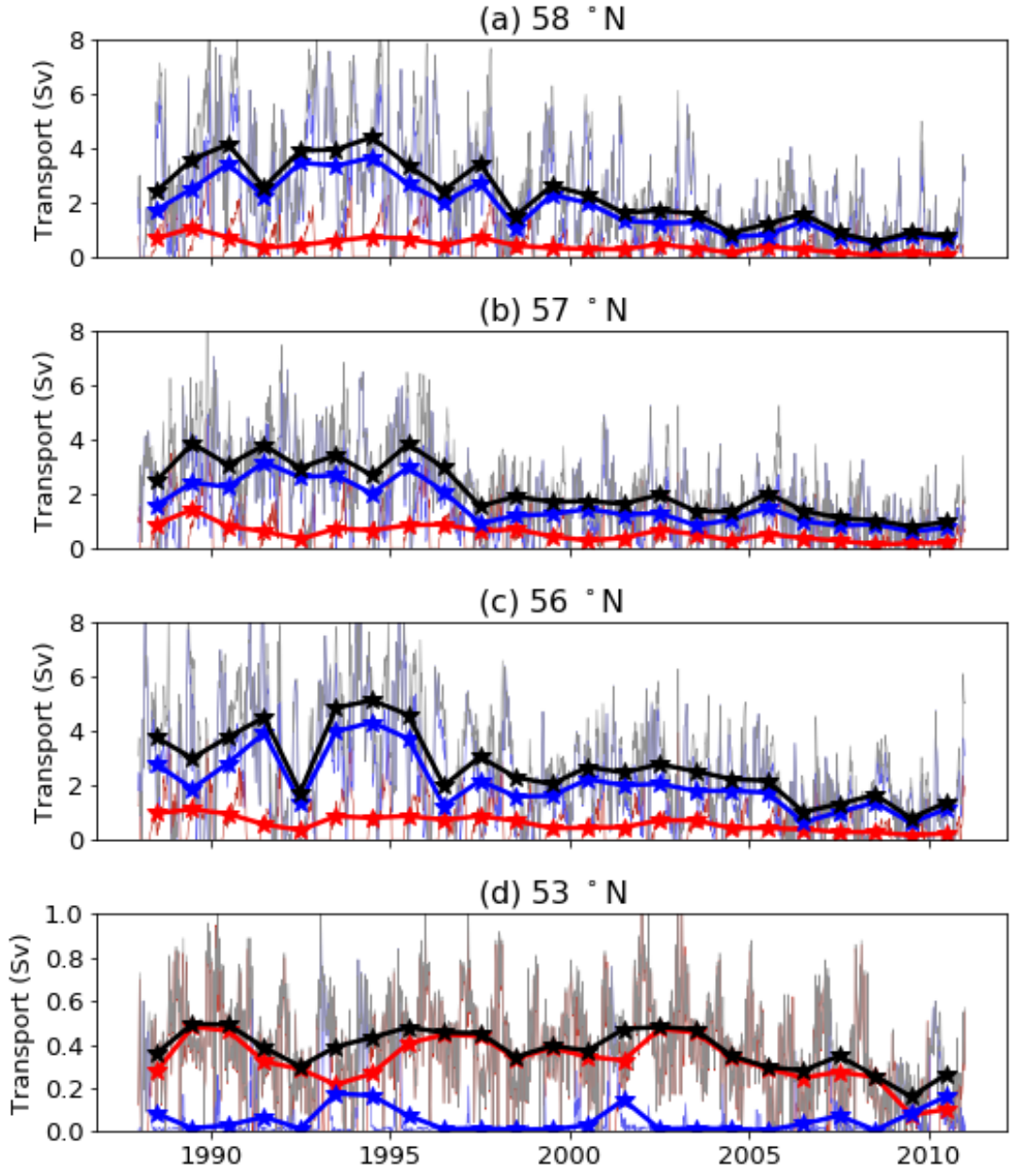

FIGURE 3.8: Northward total transport at the shelf edge from the ORCA12 hindcast, across zonal transects at (a) 58°N, (b) 57°N, (c) 56°N, and (b) 53°N (see Fig. 1). Transects are the following length, as constrained by the bathymetry: 53°N is 53.7 km; 56°N is 51.0 km; 57°N is 50.2 km; 58°N is 49.5 km. Total transport is indicated with black lines. Transport at temperatures above and below 11°C is indicated with red and blue lines respectively. Thin lines show 5-daily means. Thick lines and stars indicate the annual mean. Note that Y-axis scales on (d) are different from (a)-(c).

3.11) indicate that most particles originate from depths of approximately 100-150m. Only outside of the NAC and SPG pathway are particles traced to greater depths. The difference plot shows that overall, the 2010 hindcast saw particles become deeper by up to 100m (Fig. 3.11c), particularly the particles of subtropical origin. Flows were slower by approximately 100 days, mainly when following the NAC pathway.

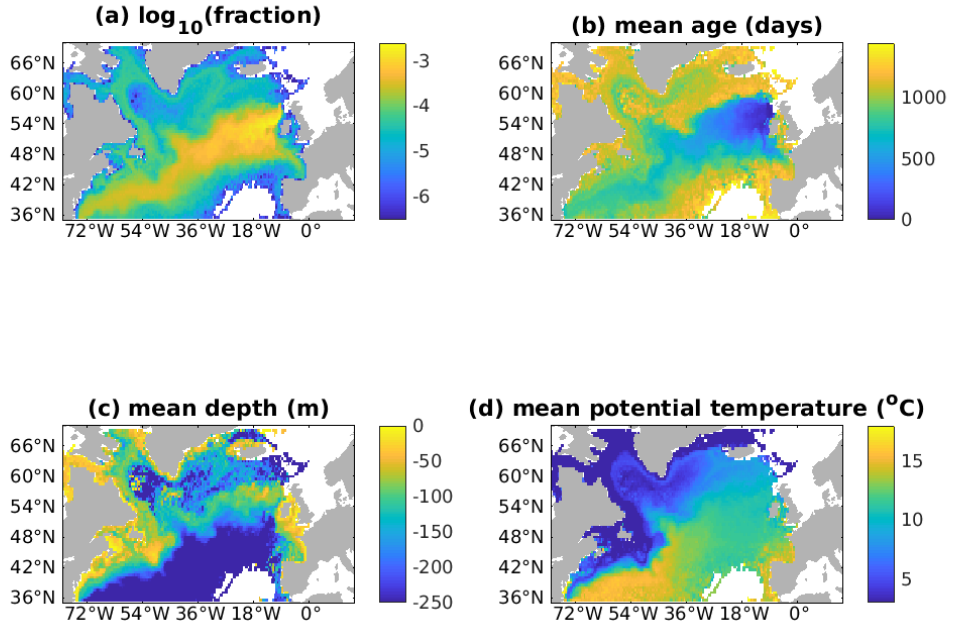

FIGURE 3.9: Ensemble mean particle statistics for the 1992-88 Ariane hindcast: (a) log10 fraction of total particles; (b) mean age in days; (c) mean depth in metres; (d) mean potential temperature in °C

Statistic	1992 hindcast	2010 hindcast	Difference
Lat.: mean	51.68 °N	50.73 °N	-0.95 °N
Lat.: median	51.72 °N	50.44 °N	-1.28 °N
Lat.: standard deviation	2.34 °	2.66 °	0.32 °
Age: mean	498 d	616 d	118 d
Age: median	420 d	535 d	115 d
Age: standard deviation	278 d	289 d	11 d
Depth: mean	177.8 m	156.9 m	-21 m
Depth: median	147.6 m	133.1 m	-14.5 m
Depth: standard deviation	138.7 m	116.9 m	-21.8 m
Temp.: mean	12.0 °C	12.9 °C	0.9 °C
Temp.: median	12.0 °C	13.1 °C	1.1 °C
Temp.: standard deviation	1.2 °C	1.6 °C	0.4 °C

TABLE 3.1: Simple statistics of crossing 30 °W to assess the spread of and difference between the two Ariane hindcasts

Comparing 2010 to 1992, there has also been a considerable increase in upstream temperature (ranging from 1 – 2 °C) of particles arriving at the shelf edge. This is confirmed in the T-S analysis (Fig. 3.7) and in the summary statistics presented in Table 3.1.

We can track particles passing a selected meridian: 30 °W is again been chosen, due to

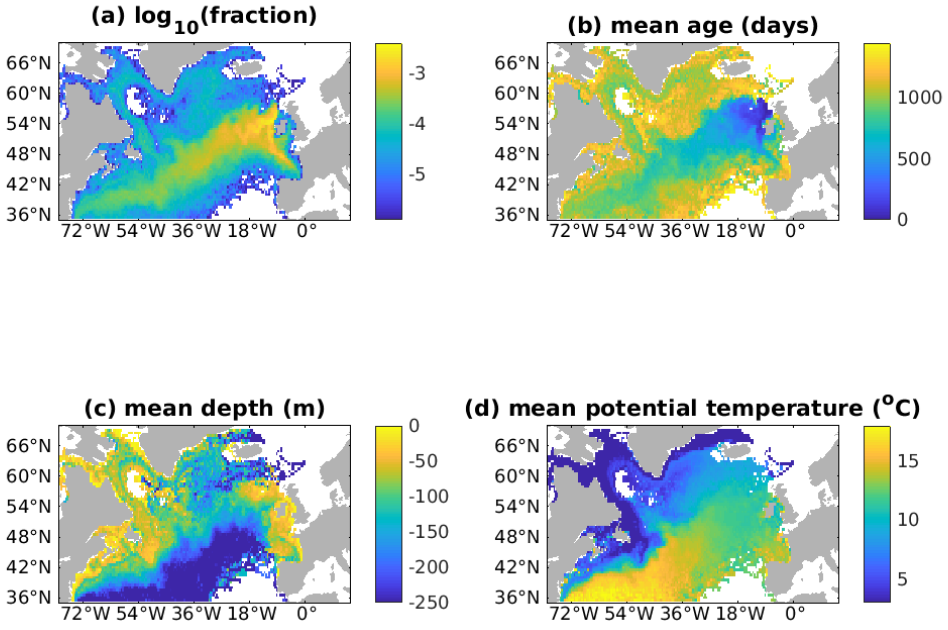

FIGURE 3.10: Ensemble mean particle statistics for the 2010-06 Ariane hindcast: (a) log10 fraction of total particles; (b) mean age in days; (c) mean depth in metres; (d) mean potential temperature in °C

the high prevalence of particles crossing that longitude in both hindcasts. Figures 3.12 and 3.13 show histograms of the two hindcasts (1992 and 2010), where particles are tracked passing 30 °W in the latitude range 40-60 °N. Figure 3.12 shows the latitude (panel a for 1992, c for 2010) and time (particle age, panel b for 1992, d for 2010) at which they crossed. Figure 3.13 shows the temperature (panel a for 1992, c for 2010) at which they crossed, as well as the depth of crossing (panel b for 1992, d for 2010). Only the first crossing (since release of the hindcast) of 30 °W is recorded in both figures. The latitude at which the particle first passes 30 °W has shifted south overall, as shown in Fig. 3.12e. The statistics shown in Table 3.1 confirm this visual analysis, with the median shifting southward by 1.2 degrees. These observations are consistent with the long-term transport changes, both geostrophic and absolute (Fig. 3.5). Even more striking is the change of particle age (Fig. 3.12f). The 2010 hindcast shows a median slowdown of 115 days. This confirms the general pattern evident in the ensemble mean difference plot (Fig. 3.11). The latitude of its first crossing of 30 °W shows a normal distribution in both hindcasts. However, the spread of the latitude at which the particles crossed increased by 0.32°, measured by standard deviation (Table 3.1). The spread of particle temperatures (Fig. 3.12e) and particle age (Fig. 3.12f) has also increased in the 2010 hindcast.

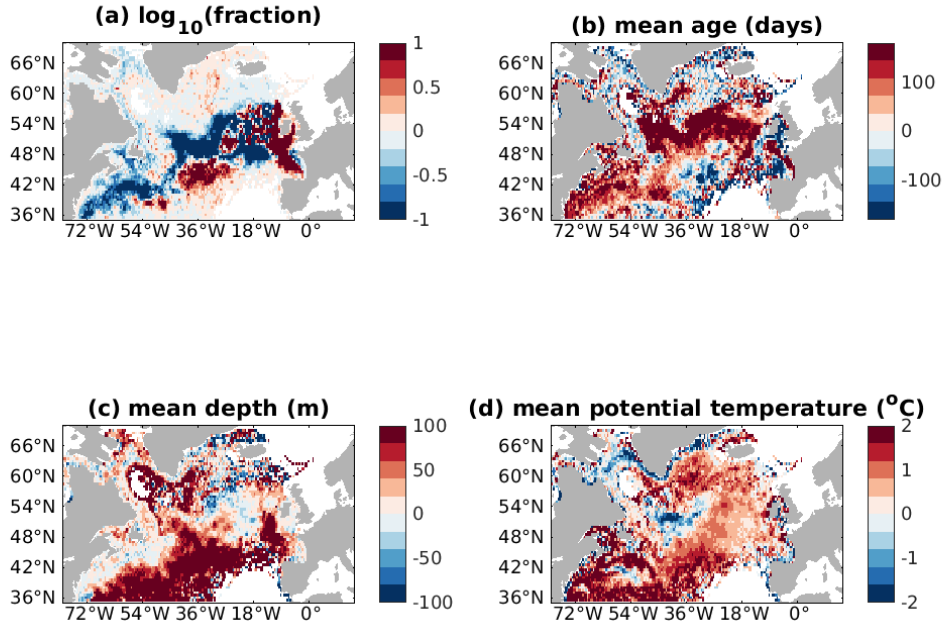

FIGURE 3.11: Difference between the ensemble mean statistical analyses of the ARIANE 4-year hindcasts: (a) 2010 mean – 1992 mean log10 fraction of total particles; (b) 2010 mean – 1992 mean age in days; (c) 2010 mean – 1992 mean depth in metres, positive = shallower; (d) 2010 mean – 1992 mean potential temperature in °C.

3.4 Discussion

As determined in a wide range of previous studies, our results have confirmed the North Atlantic is warming and transport is changing over a decadal timescale, despite being highly variable interannually and spatially. We first discuss the evidence for physical and dynamical changes in the North Atlantic and associated changes in the Slope Current, followed by consideration of the potential implications of these changes.

3.4.1 Variable hydrography and transport

Four decades of GODAS data have shown that the hydrography of the North Atlantic has changed considerably. Variation in density anomaly appears to be influenced more by temperature change than of salinity, due to the close inverse relationship between temperature and density anomalies (not shown). Until recently, the subpolar gyre was subject to long-term warming that began around 1997. In the mid-2010s, the re-establishment of positive density anomalies was associated with dramatic cooling

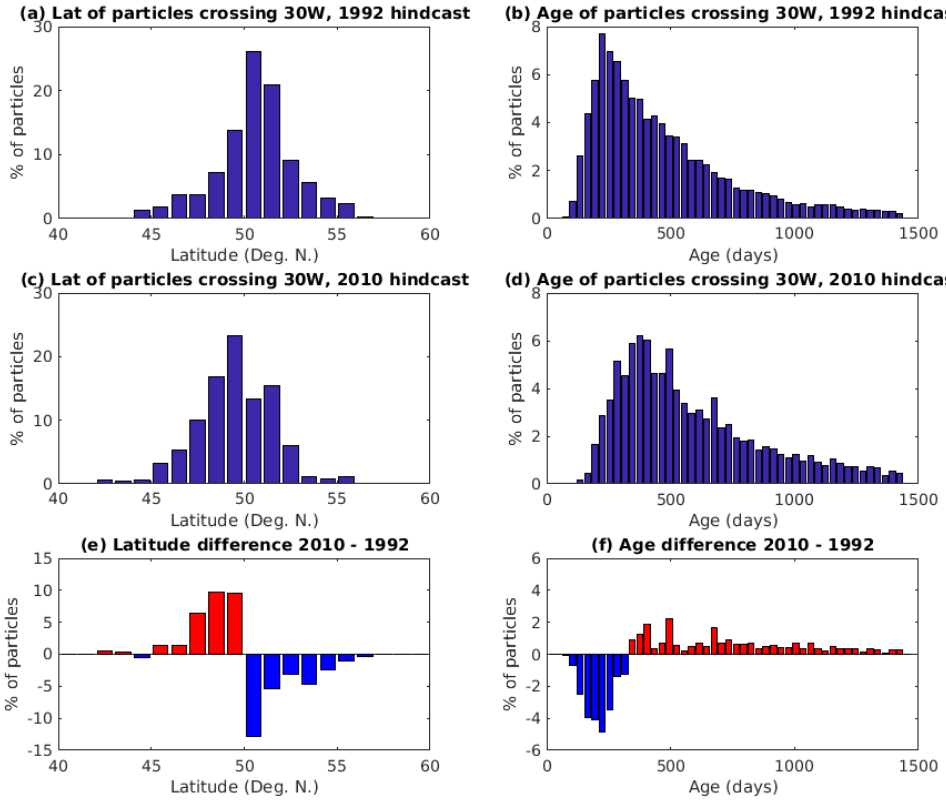

FIGURE 3.12: Histograms from the 1992 and 2010 hindcast, showing the latitude and age of unique particles crossing 30 °W for the first time (any further crossings are ignored). (a) 1992 particle latitude; (b) 1992 particle age; (c) 2010 particle latitude; (d) 2010 particle age; (e) latitude difference; (f) age difference. Positive difference = more particles in 2010. Data binned by 1° latitude and 30 days.

in the SPG region, with the core centred at 40 °W, 47 °N. This is largely associated with extensive cooling of the SPG from 2013 – 2015, which saw anomalies of up to -2.5 °C extending to at least 600m (Josey et al., 2018). This was then termed the "Big Blue Blob" (or "Cold Blob") by some within the field and indeed the media (Mooney, 2015; Josey et al., 2018).

Associated with basin-scale changes in hydrography are anomalies at the eastern boundary, expressed in density along the continental slope.

Plotting density anomalies in time and latitude (Fig. 3.4), there is meridional coherence of anomalies consistent with conveyance along the Slope Current pathway, although pulses of positive or negative anomaly appear to originate from the south and weaken poleward in some years. The early 2000s show a shift from an overall negative temperature anomaly to a positive anomaly (not shown), consistent with the decadal mean anomaly maps in Fig. 3.2. Emphasising the subtropical gyre as a driver of interannual variability, although restricted to analysis over 1992-2002, Pingree (2002) finds that poleward flow at the eastern boundary is enhanced following winters

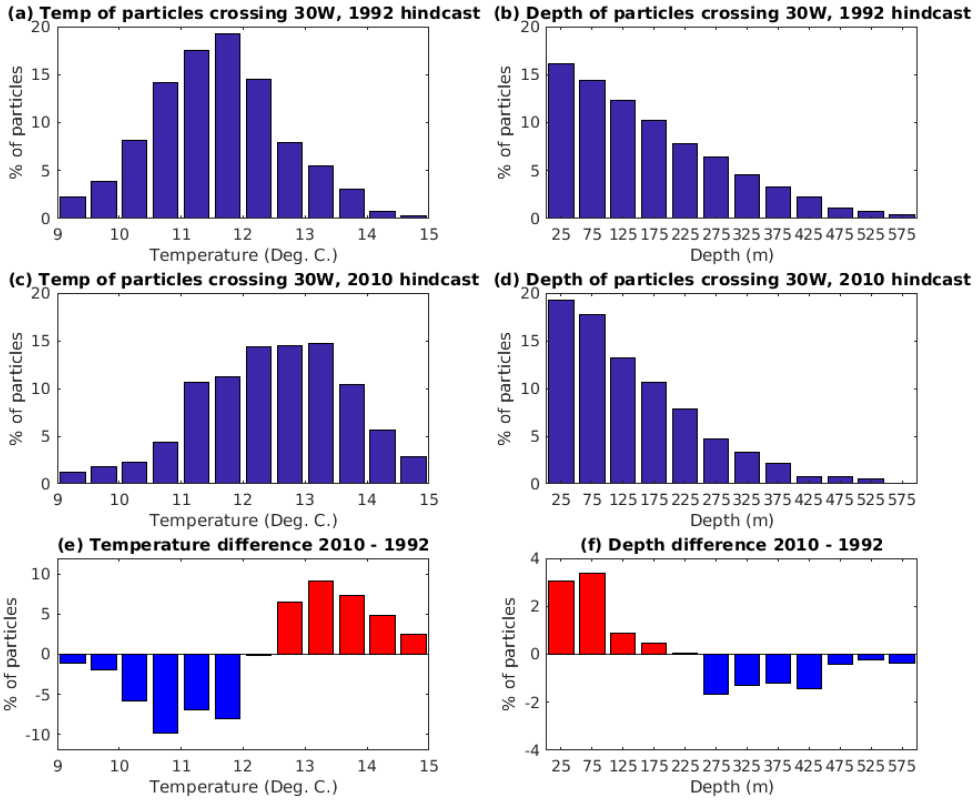

FIGURE 3.13: Histograms from the 1992 and 2010 hindcast, showing the temperature and depth of unique particles crossing 30 °W for the first time (any further crossings are ignored). (a) 1992 particle temperature; (b) 1992 particle depth; (c) 2010 particle temperature; (d) 2010 particle depth; (e) temperature difference; (f) depth difference. Positive difference = more particles in 2010. Data binned by 0.5 °C temperature and 50m depth.

when the NAO index was negative. In contrast, we find here that Slope Current variability on a longer timescale is attributed to changes in the subpolar gyre that drive variations in mid-latitude flows towards the eastern boundary. At the shelf edge and Slope Current, density anomalies appear to propagate northwards over time (Fig. 3.4). Northward transport is also declining, which shows some correlation with the observed shelf edge density anomalies, albeit with a slight lag (Fig. 3.8). Any statistical correlation or significance has not been tested in our work. It is difficult to conclusively say that the observed shelf edge density changes are directly influencing the northward transport, or if indeed the density anomalies are truly propagating along the shelf edge. It is important to note that Fig. 3.4 shows the gridded shelf edge from GODAS (that is the first grid cells to the west of land ("nan") values). Due to the regular and blocky nature of the grid, it could be an artificial signal that makes it appear as if there is a lag/propagation of density values going northward. However, it is possible that the Slope Current could be aiding a propagation of the shelf edge density anomaly. Further testing is therefore required.

Examining large-scale inflow towards the eastern boundary, geostrophic and total eastward transport estimates obtained with GODAS (Fig. 3.5), show an overall decline in transport of approximately 5 Sv throughout the time series. This variability is clearly associated with changes of density and cannot be directly attributed to wind forcing (from Sverdrup balance). Partitioning water warmer or cooler than 11°C, we identify an increase in warm-water (southern) inputs to the Slope Current since late 1990's. This has been observed in the transport calculations as well as the ARIANE particle tracking (Figs. 3.9 to 3.11). The particle tracking calculations provide evidence of a southward shift of water feeding into the Slope Current over the past 3 decades by nearly 1° of latitude (Fig. 3.11). This is consistent with the observed southward transport shifts seen in the SPG region (Figs. 3.5 and 3.6). Pulses of water near the shelf edge have been observed before: transport anomalies of +4 Sv were observed through the Rockall Trough, corresponding to periods of increasing Atlantic input to the North Sea (Holliday and Reid, 2001). Plotting GODAS transports in TS space (Fig. 3.7) confirms the shift towards warmer (and more saline) transports. A warming and more saline trend has previously been observed for shelf-edge flows (Berx et al., 2013), although at the time the authors did not determine any trends in volume transport.

Our results have shown that density gradient driven transport (Fig. 3.5a) correlates strongly with northward transport at the shelf edge, and we conclude that this is the main driver of variability in Slope Current flows. Whilst wind stress and associated Ekman transport is significant in forcing local short term shelf edge and North Sea transport (Pätsch et al., 2020), there is no evidence for a long-term trend in either Sverdrup or Ekman transport. That SSH gradient anomalies closely resemble those in eastward transport time series is consistent with the steric effect of density anomalies. Principal component analysis of SSH has accordingly been used as an index of the subpolar gyre strength (Hátún and Chafik, 2018).

3.4.2 Implications of the observed changes on the Slope Current and European Shelf Seas

Changes in the meridional density gradient across mid-latitude North Atlantic drives changes in geostrophic eastward transport that subsequently feeds the shelf edge northward flow (Marsh et al., 2017). Corresponding changes in the strength and properties of the Slope Current are likely to reverberate downstream. Expansion and contraction of the subpolar gyre has already been shown to be correlated with salinity variations on an interannual and decadal timescale in the northern North Sea, strongly linked to pulses in nutrient availability, with a lag of approximately 2 years (Pätsch et al., 2020; Hátún et al., 2021, 2017; Jacobsen et al., 2019). Nitrate and phosphate fluxes in the North Sea have been linked to the local and regional wind fluxes (Pätsch et al., 2020). The SPG has been proposed as a regulator of silicate concentrations on the

central Faroe shelf (Pätsch et al., 2020). In support of this, we emphasize the strong link established here between eastward transport indices in the subpolar North Atlantic (Figs. 3.5 and 3.6) and northward transport at the shelf edge (Fig. 3.8).

The Slope Current acts to convey water with distinct Atlantic temperature and salinity, as well as nutrients from the North East Atlantic along the shelf edge and eventually into the North Sea (Reid et al., 2003; Porter et al., 2018). Water from the Slope Current is also upwelled to the surface and transferred to the shelf seas in the Whittard Canyon, south west of Ireland (Porter et al., 2016b). The amount of cross-shelf exchange varies seasonally and interannually and can switch to a downwelling mode depending on the strength and direction of Slope Current flow (Porter et al., 2016b). This provides an important mechanism for drawing nutrients such as nitrate, phosphate, and silicate from deeper flows onto the shelf (Porter et al., 2016b), making them available for biological consumption. Changes in the Slope Current may consequently impact downstream ecosystems through a number of mechanisms. There is growing evidence that recent warming trends have impacted shelf sea species distributions, leading to "subtropicalization" of the North Sea: warmer-water species of zooplankton and fish species have been observed (and in some cases, now breeding) in UK coastal waters (Montero-Serra et al., 2015; Beaugrand et al., 2009; Beare et al., 2004). Not only is the species distribution being altered, the warmer water is physically affecting fish such as cod with "heat-induced hyperglycaemia" and water oxygen saturation is decreased with the warming water (Beaugrand et al., 2008). With up to 40 percent of Slope Current flow destined for the North Sea (Marsh et al., 2017), changes to the provenance and properties of the current could have profound effects to the state of the northern North Sea in particular, and may provide the conduit for the observed subtropicalization. Whilst the species shift has not been explored in this study, it clearly warrants further work to assess the significance of Slope Current variability on North Sea inputs and ecology.

3.5 Conclusions

We have shown that broad warming of the subpolar North Atlantic Ocean, with a mean of around 1 °C between our two study hindcasts (1992 and 2010), has acted to decrease the meridional density gradient of the region, leading to a general reduction and slowdown in geostrophic transport (by up to 10 Sv) feeding the Slope Current. More recent extreme cooling events of up to 2 °C have also been a major feature, but these have been relatively short-lived. Transport towards the shelf edge has been decreasing since 1995 - 1997, although some evidence exists of a slight recovery post-2015. It remains too early to tell if this recovery will persist. Shelf edge northward transport, incorporating the Slope Current, shows a similar pattern but with a smaller magnitude of 2 Sv north of the Rockall Trough. This relationship supports the theory

that a major input to the Slope Current is subpolar gyre water. There has been a gradual, sustained southward shift (of approximately 1° of latitude) in the water flowing to the shelf edge and being incorporated in the Slope Current. Backtracked from 1992 and 2010, transport times towards the shelf edge from 30 °W have increased by an average of 118 days, based on comparison between our two particle back-trajectory ensembles. The spread (standard deviation) of particle latitudes, temperatures, ages and depths at time of crossing 30 °W have all increased, which is associated with the weakening eastward flow from the subpolar North Atlantic.

There are yet unquantified implications of these changes, with particular focus on subtropicalization and nutrient inputs to the North Sea and the rest of the UK/European shelf. Quantifying the effects of the changing Atlantic inputs to the Slope Current and surrounding shelf seas will be examined in the following chapters.

Chapter 4

Changing fate of European Slope Current waters since the late 1980s

Abstract: The European Slope Current provides a major pathway of Atlantic water entering the North Sea and other European shelf seas. Overall, geostrophic transport towards the shelf edge has reduced by 10 Sv as a result of subpolar warming reducing the strength of the poleward density gradient. However, the proportion of warmer water feeding the Slope Current has increased. Using Lagrangian particle tracking experiments in the forecast mode, we investigate how the weakening and warming of the Slope Current has affected inputs to the European shelf and the northern North Sea. Particles released in the Slope Current, proportionally to the northward volume transport, were tracked forward for a year, and calculations of shelf-edge exchange and residency times were made. North Sea inputs are freshening. A freshening of water crossing onto the shelf has been observed, with the point at which water crosses onto the shelf is shifting to the southwest. The slowdown of the Slope Current has resulted in water that makes it onto the shelf residing for as much as 100 days more since the Atlantic warming in 1997. The relatively saline signature of the Slope Current can be used as a proxy to trace inflow to the northern North Sea, but with some limitations.

4.1 Introduction

The European Slope Current (henceforth, "Slope Current" (SC)) is a northward-flowing bathymetry-constrained current flowing along the European shelf edge (Marsh et al., 2017). It is narrow, with a high velocity and salinity core at 200 – 300m below the surface (Porter et al., 2018). Since the SC is primarily driven by geostrophic inflow from the subpolar gyre region of the North Atlantic, any changes to the Atlantic basin could affect this along-shelf flow. The SC has decreased by

approximately 5 Sv since 1997: when the North Atlantic warmed considerably and became more saline. This work aims to quantify the changing cross-shelf exchange and residence times in the northern North Sea associated with the slowdown and warming of the SC and to discuss the significance of our results in terms of shelf edge dynamics.

4.1.1 Warming of the North Atlantic

The North Atlantic Ocean has warmed in the region of 1-2 °C over the past 4 decades (Berx and Hughes, 2009; Clark et al., 2022b). This trend is anticipated to continue, and has been widely linked to anthropogenic climate change (Bakun et al., 2015; Beaugrand et al., 2009; Bakun, 1990). The warming has changed the dynamics of North Atlantic circulation, as well as altering the biogeochemistry of the ocean basin and surrounding shelf seas, via various mechanisms. On shorter timescales, uneven warming of the surface ocean has altered wind patterns and changed associated Ekman flow of surface waters at basin scale (Moat et al., 2016).

4.1.2 Changing provenance of the European Slope Current and cross-shelf exchange

The highest proportion of water arriving at the European shelf edge originates from the sub-polar gyre region (Clark et al., 2022b), and is largely forced by meridional density gradients forcing an eastward geostrophic flow (Clark et al., 2022b). The warming of the North Atlantic, particularly from the late 1990s, has acted to altered and has reduced the strength of these gradients, thus reducing this eastward geostrophic transport.

Atlantic water forced eastward by geostrophic, sea surface height, Ekman or Sverdrup transport. Geostrophic transport is deflected northward upon reaching the European shelf edge. However, some of the waters can instead be pushed onto the shelf. There are various mechanisms for this cross-shelf exchange. The geostroic flow cannot directly cross isobaths so ageostrophic processes become important at the shelf edge. In the summer months in southern regions of the shelf edge, rapidly changing bathymetry in the Whittard Canyon combined with a slight SC flow reversal, a seasonal upwelling current helps transfer SC waters onto the shelf (Porter et al., 2016b). Further north at approximately 55-56 °N, SC inflow to the Malin Shelf (referred to as the Atlantic Inflow Current) is observed, associated with internal wave breaking caused by the extreme bathymetry change near the coastline (Porter et al., 2018).

Ekman processes can have an impact. An along-slope wind deflects 90 degrees to the right in the northern hemisphere so can force water onto the shelf, also enhancing upwelling (Benazzouz et al., 2014). Most importantly, horizontal Ekman transport can induce vertical transport referred to as Ekman pumping (Winther and Johannessen, 2006). Generally, Ekman transport in the North Sea and shelf edge becomes effective in the shallow and weakly stratified regions between Shetland and the Orkneys, in the early spring (Winther and Johannessen, 2006).

4.1.3 North Sea input pathways

Up to 40% of oceanic input to the North Sea is currently thought to be advected via the Slope Current (Marsh et al., 2017). There are 3 pathways for Atlantic water entering the North Sea: between Orkney and Shetland, between Shetland and Norway, and through the English Channel (near Dover) (Winther and Johannessen, 2006). These pathways of shelf edge and Slope Current waters into the North Sea are well known from observational studies using drouged drifting buoys (Pingree et al., 1999), as well as hydrographic surveys using CTD and ADCP techniques (Berx et al., 2013). As the Slope Current flows northward along the shelf edge, we can disregard the English Channel pathway. The English Channel inflow is on the order of 0.1 Sv (Marzocchi et al., 2015). Changes in the North Atlantic are already known to directly link to change in the shelf edge exchange and inputs into the North Sea (Holt et al., 2018). Warmer and more saline inflow, from the Atlantic via the Faroe-Shetland channel to the northern North Sea, has been observed with CTD measurements (Berx et al., 2013).

4.2 Datasets and methods

We present the different datasets and methods used to reach our findings. Code will be made available on the open-access repository Zenodo.

4.2.1 2.1 Observing the changing North Atlantic influences on the shelf edge

The hydrography of the North Atlantic has been assessed using two datasets.

EN4 is an objective analysis product produced by the UK's Met Office Hadley Centre. It provides quality controlled salinity and temperature gridded depth profiles, mainly from ARGO floats, expendable bathythermographs and CTD probe deployments from research cruises, all presented as monthly values on a 1 by 1 degree grid (Good et al., 2013). EN4 salinity has been compared to ORCA12 salinity (see results, Fig. 4.12),

showing a strong relationship between 1995 and 2005 but weak correlation outside these limits. EN4 salinity signature in the northern North Sea is also compared to Slope Current northward transport, showing a statistically insignificant relationship (see results, Fig. 4.10).

To obtain the influence of wind-driven processes moving water onto the shelf edge, Ekman volume transport towards the shelf edge was calculated using Equation 4.1. The northward component of wind stress per gridcell in the ORCA12 model at 10 °W between 56 - 58 °N was used to calculate 5-daily and monthly mean Ekman transport (in Sverdrups), as a metric for shelf-edge exchange across the Hebridean shelf break:

$$U_{Ekman} = \sum_{56^\circ N}^{58^\circ N} ((\frac{\tau_y}{\rho f})\Delta y)/(1 \times 10^6) \tag{4.1}$$

Where (τ_y) is the northward wind stress in each gridcell (as applied 5-day averages in the ORCA12 hindcast), ρ is seawater density (assumed constant at 1026 kg m^{-3}), f is the Coriolis parameter $2\Omega \sin\theta$ ($\Omega = 2\pi/86400$s, Earth's rotation rate) and Δy is the latitude grid step in the ORCA12 model (calculated as 111000m/12).

4.2.2 Lagrangian particle forecast experiments

The Ariane software package (Blanke and Raynaud, 1997) was used to seed virtual water particles at the shelf edge, proportional to the strength of the northward velocity vector at the shelf edge at each grid coordinate: assumed to be dominated by the Slope Current. ORCA12 5-day mean output was used to obtain the northward transport for the initial position seeding, as well as for forcing the particles in the Ariane runs. Particles were released between 54.2 °N and 58.4 °N, consistent with the same particle targeting regime as Clark et al. (2022b) (presented in Chapter 3.2.4), but across 22 2-year runs. Particles were released at the end of each month, for a year, and tracked forwards in time for a maximum of 365 days. Positions were recorded every 5 days. Ariane simulations were run annually for the years 1980-81 to 2009-10.

To obtain a metric for shelf edge exchange and residence time, a Boolean/binary area mask (shelf = 1, no-shelf = 0) was created in ORCA12 grid co-ordinates (`i, j, k`). In the mask, the continental shelf is defined as all areas of 200m water depth or shallower. The mask was further refined manually to remove non-shelf shallow areas such as the Rockall Bank and the waters around the Faroe Islands. The Norwegian Trench was also excluded from the mask. There were a few instances of "coast crashes", where particles hit the coastline or the seabed and are then counted as stopped or outside the domain by Ariane. These particles were filtered out from the calculations of particles on shelf and residence time, to remove bias in the data (a risk of particles being counted as residing on shelf for longer than they actually do). Figure

4.1 shows the refined mask, in ORCA12 grid co-ordinates. The Iberian Peninsula and the European Shelf, including the North Sea, can be seen. Land is not excluded from the mask, since water particles in Ariane cannot cross onto land in any case.

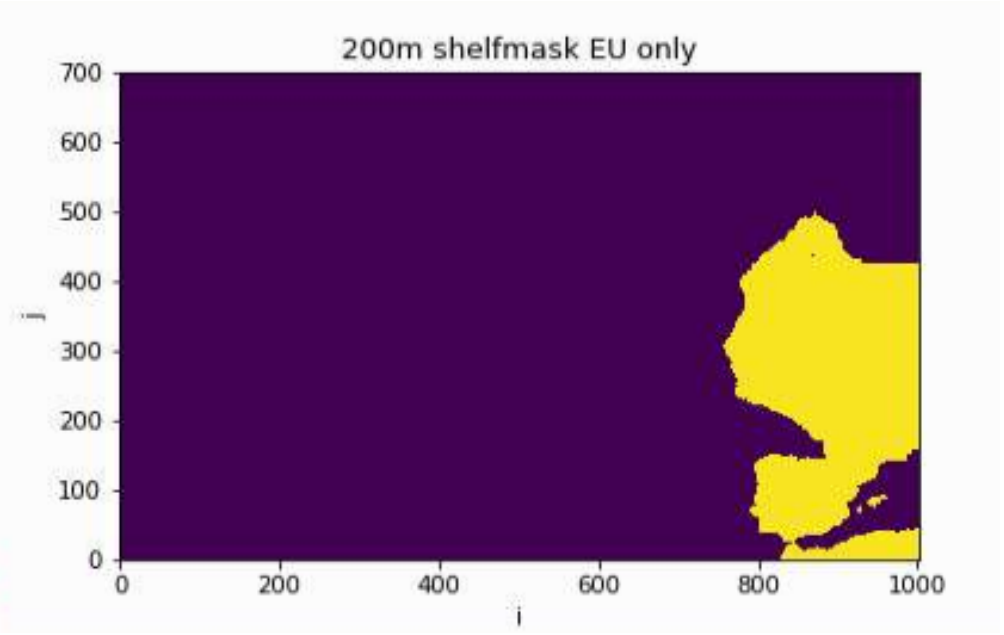

FIGURE 4.1: A plot showing the binary shelf mask used to obtain cross-shelf exchange and residence time metrics. Yellow shows regions on-shelf (defined as 200m water depth or shallower), purple shows off-shelf areas. Note that the axis show ORCA12 model co-ordinates.

4.3 Results

Here we show our results, beginning with the output and statistical analysis of the Lagrangian experiments at the shelf edge. We move then to present and quantify some drivers of the on-shelf transport, showing how salinity provides a traceable proxy of Slope Current water that has made it on-shelf. Finally, we attempt to show how Slope Current transport (and the destination of it) has changed over the past few decades by using this proxy.

4.3.1 Lagrangian analysis

We performed 22 Ariane experiments, seeded monthly and proportional to the northward transport at each grid point at each respective release time. The outputs are related to volume transport of the Slope Current and cross-shelf exchange, including inflow to the northern North Sea.

Figure 4.2 shows a time series of the total number of particle releases co-plotted with volume transport. The total number of particles released in each annual experiment

decreases, accurately reflecting a decrease in northward transport at the shelf edge. The transport calculation at 58 °N was the same as Clark et al. (2022b), Fig. 8 (see Fig. 3.8 in Chapter 3.3.3). This confirms the release mechanism for the forecast Ariane runs was working correctly and is appropriate for closely representing variable Slope Current transport. There is not an exact match between northward transport and number of particles released as the latter is proportional to local speed, and the calculation is performed across each latitude step rather than the transport at a single latitude (58 °N in the figure). Therefore, the number of particles crossing onto the shelf can be used as a representative proxy for the influence of Slope Current transport on cross-shelf exchange.

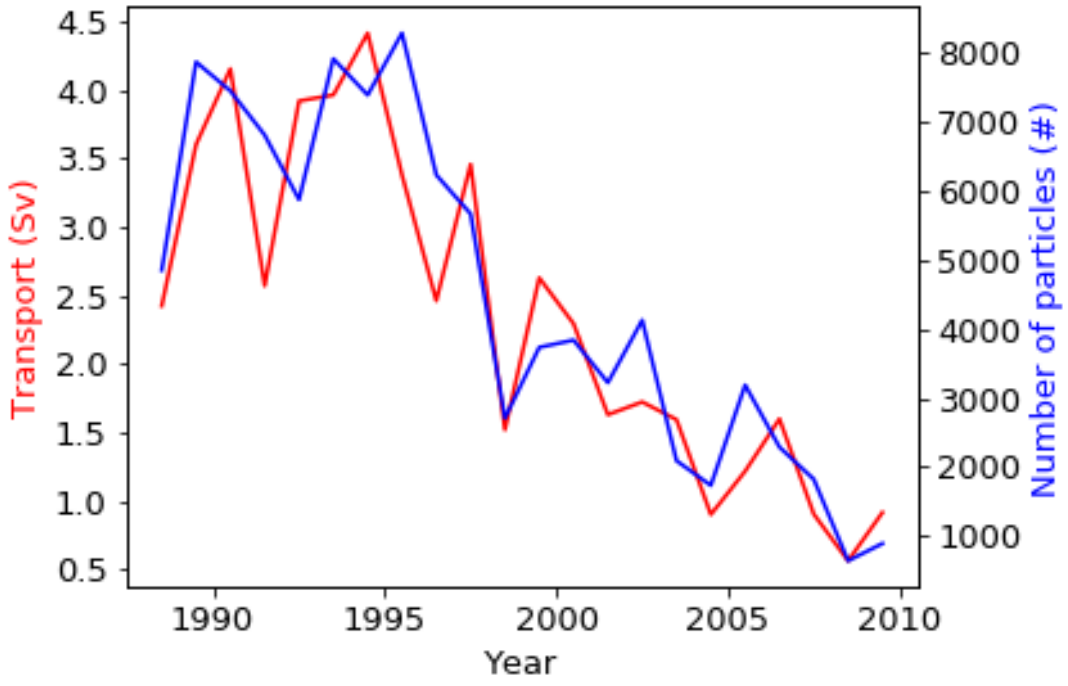

FIGURE 4.2: Line graph showing the number of particles released per Ariane experiment (blue line, right axis), co-plotted with northward total volume transport at the shelf edge (red line, left axis) from the ORCA12 hindcast at 58 °N.

Figure 4.3 shows the seasonal trends of particles moving onto the shelf (as defined by the shelf mask, see methods Chapter 4.2.2), presented as a percentage of all releases that month (left) and as an absolute number of particles (right). More particles end up on the shelf when released in the winter months (December to January) than in the summer and autumn months (June to October), with the minimum proportion and number of particles making it onto the shelf consistently being in August. Only a mean of 40% of particles make it onto the shelf in August, a 10 percent drop from the winter. When looking at the absolute number of particles on shelf, the standard deviation is much larger in the winter months compared to any other season. This likely reflects the high variability of shelf edge transport (and therefore particles)

during winter conditions. The standard deviation across all months is very similar in the proportion of particles plot, with an approximate value of ±10%.

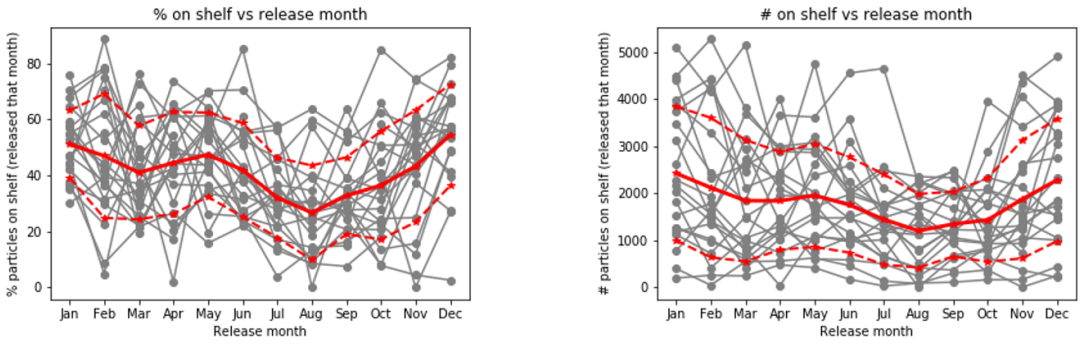

FIGURE 4.3: Time series of particles on shelf (left: as a percentage of those released, right: number of those released), split into the month of release. The grey lines represent each Ariane experiment over the 22 release years. Bold red line is the ensemble mean of all experiments, with dashed red lines being ± standard deviation.

Residence time of particles that made it onto the shelf was calculated. Since Ariane had 5 day output, any particle that was not logged as on shelf for 2 or more time steps was not counted as residing on the shelf. Figure 4.4 shows the relationship between mean residence time and the Slope Current northward transport. As Slope Current transport increases, particles spend less time on the shelf. This may be due to increased shelf flushing with greater shelf edge (Slope Current) transports, or may simply be due to less particles making it on the shelf in the first place. The correlation (r^2 of 0.29) is not particularly strong. A Wald Test (t-test) was performed to examine the significance of this correlation. The p-value obtained was 0.01, which is lower than the confidence value α of 0.05. Therefore, we can reject the null hypothesis and conclude that there is sufficient evidence of a significant linear relationship between the transport and residence time of particles on the shelf.

To better show the effect of shelf edge northward transport on the proportion of particles residing on the shelf at any given time, Fig. 4.5 presents the 5-daily output data as a time series. There is a high degree of apparent annual variability in the particle data. However, the variability can mostly be explained as an artefact of each adjacent (in time) Ariane experiment starting with the majority (greater than 15%) of the released particles off the shelf. As the transport declines, there is an increasing trend of particles making their way onto the shelf. This trend appears to accelerate after the Atlantic warming event in the mid 1990s.

4.3.2 Drivers of on-shelf transport

So far, we have shown that residence time of Slope Current water on the European shelf decreases with increasing transport. We have also shown that the number and

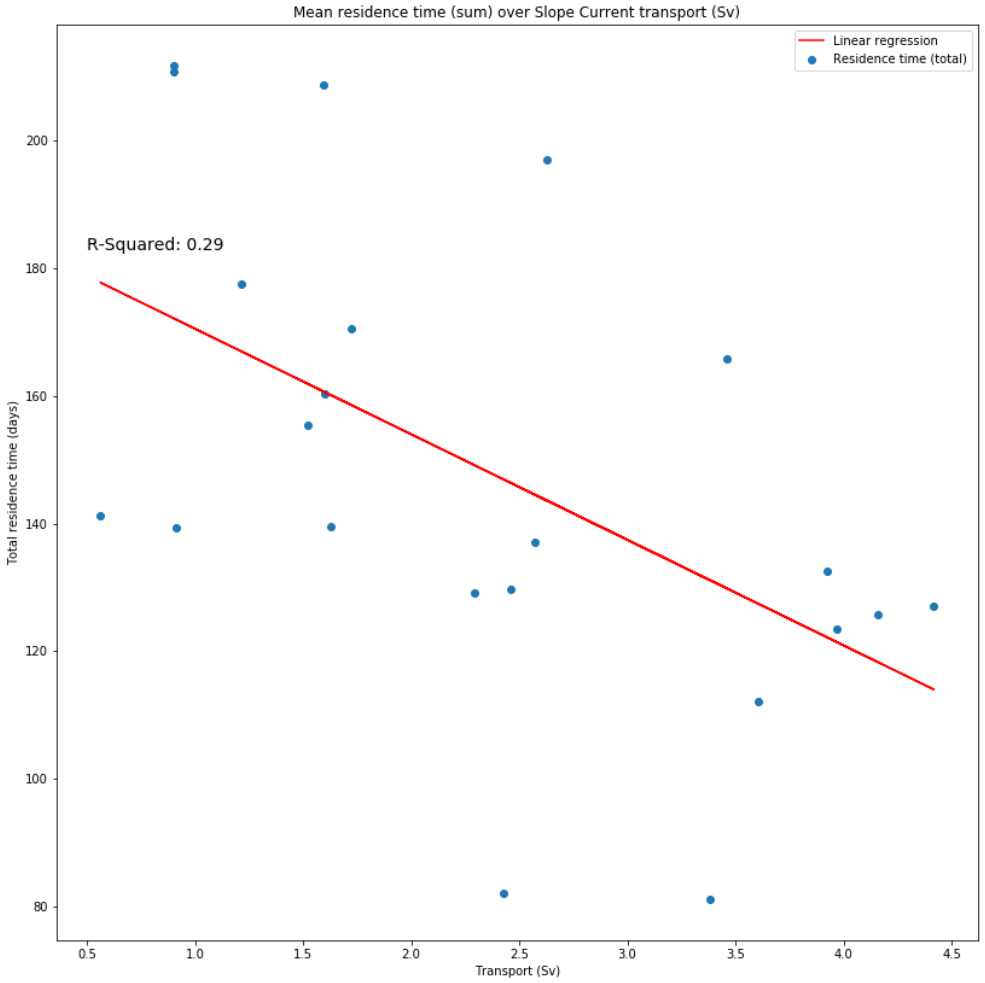

FIGURE 4.4: Mean residence time (days) of particles on the European shelf over Slope Current northward transport at 58 °N.

proportion of particles is somewhat seasonal. We shall now explore potential drivers of the cross-shelf exchange and on-shelf transport.

Figure 4.6 shows eastward Ekman transport time series, both at 5 daily output and monthly mean output. Looking at the 5 day output first, it is clear that transport is extremely variable in these short time periods, including many instances of shifting from positive (eastward) to negative (westward) in as little as 10 days. Transport is positive (eastward), consistent with the northward component of wind stress. Monthly averaging highlights a seasonal pattern of high eastward transport in the winter months and lower eastward transport (occasioning negative) mainly in the summer months. This is reflective of the typical winter and summer wind patterns in the northwestern North Atlantic. There is no apparent overall trend in the transports, though the magnitude of the variability in transport does appear to decrease from 1988 to 2000. The high monthly and inter-annual variability of Ekman transport is consistent with the low correlation with total residence time.

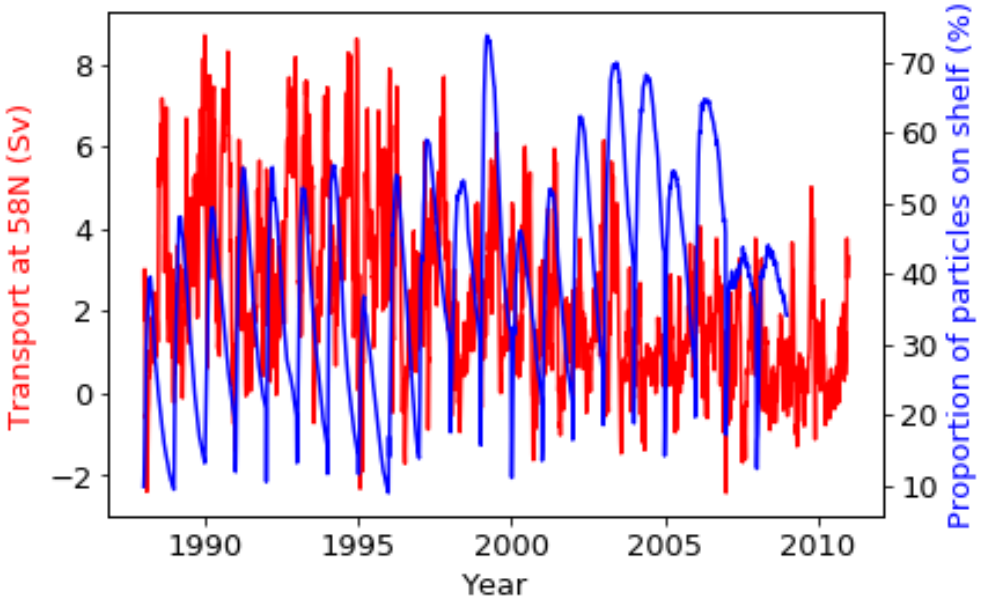

FIGURE 4.5: Time series showing 5-daily northward transport at the shelf edge at 58°N (red line, left axis) co-plotted with the 5-daily proportion of particles released in the Lagrangian forecast experiments making it onto the shelf (blue line, right axis).

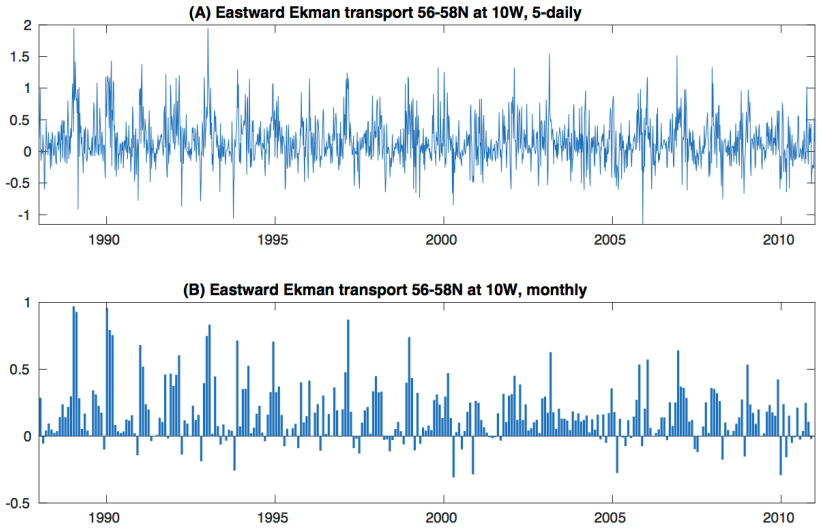

FIGURE 4.6: Time series of Ekman transport eastward total transport 10 °W, 56-58 °N, derived from ORCA12 poleward component of wind stress. (a) shows the data as a continuous time series from the 5-daily output, (b) provides monthly means provided as bars.

Figure 4.7 shows the relationship between eastward Ekman transport at the shelf edge with the total residence time on the shelf. The residence times presented here are the mean sum of residence times for each release year. Particles that went on and off the shelf and then back on were therefore recorded as their cumulative time on shelf, and then the ensemble mean of that was taken. However, particles that were not on the

shelf for 2 consecutive time steps (so 10 days) were not classed as residing. Particles that never made it on shelf were also excluded from the calculation. Particles that were originally residing on the shelf but then experienced a "coast crash" were counted as residing up until the point of hitting the coast or seabed, and then are considered "out of bounds". There is a very weakly correlated (statistically insignificant) declining trend of residence time with increasing eastward Ekman transport, with an R^2 value of just 0.02. As with increasing Slope Current transport, this might be due to increased flushing of particles from the shelf due to the increased transport.

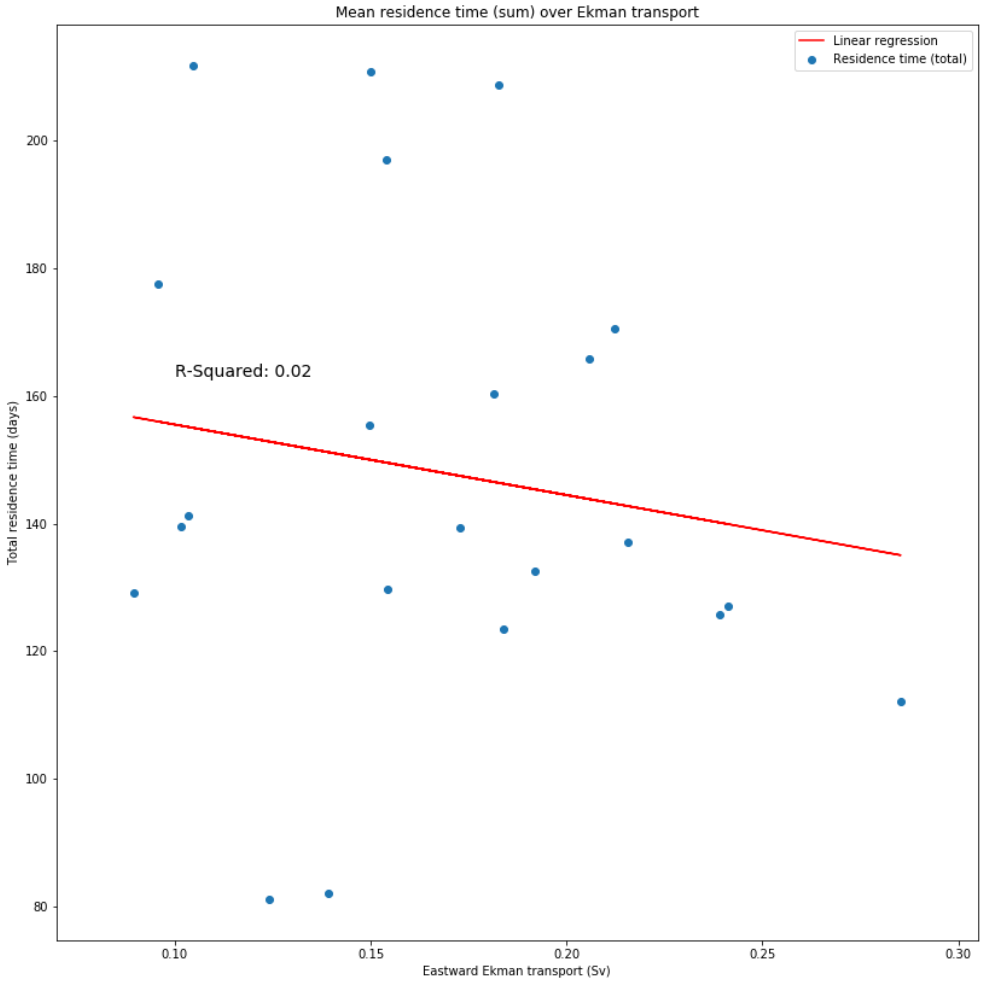

FIGURE 4.7: Scatter plot showing the relationship between annual mean residence time on the shelf and annual mean eastward Ekman transport, calculated at 10 °W, 56-58 °N. Annotated is the linear regression (R-squared value of 0.02).

The properties of particles crossing onto the shelf for the first time can tell us how Atlantic inputs to the shelf seas have changed over time and can further suggest forcing mechanisms. In Fig. 4.8, we see that the mean particle crossing latitude and longitude have consistently decreased over time, with some resurgence in 1996-7 and 2005-6. This means input to the shelf seas have shifted to the south west. The mean Atlantic inflow has also slowed (delayed arrival to the shelf) by approximately 4 days, with evidence that this slowing trend is ongoing and potentially accelerating from

2006 onwards. This reflects the previously observed changing inflow to the Slope Current caused by basin density changes (see Chapter 3.3.3, (Clark et al., 2022b)). Inflow salinity has been steadily decreasing, with a more rapid decrease of over 0.1 detected from 2007. There were no observable trends in inflow depth or temperature. This is most likely due to localised ocean-atmosphere (wind) interaction, which will help mix the water column, particularly on the shorter (daily to monthly) time periods. Salinity is a better conserved tracer even after water column mixing.

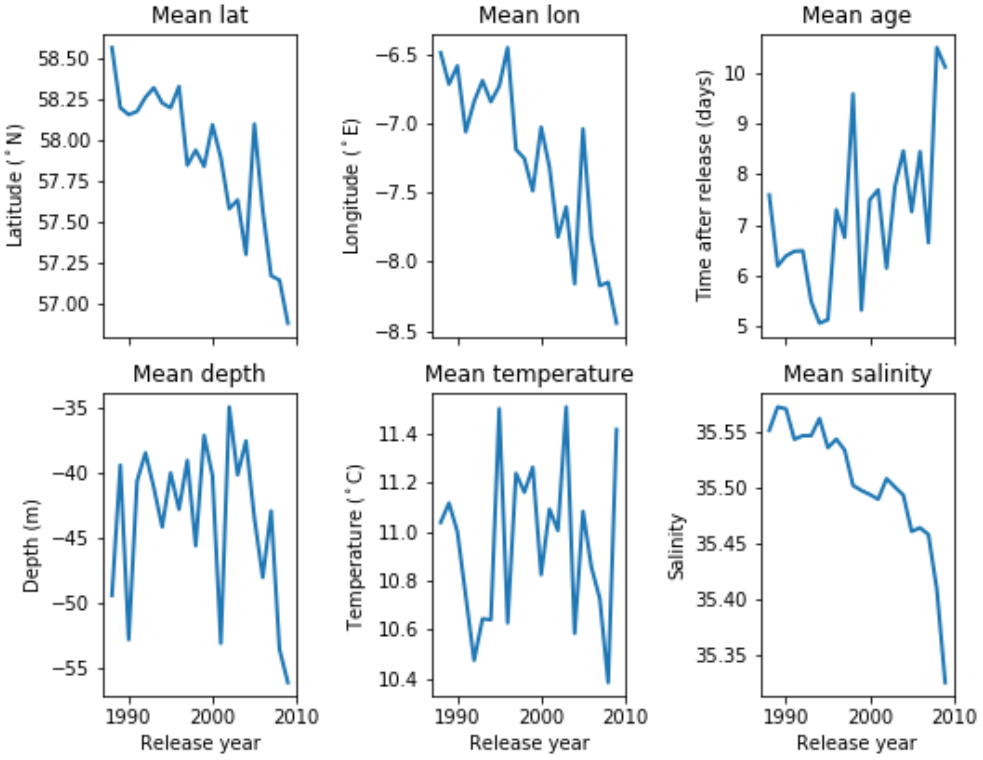

FIGURE 4.8: Time series of ensemble annual mean particle properties (longitude, latitude, age, depth, temperature and salinity) crossing onto the shelf for the first time.

Figure 4.9 reintroduces the European Slope Current northward transport (from Fig 8 in (Clark et al., 2022b), Ch. 4, at various sections along the shelf edge. Panel (a) is at 58 °N, just before the point at which the Slope Current turns and where a portion of the flow crosses the shelf and into the North Sea. It shows that the trend of total volume transport is declining. The trend appears to match the declines in latitude, longitude and salinity seen in Fig. 4.8. This suggests that there is indeed a strong link in the strength of the Slope Current and changing inputs to the shelf seas. This will be examined in more detail, through salinity as a tracer of Atlantic water going onto the shelf.

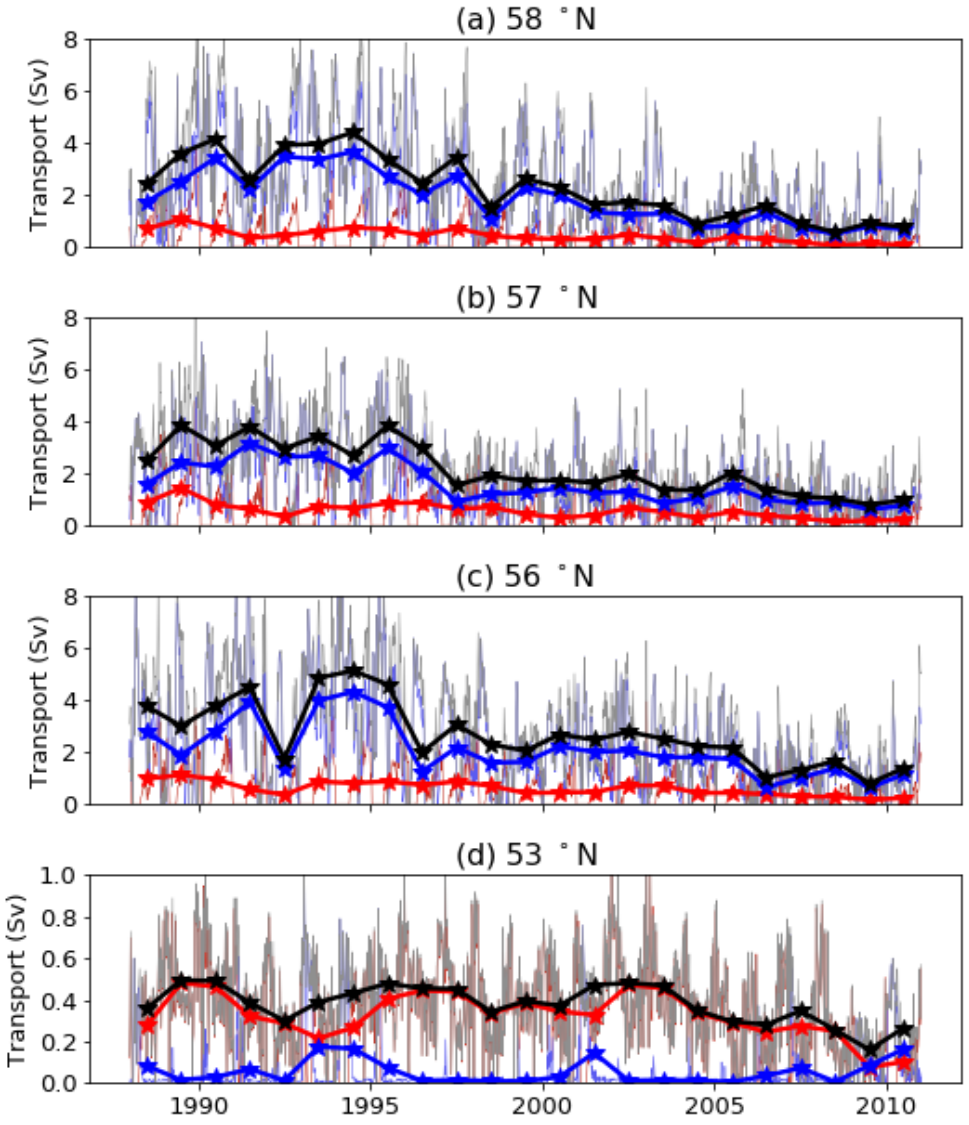

FIGURE 4.9: Slope Current northward transport at the shelf edge at 53, 56, 57 and 58°N (as Clark et al., 2022b, Fig. 8). Total transport is indicated with black lines. Transport at temperatures above and below 11°C is indicated with red and blue lines respectively. Thin lines show 5-daily means. Thick lines and stars indicate the annual mean.

4.3.3 Salinity as a proxy for Slope Current transport

The Slope Current has previously been characterised as an along-slope jet with a high salinity core. This, in theory, makes the Slope Current traceable along the shelf edge, and could help to distinguish when Slope Current waters are moved across onto the shelf. An elevated salinity signature in an otherwise relatively fresh North Sea should therefore be detected where Slope Current waters inflow. It has already been shown that salinity has been declining in waters arriving on the shelf (Fig. 4.8). Figure 4.10 shows the regional salinity in the northwestern North Sea (from EN4 dataset) plotted against the northward Slope Current transport as calculated in (Clark et al., 2022b)

(see Chapter 3.3.3. For comparison, the same region is plotted but with salinities from ORCA12 in Fig. 4.11. There are some major differences that are immediately apparent. In the first instance, the ORCA12 salinity values are higher than those of EN4. The range of salinity is also different: EN4 has a salinity range of approximately 0.5, whereas the ORCA12 is more constrained at only 0.25. The correlation between salinity and Slope Current transport is much stronger in ORCA12 (r^2 = 0.72) than EN4 (r^2 = 0.02). This is not surprising, as the transport calculations used ORCA12 velocities and EN4 is on a much coarser resolution. The 1 degree resolution of EN4 makes it likely that the fine scale of the Slope Current and it's associated inputs are lacking, despite the salinity values being most likely closer to observations, when and where these are available.

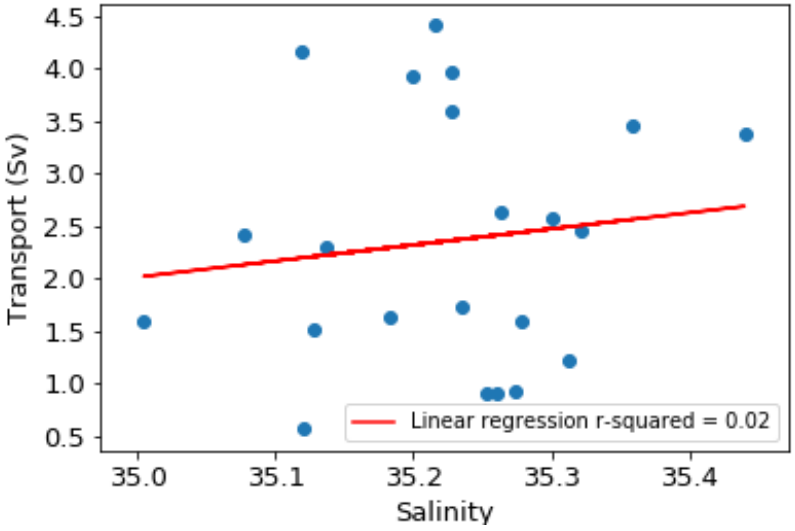

FIGURE 4.10: Scatter of annual mean regional salinity from the EN4 dataset against Slope Current northward transport. The region is 1°W to 1°E, 58 to 60°N, 40 - 50m.

Figure 4.12 presents the same data as time series: here we compare the Slope Current transport time series at 58 °N to time series of salinity in both the EN4 (blue) and ORCA12 (purple) datasets. Both salinity series show some similar trends from 1988 to 2001. The magnitude of salinity variability in EN4 and ORCA12 are completely different. EN4 shows much greater interannual variability of salinity than ORCA12, on the order of $\pm$0.2. EN4 salinity values are consistently lower than ORCA12 by at least 0.10. Comparing the salinity values to the volume transport of the SC, both EN4 and ORCA12 salinity seem to match the pattern of variability of transport up to the year 2000. After 2000, the time series diverge especially in the case of EN4 salinity values. Again, this is not necessarily surprising due to the SC transport was calculated using ORCA12 northward velocity. The interpolation of likely sparse hydrographic data presented in EN4 (on a 1 degree regular grid) is also likely to have affected these values. ORCA12 salinity better follows the variability of transport, tracing the general

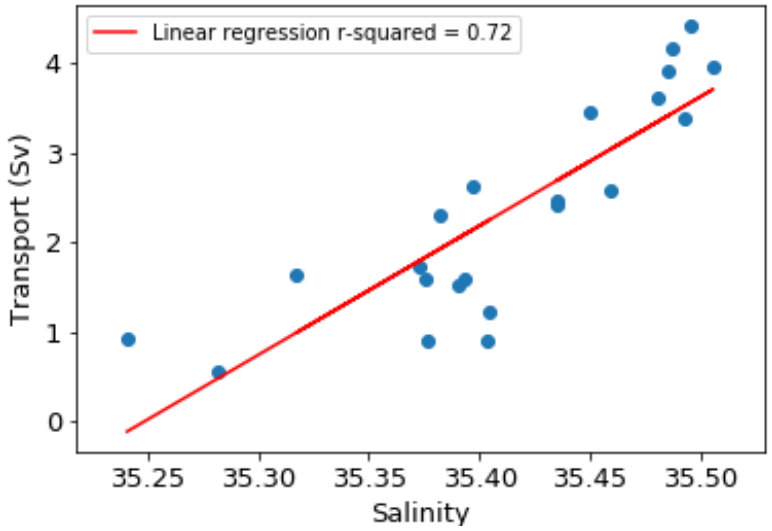

FIGURE 4.11: Scatter of annual mean regional salinity from the ORCA12 dataset over Slope Current northward transport. The region is 1°W to 1°E, 58 to 60°N, 40 - 50m.

decline in transport with a decline in salinity, albeit with a slight salinity increase from 2003-5, consistent with an associated reduced salt transport to the northern North Sea.

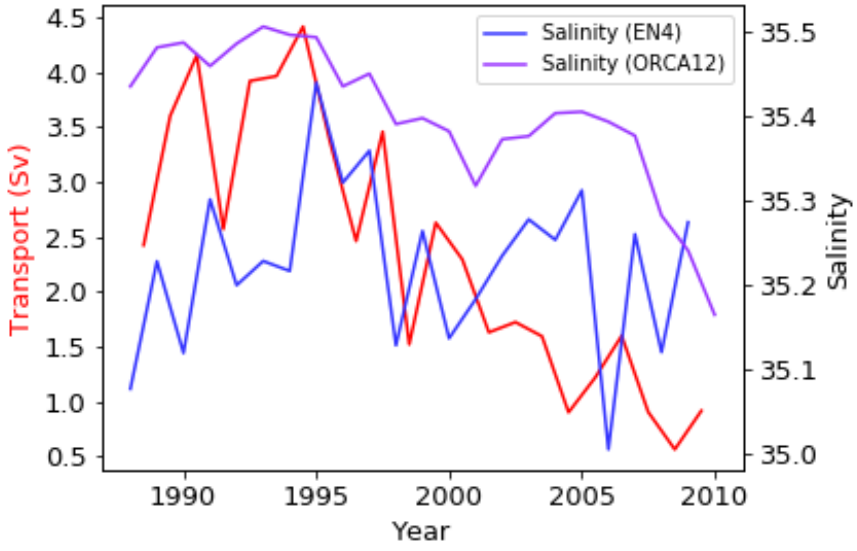

FIGURE 4.12: Time series of regional annual mean salinity from the EN4 dataset (blue) and ORCA12 model (purple), co-plotted with Slope Current northward transport at 58°N (red). The region is 1°W to 1°E, 58 to 60°N, 40 - 50m.

4.3.4 Reconstruction of Slope Current transport

By using the salinity-transport relationships in Fig. 4.11, we estimate the Slope Current transport back to the 1950s. The transport proxy has been adjusted for the

mean difference between ORCA12 and EN4 salinity values. Firstly, looking at the period between 1988 to 2000, the salinity-derived proxy reproduces the Slope Current transport well in both magnitude and variability. Post-2000, the proxy fails. Where there is a clear decline in Slope Current transport, the proxy suggests a slight increase until 2005, when the transport briefly collapses. The proxy suggests that from the mid 50s to 1980, there was a slight decline in overall transport but with large amount of inter-annual variability of ± 3 Sv. There are 2 periods of mean negative (southward) transport: in 1961-2 and in 1984-5. After 1985, the Slope Current shows a sustained recovery to it's mean northward flow, peaking at approximately 4.75 Sv in 1995.

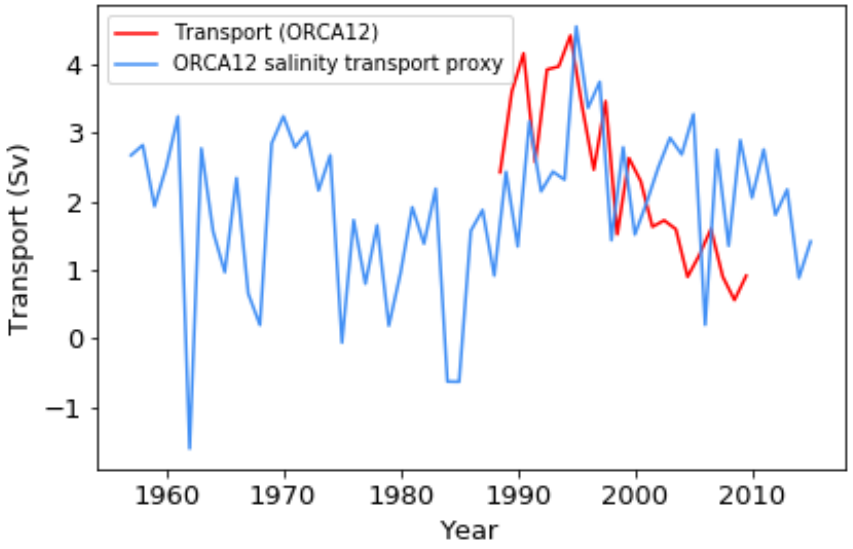

FIGURE 4.13: Reconstruction of Slope Current transport at 58 °N based on the salinity trend and correlation in ORCA12 from Fig. 4.11, adjusted for the difference between salinity values in EN4 and ORCA12.

4.4 Discussion

Here we summarise our findings and discuss the main trends and implications of the changing fate of the Slope Current. We discuss the changing transport at the shelf edge and relate these findings to the changing on-shelf and North Sea residence time of Atlantic water inflow. Finally, we discuss the consequences of these changes on the fate of Slope Current waters.

4.4.1 Changing localised transport at the shelf edge

We have shown that along-shelf transport at the shelf edge peaks at 1995 before declining (Fig. 4.9). The peak in northward transport corresponds to enhanced negative winter NAO index in 1994-5, with a lag of up to 1 year (Pingree, 2002). This

also correlates strongly with the previously observed changes of water influx to the Slope Current and shelf edge (Clark et al., 2022b). Peak cross-shelf exchange happens in the winter months (Fig 4.3), which suggests that cross-shelf exchange is dependant on strong enough flows to inertially "push" water onto the shelf, rather than be drawn on-shelf via stronger eastward Ekman transport (see below). If this assumption is correct, then the slowdown of the Slope Current could reduce the amount of water that makes it onto the shelf and into the North Sea. The exact mechanism of how Slope Current water is transferred onto the shelf remains unclear. Our Ekman calculation had no real correlation to shelf residence time (Fig. 4.7), suggesting that it is not a main driver of shelf edge exchange in this region. Porter et al. (2018) identified an "Atlantic Inflow Current" (AIC), with an abrupt change in the bathymetry at approximately 55.4 °N increasing shear, causing part of the SC to deflect onto the shelf. This is nearly 2 degrees further south of the cross-shelf exchange that we observed in Fig. 4.8. However, Porter et al. (2018) state that the AIC is not observed in models (they use the 7km resolution AMM7 model) but is traceable using drouged drifters and glider observations, which could explain why the AIC inflow does not appear to be captured in our results.

4.4.2 Increasing residence time of Slope Current water on-shelf and their consequences

Greater volumes of Atlantic water is reaching the shelf (Fig. 4.5) and the water that does is spending longer on-shelf than it used to (Figs. 4.4 and 4.7). This is significantly (yet weakly) correlated to the decrease of transport strength of the SC. This may be due to weaker and slower flow, meaning the SC waters are not as actively flushed from the shelf seas.

The changing provenance of the Slope Current has had a direct impact on the fate of the Slope Current, especially when it comes to shelf edge exchange and inputs to the North Sea. We have demonstrated that the slowdown of the Slope Current has increased the residence time of Atlantic water on the European Shelf. Upwelling systems along the eastern Atlantic boundary (Varela et al., 2018) provide nutrients at the shelf edge, which the Slope Current helps to convey. The same wind stress and Ekman processes that have been found to deflect the Slope Current onto the shelf have aided nutrient upwelling and mixing of waters on the shelf (Porter et al., 2018). Another source of nutrient inputs are from terrestrial sources, conveyed through rivers and estuaries (Vermaat et al., 2008). This may include anthropogenic nutrient inputs such as agricultural fertiliser run-off, though this is thought to be decreasing in the North Sea (Vermaat et al., 2008). Clearly, any future attempts to quantify nutrient inputs to the North Sea from the North Atlantic via the Slope Current will need to consider this.

4.5 Conclusions

We have confirmed that the changing provenance of the European Slope Current, as observed in our previous study (Clark et al., 2022b), does indeed lead to a changing fate of the same waters. The overall Slope Current volume transport has been steadily reducing. It remains highly seasonal, which in turn forces the seasonality of the cross-shelf exchange. Cross-shelf exchange remains lowest in the summer months, consistent with lower wind forcing at the shelf edge and reduced temperature and density gradients hence weaker Slope Current transport. There is no discernible trend in wind-driven Ekman transport at the shelf edge. Additionally, it has a surprisingly limited effect on the residence time of particles crossing onto the shelf from the Slope Current. The mechanisms behind how Slope Current water diverges onto the European shelf remain unclear. Inflow to the shelf seas has become from a more southwesterly origin, with our analysis showing an inflow at 57 °N, 8.5 °W, with a rapidly freshening salinity signature. The freshening signature is likely down to lessened Atlantic inflow. However, the relationship between salinity signature of the northern North Sea and the inflow of the Slope Current was not as strong as expected in the EN4 dataset. There appears to be a very strong relationship between ORCA12 salinity and the Slope Current transport. This is expected to have been biased since the transport calculation utilised ORCA12 velocity. A transport proxy based from ORCA12 salinity, corrected for bias with EN4, has accurately reproduced the trend and magnitude of the calculated Slope Current northward transport between 1988 and 2000. Whilst the relationship does appear to collapse after 2000, it opens up the possibility to use longer-term salinity measurements in the North Sea to potentially reconstruct the Slope Current. The changing fate of the Slope Current has implications on nutrient inputs from the Atlantic eastern boundary upwelling zones and cycling/utilisation whilst in the North Sea, which will be explored in the following Chapter 5.

Chapter 5

Biogeochemical consequences of changing Slope Current transport in the northern North Sea.

Abstract: The Slope Current has slowed on the order of 5 Sv since a major subpolar warming event in the late 1990s. Despite this, warmer and more saline water from the North Atlantic basin is drawn via the Slope Current to the shelf edge, across the slope and into the North Sea. This Atlantic inflow provides a variable flux of key nutrients such as dissolved inorganic nitrate (DIN). By using a shelf seas biogeochemistry model with three proxies for surface DIN flux into the North Sea, we find that net primary production in the northern North Sea is decreasing with the declining Atlantic inflow. The phytoplankton primary production in the autumn bloom has decreased by at least 50% in the year following the subpolar Atlantic warming event, and the declining trend in productivity has continued but at a lessened rate. This in turn is affecting the distribution of various fish and zooplankton species. The warming of the subpolar North Atlantic has increased the number of "warm-water" species being able to survive in previously "too cold" water. This subtropicalization of the ecosystem is not captured in the model, so it is likely that our results are only part of what is really occurring. By comparing and combining shelf sea biogeochemistry models with observations from previous studies, we determine how the changing physical environment and nutrient flux from the Atlantic is affecting the local ecosystem response.

5.1 Introduction

The northwest European shelf edge and shelf seas are highly dynamic, and respond on daily, monthly and seasonal timescales to wind and other surface ocean forcing

(see Chapter 1.2). They are also sensitive to longer-term changes in circulation in the wider North Atlantic basin. The along-slope European Slope Current is located at an interface between the Atlantic waters and the shelf waters and provides a conduit for North Atlantic influence over the current and shelf seas (Clark et al., 2022b). The Slope Current is at times deflected onto the shelf (Porter et al., 2018), and into the North Sea (see Ch. 4 and Marsh et al. (2017)). Here, we provide a summary of the physical changes to the North Atlantic, shelf edge transport and associated Atlantic inflow to the North Sea. We then relate these physical changes to previously observed patterns of nutrient and ecosystem variability.

5.1.1 The warming shelf seas and changing Atlantic inputs

As the North Atlantic has warmed over the past decades, so too have the shelf seas. The Northwest European shelf seas have been particularly sensitive to this due to the shelf edge currents moving warmer Atlantic water northward and, at times, across onto the shelf. With the warming Atlantic over the past few decades, the changes in the meridional density gradients and circulation of the subpolar gyre has acted to reduce the geostrophic inflow to the Slope Current, thus reducing the poleward transport of the Slope Current (Clark et al., 2022b). This has had implications for cross-shelf exchange.

The rapidly changing bathymetry at the shelf edge is one mechanism for Slope Current water making it onto the shelf (Porter et al., 2016b). Porter et al. (2016b) found that seasonal fluctuations in Slope Current strength and direction is strongly linked to cross shelf exchange of nutrient-rich waters. The associated inflow via this mechanism has been estimated to contribute 0.2 Sv of Atlantic water to the shelf and North Sea (Porter et al., 2018). The abrupt changes in bathymetry at the Goban Spur combined with seasonal summer flow reversal also leads to cross-shelf exchange (Pingree et al., 1999).

5.1.2 Shifting patterns of ecology and nutrients

Many previous studies have identified a shift of various pelagic and benthic species in the shelf seas over the past >50 years (Hátún et al., 2009; Beaugrand et al., 2009; Beaugrand and Reid, 2003). The term "subtropicalization" is frequently used to describe these changing as the act of replacing local temperate species with species that originate from more subtropical and tropical waters. This is occuring across all trophic levels: from the plankton to the megafauna. Two main potential drivers to make these changes occur have been previously identified.

The main driver is the warming water itself, which in the North Sea can vary with changing Atlantic inflow (Reid et al., 2003). As the water warms, the species that reside in the region find it difficult to survive, either due to their bodies not being to cope, or their breeding strategy does not allow for warmer temperatures (eg: eggs won't survive or conditions aren't right for migration/dispersal) (O'Connor et al., 2007). Warmer water is also less able to store dissolved oxygen (O_2), which inhibits respiration in all marine organisms (Beaugrand et al., 2008). The Continuous Plankton Recorder (CPR) survey, now managed by the Marine Biological Association (MBA), has provided a nearly 60 year record of phytoplankton and zooplankton distribution in the North Atlantic and surrounding shelf seas (see the CPR survey website at `https://www.cprsurvey.org/` for historical context, sampling areas and up-to-date CPR data. The CPR device is towed behind voluntary "ships of opportunity" and then returned to the MBA for analysis along with the shipping GPS logs (Batten et al., 2003; Warner and Hays, 1994; Hays and Warner, 1993). The CPR record has revealed a changing distribution of plankton since the 1950's associated with the long-term warming trend of the North Atlantic basin.

In the North Atlantic basin, the warming is changing the distribution of native species. Krill, a pelagic crustacean that forms a key part in the food chain for many commercially important species, have seen their range decline by 50% as the temperature has limited the area in which they can survive (Edwards et al., 2021). Similar trends have been observed on the shelf and in the North Sea. A warming trend observed from 1988 linked to a positive North Atlantic Oscillation (NAO) anomaly showed a strong migration of plankton in the CPR record northeast onto the shelf and into the North Sea (Reid et al., 2001a). This corresponded to an increase in horse mackerel catch by commercial fishing (Reid et al., 2001a).

The other driver of ecological change and variability is changes in nutrient distribution. As circulation patterns in the North Atlantic and North Sea have changed, so too has the distribution of nutrients. Atlantic inflow remains the dominant source of nutrients in the North Sea, with seabed flux being second, followed by terrestrial (run-off entering via rivers) and anthropogenic sources (Vermaat et al., 2008; Brion et al., 2004). The shelf edge vertical mixing provides key upwelling of subpycnocline nutrients to the surface waters (Mathis et al., 2019), which can then be advected into the North Sea. Along the northwestern boundary of the Atlantic are a series of upwelling zones. The most notable ones are in the Iberian Peninsular and the Canary Current (Varela et al., 2018). Warming of the oceans has reduced winter convection, limiting the upwelling of key nutrients and thus expected to limit North Atlantic plankton blooms (Hátún et al., 2021). This also raises the likelihood of lessened primary production in the North Sea, through declining Atlantic nutrient flux via the Slope Current.

5.2 Datasets and methods

This work builds on the results from Chapters 3 and 4 to relate the changing shelf edge physical dynamics to a biogeochemical response. We use a 1D shelf seas primary production model, to assess how the warming Atlantic and decreasing Slope Current inflow to the North Sea is effecting net primary production in the northern North Sea.

5.2.1 Lagrangian metrics for shelf edge exchange and associated nutrient flux

In Chapter 3 (Clark et al., 2022b), we present the results of two Lagrangian Ariane hindcast experiments which aimed to assess the changing provenance of waters arriving at the shelf edge. The first was run for 1992 to 1988 hindcast, the second was 2010 to 2006 hindcast. These experiments captured an increased time taken to get to the shelf edge. The shelf edge inflow has also warmed by 1 °C and become shallower by approximately 20m. A corresponding decrease of the shelf edge northward transport (of 2 Sv at 58 °N) was observed at 4 latitudes (Fig. 3.8), capturing a decrease of the Slope Current transport. Chapter 4 builds on this work by running 22 Ariane forecast experiments to quantify the changing destination of Slope Current waters. We found that the amount of particles getting onto the shelf was highly seasonal, with more particles getting onto the shelf in the winter months than in the summer months. The inflow to the shelf is shifting to the southwest. Residence time of those particles showed a negative correlation with increasing Slope Current transport. We use these findings to inform forcing of the shelf sea biogeochemistry model, as discussed next.

5.2.2 1D S2P3 shelf seas primary production model

A shelf seas coupled physics and primary production "S2P3" model was used to assess the effects of changing Atlantic input to the northern North Sea. First developed in Sharples (1999), it has since been updated in Simpson and Sharples (2012) and this updated version has been used in this work - please see those works for details of model parameters and calculations. The S2P3 model requires forcing with a set dissolved inorganic nitrate (DIN) flux, both from the seabed and from the surface, for each year. The seabed flux has been set as a constant across all model runs at 2.64 mmol m^{-2} d^{-1}. This value has been chosen as representative for the northern North Sea, based on work by Vermaat et al. (2008). Surface DIN fluxes into the northern North Sea vary with Atlantic inflow, as well as from terrestrial sources. Under the assumption that the main DIN input occurs from Atlantic inflow, three annual mean proxies have been tested: one based on northward transport of the Slope Current at 58 °N, another based on the number of particles on shelf and a third based on salinity of

the Atlantic inflow from the Slope Current to the North Sea (see Table 5.1 for all proxy DIN values, and Fig. 5.1 for a graphical representation). This develops on work already done Irene Ma for her Masters dissertation (Ma, 2022).

In order to produce a DIN proxy based on the salinity of inflow, salinity values from the northern North Sea (from the EN4 dataset) were regressed against the northward transport of the Slope Current at the shelf edge (at 58 °N) using a simple linear regression (form $y = mx + c$), with an adjustment value based on the mean difference between ORCA12 salinity (since ORCA12 was used to analyse Slope Current transport and cross-shelf exchange) and EN4 salinity:

$$Transport_{EN4Proxy} = (10.009 \times (EN4_{salinity} + 0.1877417)) - 352.0593 \quad (5.1)$$

The EN4 transport was then scaled by 1995 (as with the other proxies) to obtain a annual mean DIN flux estimate. The salinity-derived proxy shows less annual variation in DIN flux, as the salinity values themselves show less inter-annual variability than the other parameters. The model was run from 1988 to 2009, once per DIN proxy, for 1 °W, 58 °N. This location was chosen to capture the inflow from the Orkney-Shetland Channel: one of the main inflow pathways (Winther and Johannessen, 2006).

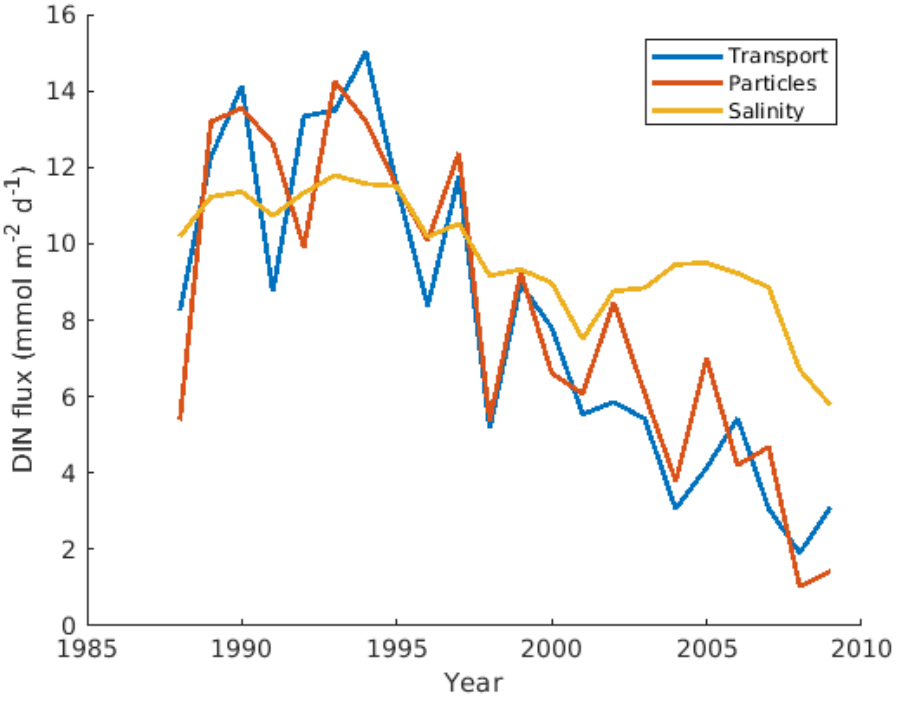

FIGURE 5.1: Time series of the DIN fluxes associated with Atlantic inflow derived from each of the proxy values as listed in Table 5.1. Each line colour indicated a different DIN flux proxy: blue for transport-derived proxy, orange for particle on shelf derived proxy, and yellow for salinity-derived proxy.

The model uses M2, S2 and N2 tidal constituents for the chosen location. It also utilises daily meteorological forcing with values of wind velocity, cloud cover, air temperature and relative humidity. The biological component of the model actively responds to the physical and meteorological forcing. For example, the model utilises the cloud cover values to provide light available for photosynthesis (and therefore primary production). Nitrogen is utilised by phytoplankton cells in proportion to the available DIN. Biological grazing of phytoplankton is also simulated, with 50 percent of organic nitrate going back into the water column.

5.3 Results and Discussion

Here we show the results of the S2P3 simulations, and relate them to real-world observations. We quantify the the effects of variable Atlantic influences on nutrients and ecology in the northern North Sea in terms of the varying DIN and chlorophyll signatures present.

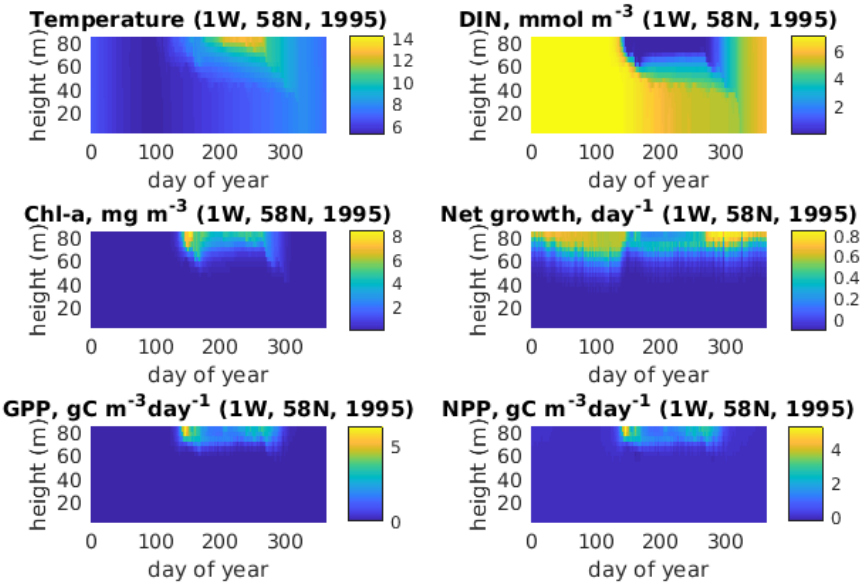

FIGURE 5.2: Hovmuller plot of daily output for the 1995 run of the S2P3 model, at 1 °W, 58 °N, for the 6 output values: temperature, dissolved inorganic nitrate (DIN), chlorophyll-α, net growth, gross primary production (GPP) and net primary production (NPP). Note that the y axis is height in meters above the seabed.

The S2P3 was forced by variable surface DIN rates derived from 3 different proxies (see section 5.2.2 for the model run information, and Table 5.1 for DIN values used). All the proxy DIN rates were scaled by 1995, which was given a constant DIN rate of 11.5 mmol m^{-2} d^{-1} based on the work by Ma (2022): based on a mean Faroe-Shetland Current flow to represent Atlantic inflow to the northern North Sea (Ma, 2022). Figure 5.2 shows the S2P3 output of the 1995 run. The output is daily and is presented as

YEAR	Nward transp. (Sv)	Scale	DIN rate	On shelf #	Scale	DIN rate	Salinity	Proxy Transp. (Sv)	Scale	DIN rate
1988	2.424	0.717	8.242	1169.86	0.467	5.369	35.4352	4.491	0.885	10.182
1989	3.604	1.066	12.255	2874.45	1.147	13.191	35.4812	4.951	0.976	11.225
1990	4.157	1.229	14.135	2951.41	1.178	13.544	35.487	5.009	0.988	11.357
1991	2.571	0.760	8.742	2751.79	1.098	12.628	35.4592	4.731	0.933	10.726
1992	3.922	1.160	13.336	2158.59	0.861	9.906	35.4858	4.997	0.985	11.330
1993	3.966	1.173	13.486	3103.75	1.239	14.243	35.506	5.199	1.025	11.788
1994	4.418	1.306	15.023	2877.45	1.148	13.205	35.4962	5.101	1.006	11.566
1995	**3.382**	**1.000**	**11.500**	**2505.98**	**1.000**	**11.500**	**35.4933**	**5.072**	**1.000**	**11.500**
1996	2.462	0.728	8.372	2196.33	0.876	10.079	35.4351	4.490	0.885	10.179
1997	3.459	1.023	11.762	2696.93	1.076	12.376	35.4502	4.641	0.915	10.522
1998	1.519	0.449	5.165	1171.87	0.468	5.378	35.3904	4.042	0.797	9.165
1999	2.629	0.777	8.940	2015.64	0.804	9.250	35.3975	4.113	0.811	9.326
2000	2.294	0.678	7.800	1439.22	0.574	6.605	35.382	3.958	0.780	8.974
2001	1.629	0.482	5.539	1323.49	0.528	6.074	35.3173	3.311	0.653	7.506
2002	1.722	0.509	5.855	1844.07	0.736	8.462	35.3725	3.863	0.762	8.759
2003	1.593	0.471	5.417	1325.5	0.529	6.083	35.3761	3.899	0.769	8.840
2004	0.899	0.266	3.057	826.387	0.330	3.792	35.4033	4.171	0.822	9.458
2005	1.216	0.360	4.135	1523.65	0.608	6.992	35.405	4.188	0.826	9.496
2006	1.598	0.473	5.434	915.308	0.365	4.200	35.3932	4.070	0.802	9.228
2007	0.902	0.267	3.067	1020.49	0.407	4.683	35.3767	3.905	0.770	8.854
2008	0.561	0.166	1.908	224.866	0.090	1.032	35.2821	2.958	0.583	6.707
2009	0.914	0.270	3.108	309.381	0.123	1.420	35.2406	2.543	0.501	5.766

TABLE 5.1: Annual mean DIN input flux proxies (in mmol m^{-2} d^{-1})to the northern North Sea based on annual mean northward Slope Current at 58 °N, number of particles on shelf, and a transport proxy based on inflow salinity . All indices are scaled by 1995, at a constant 11.5 mmol m^{-2} d^{-1}, based on the work by Ma (2022).

values at height above the seabed. Because the model incorporates meteorological forcing, the temperature panel shows a well-mixed profile for the first 100 days, before gradually becoming more stratified. In this location, the tidal forcing is sufficiently weak (and the depth is sufficiently deep) that positive net heat flux in spring and summer can stratify the water column effectively. This stratification holds phytoplankton in the warm surface layers that form the photic zone, providing optimal light conditions for growth. The surface waters begin to warm at approximately day 120. Stratification peaks between days 200 and 275, before being mixed away. Beyond day 300, the water column becomes fully mixed once again. Temperature is not the only value to show stratification. DIN shows a strong inverse relationship with temperature stratification, indicating that the distribution and variability of DIN is linked. Chl-α is an indicator of phytoplankton presence. It is also stratified in what begins as the "spring bloom" at approximately day 120, where the chlorophyll goes from near 0 mg m^{-3} to a peak of 8 mg m^{-3} in only a few days. The signature persists in the upper 20 m of the water column. This follows a corresponding drop of DIN, which the phytoplankton utilise in order to bloom. When the stratification breaks down, the chlorophyll signature (and hence the phytoplankton) are mixed through the water column. This is evident after day 275, where the chl-α signature breaks goes below the 20 m surface layer threshold. Net growth is the rate of phytoplankton growth, proportional to the local biomass (high in winter, but when phytoplankton levels are low). The net growth is at a minimum in the surface waters where DIN is exhausted. GPP and NPP are gross and net primary production respectively, net being GPP minus the rate of energy loss due to respiration and metabolism (carbon fixation). They show very similar time and depth profiles, but of course NPP is always lower than GPP. These values are highest at the point the spring bloom starts, and are at or near 0 when the water column is well-mixed. They are also concentrated in the upper 10 to 20m of water. There is no growth (hence no NPP) between the seabed and 40m, despite maximum concentration of DIN being present. This is due to the DIN being inaccessible and unusable for phytoplankton, as it is outside the photic zone.

The following subsections focus on the changing nutrient fluxes from the subpolar North Atlantic. Chlorophyll concentrations and a model estimate of NPP are used to quantify the biogeochemical effects of changing Slope Current inputs. Finally, we discuss the wider implications for the simulated changes to nutrient fluxes from the Atlantic.

5.3.1 Net primary production under variable nutrient fluxes

Chlorophyll concentration and the corresponding net primary production signatures are important markers for biological activity. By using the S2P3 model, we can look at

the effects of changing nutrient flux from the Atlantic into the northern North Sea. By using the three different proxies for tracing Atlantic inputs to the northern North Sea, we can identify the effects of the observed slowdown of the European Slope Current.

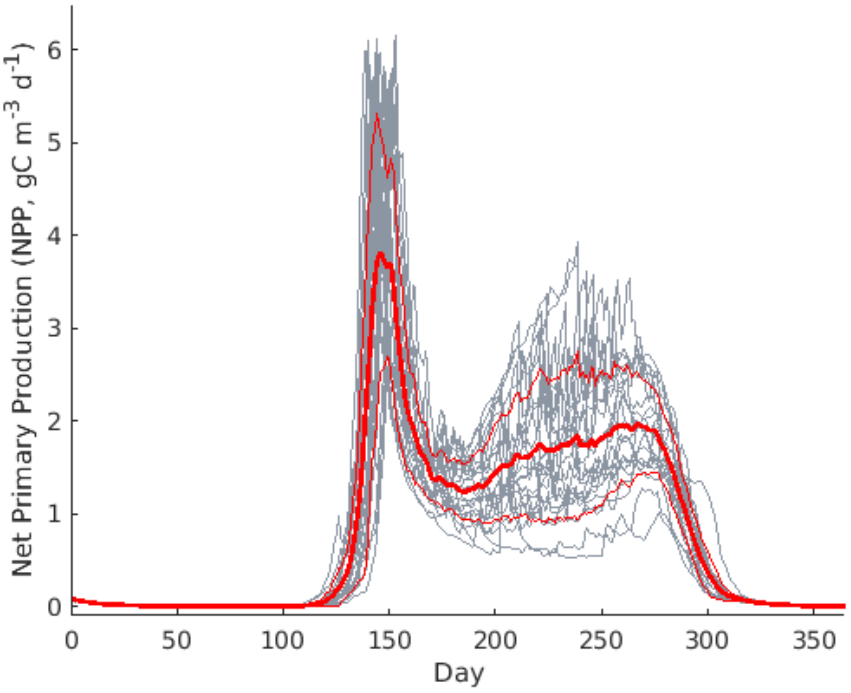

FIGURE 5.3: Surface values of net primary production (NPP) over each model run year, obtained using the particles on shelf DIN flux proxy. Grey lines represent the 22 model runs (1988 - 2009). The thick red line is the ensemble mean of the runs, with the thin red lines indicating $\pm$ standard deviation.

Figure 5.3 shows surface NPP values for the 22 model runs, using the particle proxy, with Fig. 5.4 showing the corresponding surface Chl-α values. Surface values have been chosen to best reflect production and is more comparable with previous observations (from satellites or Continuous Plankton Recorder survey). However, we acknowledge that sub-surface production and Chl-α is also important in the summer and may be variously affected by changing surface level nutrient fluxes. The spring bloom is clearly identified as the sudden peak of NPP and Chl-α starting from day 120. There is approximately 20 days variability in the start of the spring bloom in the model runs. The peak of the spring bloom occurs just before 150 days, but again there is 20 days variability in the peak timing, most likely dependent on the meteorological conditions prevailing in the run-up to the bloom. The peak vale of both NPP and Chl-α is extremely variable. The peak mean NPP is 3.8 gC m^{-3} d^{-1}, with approximately 1.7 m^{-3} d^{-1} standard deviation. For Chl-α, the peak mean is 8.3 mg m^{-3}, with approximately 0.8 mg m^{-3} standard deviation. After the peak of the bloom, NPP decreases rapidly to a mean (and temporary minima) of 1.2 gC m^{-3} d^{-1} in the space of 30-40 days (on day 190) before beginning to rise again. Chl-α also does show a mean decline over this time period, but does not reach a temporary minima. Instead,

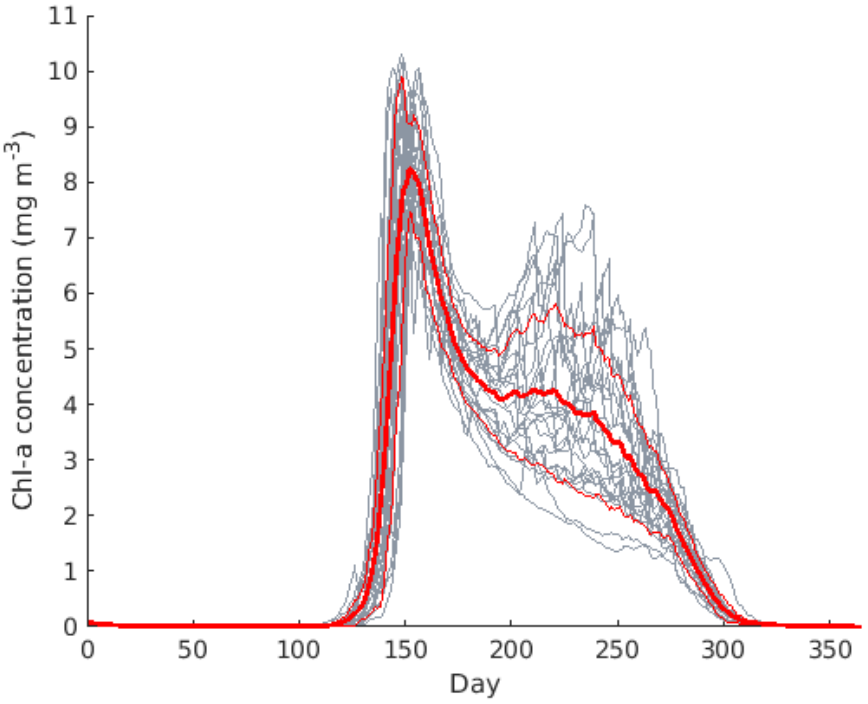

FIGURE 5.4: Surface values of chlorophyll-α over each model run year, obtained using the particles on shelf DIN flux proxy. Grey lines represent the 22 model runs (1988 - 2009). The thick red line is the ensemble mean of the runs, with the thin red lines indicating $\pm$ standard deviation.

the rate of decline slows to almost nothing before continuing to decline as an increasing rate from day 230. The timing of this NPP decline and minima at day 170 matches a deepening of the surface DIN minima seen in Fig 5.2, which extends 20 m down through the water column. As DIN is not as available, growth (NPP) slows until it can be sustained once again by any remaining DIN. From day 170 onwards, mean surface NPP increases once again, but does not reach the levels seen at the start of the bloom. However, it does reach a new mean peak at day 270 of 1.9 gC m^{-3} d^{-1}. Between the minima at day 190 and the second NPP mean peak at day 270, there is an increasing trend of NPP. This second bloom shows highly variable NPP rates between the different model runs, with an increasing standard deviation. Whilst the mean of chl-α shows a declining trend for the same temporal range (the second bloom period), there are many years showing an increase. At no year does the second chlorophyll peak exceed the first. After the second peak of NPP at day 270, NPP rapidly declines back to near-zero in 30 days (by day 300). Chl-α also follows the same decline back to near-0. The declines in NPP and Chl-α are a result of the breakdown of stratification and remixing of the water column. Whilst more DIN is available for growth, any phytoplankton are mixed away from the photic zone (since they are no longer held in place by thermohaline stratification) so are unable to utilise the available nutrients.

Annual means of surface NPP and chl-α are presented in Fig. 5.5. A clear declining

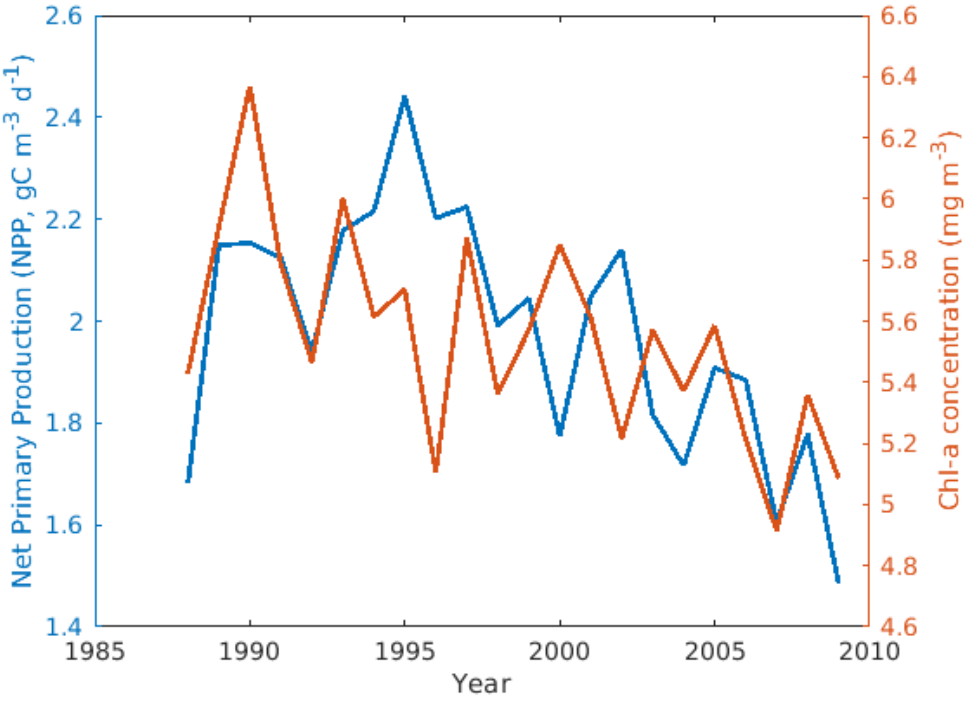

FIGURE 5.5: Time series of annual mean surface net primary production (left y axis, blue) and chlorophyll-α (right y axis, orange), obtained using the particles on shelf DIN flux proxy.

trend of both NPP and chl-α are observed. In both time series, high inter-annual variability is present. From 1988 to 1993, peaks of NPP match with peaks of chl-α. This relationship breaks down between 1994 to 2005 to an opposite mode: when there is a peak of NPP, there is a trough of chl-α. A possible explanation for the lack of direct correlation is that peak chl-α is a consequence of the time integral of NPP. This means that a short-lived but high peak in NPP may result in only a modest chl-α peak, whereas a high chl-α peak may be the result of sustained NPP but at a modest level. The overall declining trend in both indices matches the profile of decline of Slope Current transport observed in Chapters 3 (Clark et al., 2022b) and 4. This is not surprising, as the DIN flux used to force the S2P3 model in this instance were based on particles from the Slope Current making it onto the shelf and the majority entering into the North Sea. Figure 5.5 therefore confirms that the slowdown of the Slope Current is indeed affecting the ecological response of the northern North Sea. As Slope Current transport declines, less water makes it onto the shelf and brings less nutrients into the North Sea, thus causing a corresponding decline in NPP.

We will now look at the other DIN flux proxies used to force the ecosystem model. Salinity of the North Sea was used in Ch. 4 to trace Atlantic inflow. Figure 5.6 shows daily output NPP values and Fig. 5.7 shows chl-α output for the salinity DIN proxy. The overall mean trends in both values are similar to the particle proxy as presented in Figs. 5.3 and 5.4, yet the magnitude of the mean peaks (thick red lines) is slightly

higher. There is also less variation in the different experiment years in the second bloom. This may be a feature of the lack of variation of the salinity values used to create the DIN proxy. Whilst there is a declining trend of salinity, the decline is fairly constant without much interannual variability.

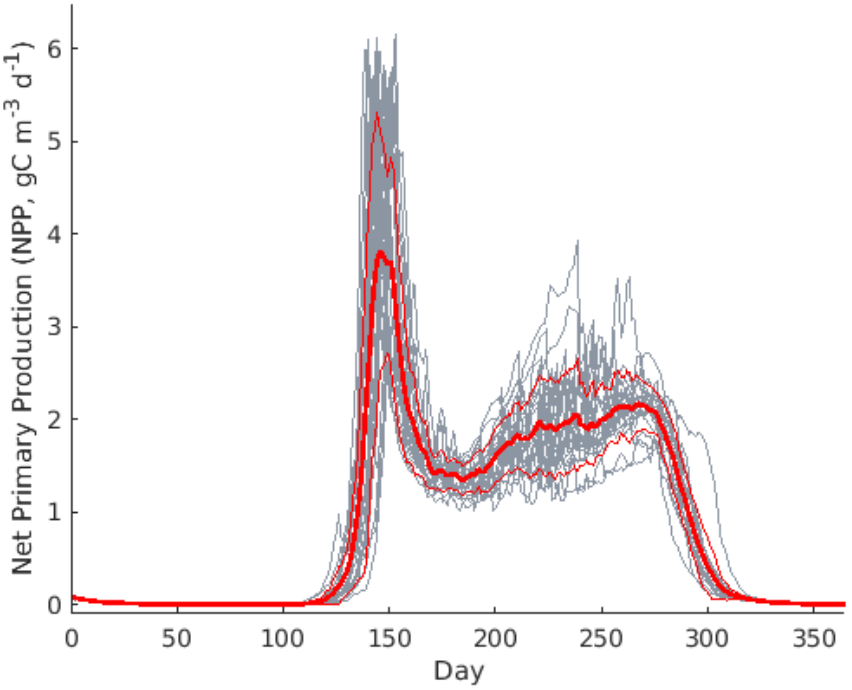

FIGURE 5.6: Surface values of net primary production (NPP) over each model run year, obtained using the salinity DIN flux proxy. Grey lines represent the 22 model runs (1988 - 2009). The thick red line is the ensemble mean of the runs, with the thin red lines indicating ± standard deviation.

Looking at NPP and chl-α annual mean time series from the salinity proxy forced model (Fig. 5.8), we see that the the trend is very different to the time series seen in the particles on shelf proxy presented in Fig. 5.5. The salinity based DIN proxy was derived from a shelf edge transport proxy first developed in Ch. 4.3.4 (see Fig. 4.13. This proxy accurately recreates transport from 1988 to 2000, but after that the regression breaks down. This may factor into why the declining trend from the year 2000 is largely missing from this salinity-derived DIN proxy model simulation.

The final proxy was based on northward transport of the Slope Current at 58 °N, using the transport data presented in Fig. 3.8a, Ch. 3.

The time series of NPP and chl-α for the transport proxy (Fig. 5.11) looks very similar to the particles on shelf proxy. This was to be expected, as particles making it onto the shelf has been shown to be strongly influenced by the strength of Slope Current transport (see Ch. 4.3). There is no material change to the mean peak timing or magnitude of either bloom, however there appears to be slightly more variability in the second bloom when using the particle proxy.

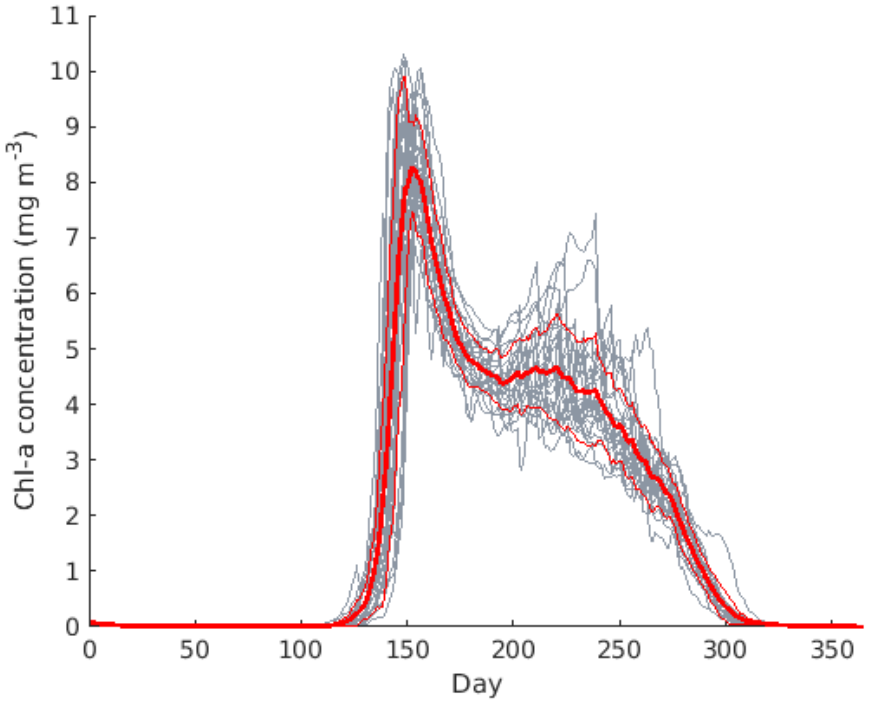

FIGURE 5.7: Surface values of chlorophyll-α over each model run year, obtained using the salinity DIN flux proxy. Grey lines represent the 22 model runs (1988 - 2009). The thick red line is the ensemble mean of the runs, with the thin red lines indicating $\pm$ standard deviation.

Using the time series of DIN flux values from the 3 proxies as shown in Fig. 5.1, we now examine the variability of chlorophyll and NPP throughout the water column between the highest (1995) and lowest (2007) DIN flux years. Figure 5.12 plots the daily output from the S2P3 model for 1995 and 2007 for the two values, over the height above the seabed. The evolution of the spring and autumn blooms can clearly be seen in both years. As expected, surface manifestation of both blooms is strong, however the signatures do penetrate up to 40m into the water column in the case of chlorophyll, 30m for NPP. The initial spring bloom provides the highest DIN and chl-α values, as expected. The initial spring blooms approximately at day 150 are of similar magnitude in both years, confirming our previous analysis. This bloom occurs in the upper 20-25m, and extends slightly deeper when the DIN inflow is weaker (2007). Peak chl-α and NPP rapidly reduces within the space of a month to a more background value of <6 mg m^{-3} level of chl-α and <3 gC m^{-3} day^{-1} NPP. In 2007, there is limited evidence of a second bloom peak. Instead, chl-α and NPP gradually decline over the next 100 days, with a very slight increase in NPP at approximately day 250, which ends just before day 300. Chlorophyll concentration does not show an increase over the same period. Instead, the chl-α signature is mixed deeper (to 70m above the seabed), indicating the start of the breakdown of seasonal thermohaline stratification. In 1995, there is a clear but weaker second (autumn) bloom seen in the both values. After day 200, both chl-α and NPP begin to increase once again, peaking at 6 mg m^{-3} chl-α, 3.5

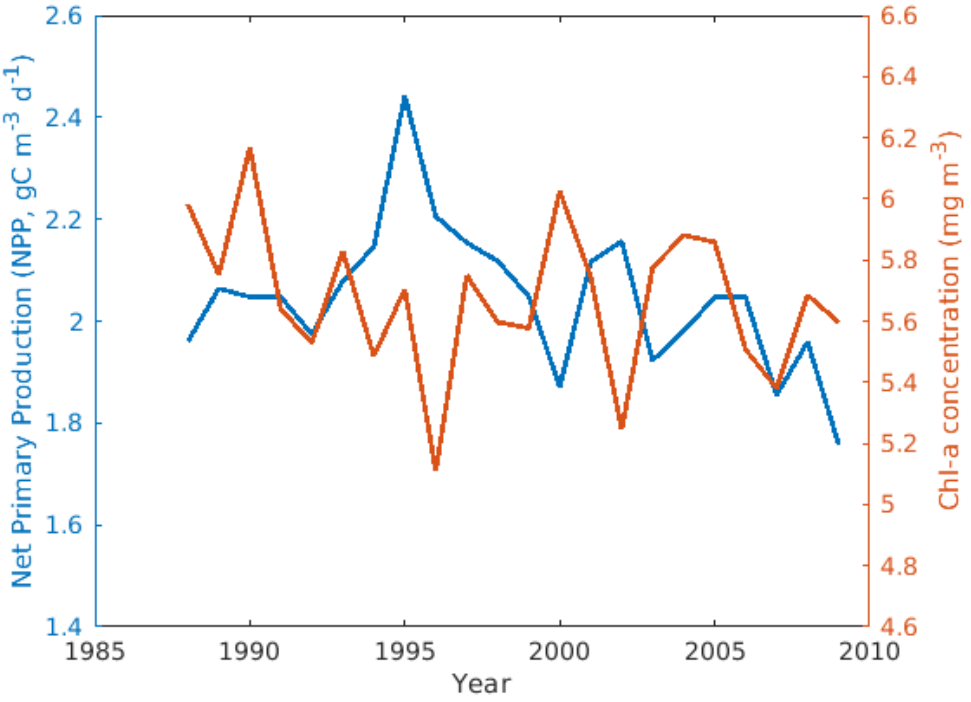

FIGURE 5.8: Time series of annual mean surface net primary production (left y axis, blue) and chlorophyll-α (right y axis, orange), obtained using the salinity DIN flux proxy.

gC m^{-3} day^{-1} NPP, by approximately day 250 before the breakdown of the thermocline occurs soon after. The chlorophyll signature is mixed to the same level as 2007. In both cases, no chl-α or NPP signatures are detected after day 320. The timings of the blooms are most likely down to meteorological conditions, as timing of the Atlantic inflow is not set when configuring the model. However, the magnitude of the blooms are reflective of the changing availability of DIN in the water column.

5.3.2 Implications for the wider ecosystem and carbon cycling

So far, we have shown that the weakening of the European Slope Current has decreased the mean flux of nutrients to the northern North Sea. This has decreased the overall net primary production and associated chlorophyll-α signatures in the region (as shown in Figs. 5.5, 5.8 and 5.11). Figure 5.13 shows the maximum values in both the first/main spring bloom (as solid lines), as well as the smaller second bloom (as dashed lines). There is no overall trend in the magnitude of the first bloom. Inter-annual variability remains fairly constant with the notable exception in 2002, where both NPP and chl-α rapidly decline (especially chl-α, which declines by nearly 3 mg m^{-3}, before recovering to the previous value the following year. The second bloom maxima, however, do show a trend with time. Additionally, the second bloom also shows high inter-annual variability before 1997. Between 1988 and 1997, the

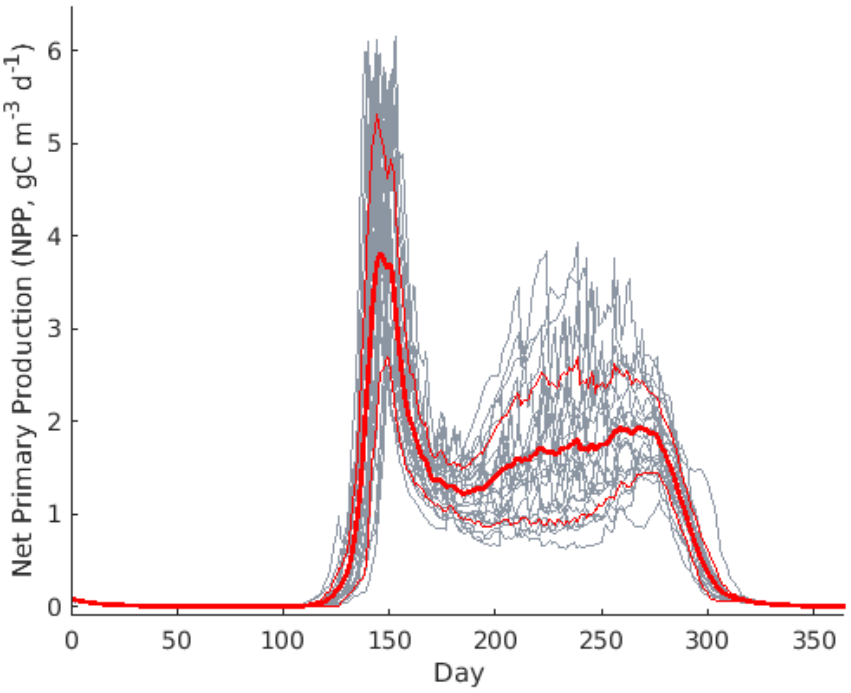

FIGURE 5.9: Surface values of net primary production (NPP) over each model run year, obtained using the Slope Current transport DIN flux proxy. Grey lines represent the 22 model runs (1988 - 2009). The thick red line is the ensemble mean of the runs, with the thin red lines indicating ± standard deviation.

maximum values of NPP and chl-α, increase to a peak of 3.8 gC m^{-3} d^{-1} NPP, 7.5 mg m^{-3} chl-α. In 1998, the maximum peaks of both NPP and chl-α rapidly drop to 1.9 gC m^{-3} d^{-1} NPP, 4.2 mg m^{-3} chl-α: a decrease of approximately 50% NPP. The declining trend continues in both values, albeit with a slower rate. The 2009 model run showed the lowest values for the second bloom peak. The pattern and trends of DIN and chl-α variability in the second bloom closely resemble the Slope Current transport variability as shown and discussed in Ch. 3.3.3, Fig. 3.8, as well as the salinity variability seen in Ch. 4.3.3, Fig. 4.12. This provides strong evidence that nutrient flux from the Slope Current is an important driver of the spring bloom, but much more importantly the later second (autumn) bloom.

The difference between the "spring" and "autumn" bloom peaks, and the decline of the autumn bloom signal since the late 1990's is potentially a remarkable finding that can be directly explained by the reduction in Atlantic inflow via the Slope Current. In the spring, nutrient flux originating from the seabed (set at a constant rate of 2.64 mmol m^{-2} d^{-1} as a representative value for the North Sea, see section 5.2.2) is utilised, as well as any nutrients from surface fluxes (considered here to be the Atlantic inflow). Whilst this is presented as a daily mean flux, the seabed nutrient supply is only replenished once a year. Once that is exhausted in the spring, the seabed nutrient supply is negligible for the rest of the year. The surface nutrient flux, however, is

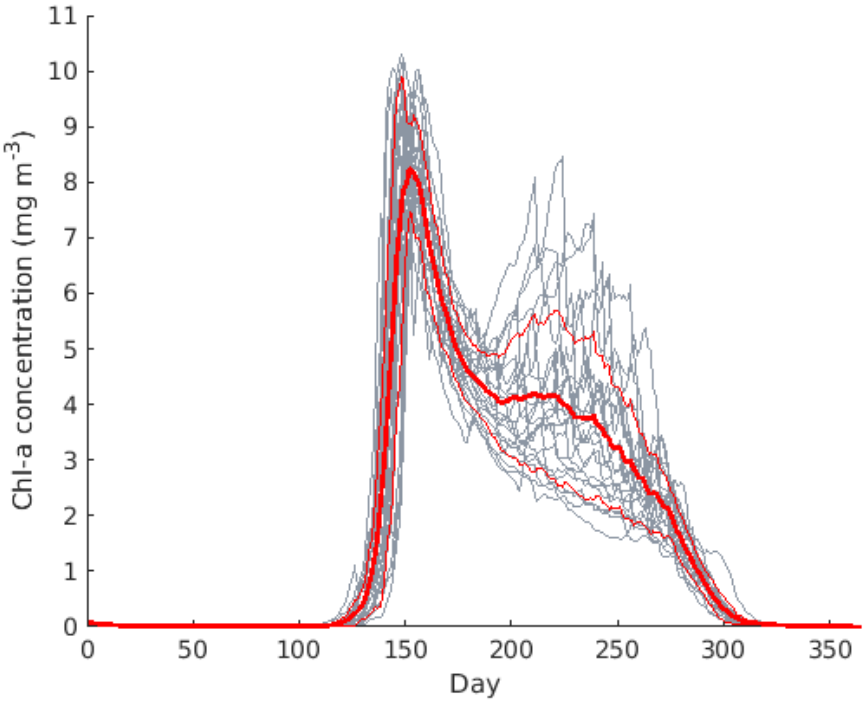

FIGURE 5.10: Surface values of chlorophyll-α over each model run year, obtained using the Slope Current transport DIN flux proxy. Grey lines represent the 22 model runs (1988 - 2009). The thick red line is the ensemble mean of the runs, with the thin red lines indicating $\pm$ standard deviation.

assumed to be continuous. It varies with changing Atlantic inflow which, from results presented in this Thesis, is influenced heavily by the strength of the Slope Current. This means that surface nutrients are resupplied after the spring bloom completes, triggering the second later autumn bloom. This is always less as total nutrient availability cannot be as high as at the start of the year. It is important to note that fluvial nutrient flux has not been considered in the DIN rates used in this study, as the point at which the model was run was away from any major rivers. A continued surveying effort using CPR or Niskin sampling in conjunction with CTD profiles in the northern North Sea would help to confirm the reduction of the autumn bloom strength as a "true" signal.

It is important to note that there may be other variables that are affecting the strength and timing of the spring blooms. Surface water temperature can affect phytoplankton growth to some degree but temperature is a larger control on zooplankton and fish species and can affect breeding and spawning success (Montero-Serra et al., 2015; Beaugrand and Reid, 2003), which in turn will affect grazing, but note that changes to grazing is not included in the model. Temperature and the North Atlantic Oscillation (NAO) has been linked to the redistribution of plankton species and introduction of warmer-water species to the North Sea (Beaugrand et al., 2002). Perhaps more important is wind-driven mixing. Wind stress at the sea surface acts to break down

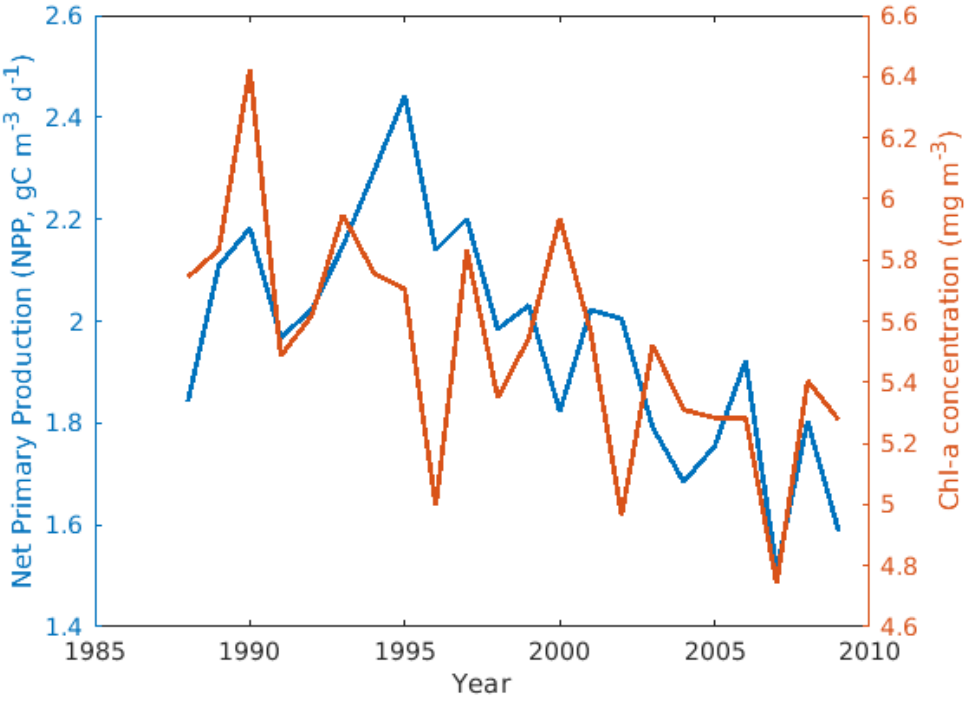

FIGURE 5.11: Time series of annual mean surface net primary production (left y axis, blue) and chlorophyll-α (right y axis, orange), obtained using the Slope Current transport DIN flux proxy.

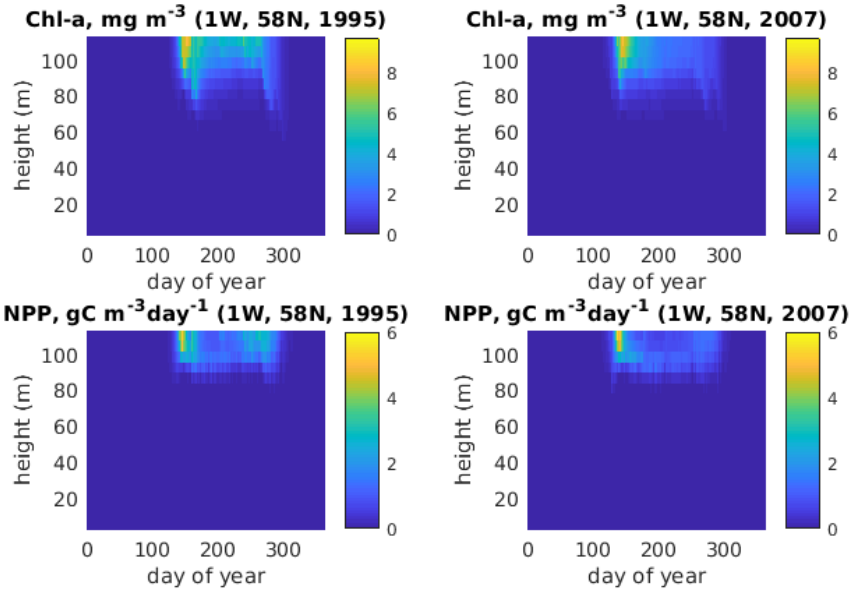

FIGURE 5.12: Hovmuller plot of daily model output time series for the high (1995) and low (2007) DIN flux years, showing the chlorophyll concentration and the NPP rates only. This run was initialised with the Slope Current transport DIN flux proxy. Note that the y axis is height above seabed. The colour scales for chl-α and NPP are fixed respectively for easier direct comparison.

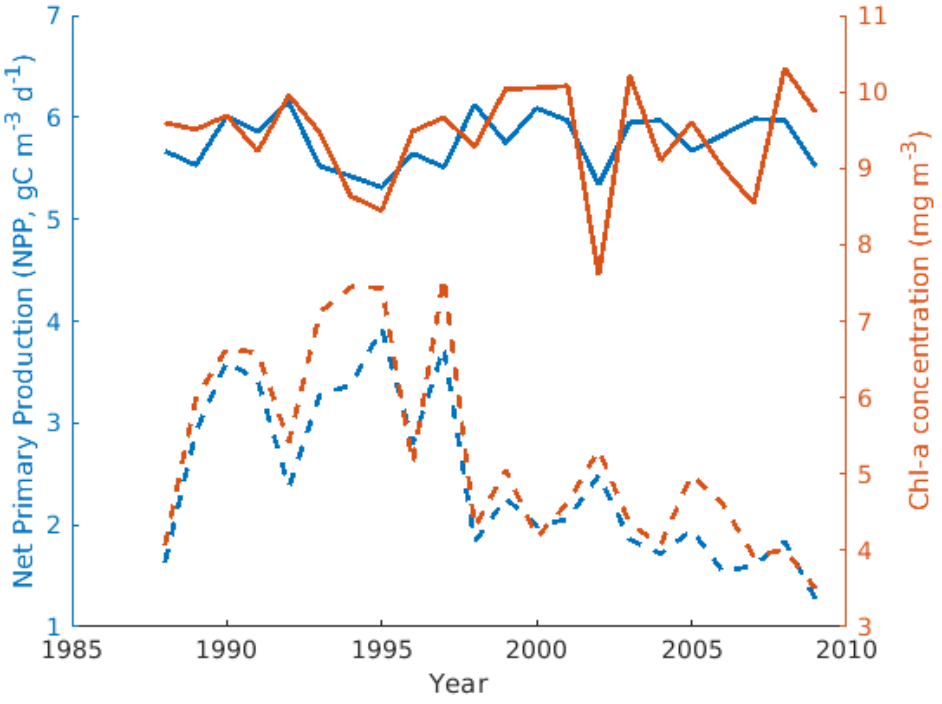

FIGURE 5.13: Time series of maximum surface net primary production (left y axis, blue) and chlorophyll-a (right y axis, orange), obtained using the particles on shelf DIN flux proxy, in the phytoplankton spring and autumn blooms. Solid lines are maximum values in the first spring bloom peak. Dashed lines are maximum values from the second (autumn) bloom.

stratification (van Haren, 2000), which means that plankton held in the photic zone get dispersed. Productivity will decrease as a result. Wind stress and air temperature at the sea surface are accounted for in the S2P3 model. However, this does make it difficult to completely disentangle the effects of Slope Current and the effects of atmospheric forcing on primary production. Since we have shown that the Slope Current actively conveys a high salinity signature from the North Atlantic to the North Sea, we can assume that surface temperatures are also conveyed in this way.

The decline in overall net primary production and phytoplankton abundance (as indicated by the chlorophyll concentration), as well as the weakening of the second bloom, has wide-ranging implications for the wider ecosystem of the North Sea. A weakened second phytoplankton bloom means less availability of phytoplankton for zooplankton and other phytoplankton-grazing species. This could then have an effect on the productivity (biomass and breeding success) of higher trophic levels, but it is important to remember that changes in plankton grazing is not covered in the model. For example, gross production in some species of zooplankton and fish have been shown to have declined since 1973 (Heath, 2005), in a manner consistent with the trends and decrease shown in the surface net primary production of the spring bloom (Fig. 5.13). Cod is commercially/economically important fish stock in the North Sea.

The early life cycle of cod is highly dependant on water temperature as well as availability of their main prey species of zooplankton: *Calanus finmarchicus* (Sundby, 2000). With the increasing temperature of Atlantic inflow, as well as less nutrients being brought from the Atlantic to the North Sea, cod development could be put at risk. Cod distribution in the North Sea has shifted northwards, attributed to the warming of the region (Engelhard et al., 2014). This is on top of an already declining adult cod population, particularly in the western North Sea, from over-fishing pressure (Engelhard et al., 2014; Cook et al., 1997).

The decline in primary productivity in the North Sea could have implications for wider carbon fluxes, which is of consequence to the local and global climate system on the long term. Gross carbon flux is associated with North Atlantic Ocean inflow, bringing DIN and DOC, but in net terms the North Sea acts as a carbon sink (Thomas et al., 2005). 98% of North Sea carbon is a consequence of Atlantic inflow, with 90% of the inflow occurring on the northern boundary consisting of the Shetland Channel and Fair Island Channel (Thomas et al., 2005). Greater than 99% of that carbon inflow is exported from the North Sea in flows through the Norwegian Trench, with the remaining carbon sinking as particulate organic carbon (POC) and forming seafloor sediments (Thomas et al., 2005). During a plankton bloom, nutrients are used to fuel a bloom. Once nutrients are exhausted, the bloom primary production slows and plankton such as coccolithophores sink through the water column, exporting carbon as POC to the sediment (Foster and Shimmield, 2002). With less Atlantic water coming into the North Sea from the Slope Current, this means less Atlantic-derived carbon as well as nutrients such as DIN being available for primary production. The changing Atlantic flux therefore has the possibility of reducing the carbon sink (as POC to the sediment) in the North Sea.

The S2P3 shelf seas physics and primary productivity model used in this chapter does have one major limitation. Whilst it allows for the vertical migration of plankton (through mixing and through self-induced motion), it is unable to replicate the lateral migration of plankton species. This may be particularly important, as previous studies have shown that there are an increasing amount of typically more southern, warmer-suited species arriving at the shelf edge and into the North Sea (Beaugrand et al., 2009). Data from the CPR survey to track changing plankton (both zooplankton and phytoplankton) has also shown that "native" North Sea species are being displaced by those sub-tropical species being carried in on Atlantic inflow (Beaugrand et al., 2009). This is a key aspect of "subtropicalization": where species from typically warmer waters are migrating into typically cooler waters that they originally would not have been able to survive in. It is known that different phytoplankton species utilise (or uptake) nutrients in different ways, with some species being able to regulate the types of nutrients that they require based on availability (Bonachela et al., 2011). Therefore, the species present in the North Sea could also have an effect in the strength

and timing of the spring bloom. However, since primary production depends on the availability of nutrients, we believe that our results are still valid in showing the effect of changing nutrient fluxes from the North Atlantic, conveyed by the Slope Current. Subtropicalization is not only shown in plankton species. Pelagic fish species (such as herring, another economically important species) have been displaced by other typically warmer-water inhabiting species such as mackerel and pilchard (Montero-Serra et al., 2015).

Another limitation of the S2P3 is the exclusion of terrestrial run-off. Riverine input to the North Sea can transport naturally occurring nutrients, as well as anthropogenic nutrients (such as those from agricultural fertilisers that run off into rivers) (Thomas et al., 2005). They are another source of nutrients and dissolved carbon (Thomas et al., 2005), therefore being another important part of the North Sea carbon budget. Taking the Humber Estuary as an example: whilst river input has increased by at least 20% since 1995 (Tappin et al., 2002) , fertiliser input to the North Sea is estimated to have decreased by 10-15% due to lower application of fertiliser (Tappin et al., 2002). The model does not account for other nutrient inputs: it only uses user-selected values of surface (from any source) and seabed DIN fluxes. Without knowing specific values of riverine DIN inputs or how riverine water is distributed throughout the North Sea, it is impossible to say how this might actually effect primary production rates or if it is of significance.

Regretfully, there was insufficient time for the model results to be validated with observational data. This study could, in the future, be validated with data from remote sensing or hydrographic approaches. Satellite sea surface chlorophyll records are readily available and would provide a suitable indicator for phytoplankton abundance. Although data cannot be collected when it is cloudy, monthly mean analysis is usually available, which should still be able to capture blooms (albeit at lower temporal resolution).

Another method to ground-truth the data would be using the Continuous Plankton Recorder (CPR) dataset. The Continuous Plankton Recorder (CPR) Survey refers to a towed mechanical sampler of the same name. The CPR was invented and tested by Sir Alister Hardy in 1931, in the North Sea (Association, 2022). It is a rectangular box with a small 1.27 cm^2 opening on the nose. Water enters through this aperture and passes through a moving gauze mesh (see Batten et al., 2003, Fig. 1, tag B). This gauze is moved by a rear-mounted impeller which drives two rollers, which sandwich any sampled material on the gauze with another piece of gauze, and into a storage chamber filled with formaldehyde (see Batten et al., 2003, Fig. 1, tag I for the storage spool chamber). Given that the moving gauze is driven by the passing water, it is important to maintain a constant speed when towing the CPR (Batten et al., 2003; Hays and Warner, 1993).

As of 2018, the CPR instruments and database are now managed by the Marine Biological Association in Plymouth, UK. The dataset records species abundance and a metric of sampling effort per month for each grid co-ordinate (averaged over a 1 by 1 degree grid). The dataset is split into many species of zooplankton and phytoplankton. CPR abundance is the mean count per cubic metre of water filtered, per month. CPR sampling effort is the mean number of samples at selected grid position, per month. By targeting some of the species seen used in other similar studies (eg: Beaugrand et al. (2009) using the copepod *Calanus finmarchicus* to track North Sea subtropicalisation), a comparable study could be achieved.

Niskin sampling, usually undertaken in conjunction with CTD deployment, could be used to obtain surface and deep water chlorophyll data as well as phyto-/zooplankton species distribution and concentration. This, however, would be a time consuming, expensive and considerably lower spatial and temporal way of comparing to the model output, given the other options available.

5.4 Conclusions

Using a 1D shelf seas ocean biogeochemical model, we have been able to determine that the slowdown of Slope Current transport and subsequent less Atlantic water making it onto the shelf is reducing the flux of nitrate into the northern North Sea. This in turn is reducing primary production in the surface waters. From all 3 dissolved inorganic nitrate flux proxies used to run the model, the resulting net primary production rate and chlorophyll-α concentration shows a variability of about 20 days in the start of the spring bloom. The magnitude of the bloom has very high variability. The first peak of the bloom around day 150 shows no overall trend. However, the maximum values of NPP and chl-α in the second autumn bloom (between day 175 and day 275) shows an overall declining trend, with a 50% decrease in NPP in the year after the subpolar Atlantic warming. The trend and inter-annual patterns of variability resemble the patterns of Slope Current northward transport variability. We conclude that the Slope Current is a key driver of the later autumn bloom by supplying nutrients (namely dissolved inorganic nitrate) to the northern North Sea year-round through cross-shelf exchange.

Chapter 6

Synthesis and Conclusions

Through this research, we have aimed to observe and quantify the changing North Atlantic Ocean forcing on the European shelf seas and their effects on the biogeochemistry of the northwest European shelf seas. The research has been motivated and directed by the following research questions, which were first introduced in Chapter. 1:

1. Do physical (hydrographic) changes in the subpolar North Atlantic significantly influence flow and cross shelf exchange at the European shelf edge?
2. Does the slowdown of shelfward geostrophic transport effect the fate of European Slope Current waters?
3. What are the potential impacts on shelf sea and North Sea biogeochemistry from the past 4 decades of changes to the subpolar North Atlantic and reduction in associated shelf edge transport?

To answer these questions, the following lines of work were undertaken as presented in Chapters 3 to 5:

- Obtaining time series of temperature, salinity and corresponding density change in the sub-polar North Atlantic.
- Quantifying the decline of the density gradient in the sub-polar North Atlantic and subsequent decline in shelfward (zonal) geostrophic volume transport.
- Determining the relationship between oceanic physical property change to changes observed at the shelf edge, through the use of Ariane particle tracking simulations.
- Quantifying the reduction of the northward-flowing European Slope Current and the changing inflow of Atlantic water to the North Sea.

- Determining the biogeochemical changes in the northern North Sea related to changing nutrient fluxes as a result of the Slope Current and shelf edge exchange.

In this chapter, the main findings of the research will be presented. They provide new perspective to the North Atlantic's changing hydrography, circulation and corresponding influence on the shelf seas via the European Slope Current. The key findings will be discussed in terms of the three research questions quoted above, as well as the working objectives introduced in Chapter 1. The significance to the wider shelf sea environment, particularly the North Sea, in terms of the physical and ecological changes will be discussed in context to previous studies and in terms of long-term changes to the viability of commercially important fisheries. Finally, directions for future research in the research field will be presented.

6.1 Changing circulation of the North Atlantic and shelf-edge currents

The dynamics and physical properties of the North Atlantic Ocean have been changing over the past 40 years. Analysis of the GODAS reanalysis product in Ch. 3 has shown that the sub-polar North Atlantic has warmed by 1 °C from 1997 to 2015 (Clark et al., 2022b). This has acted to weaken the meridional density gradients and invert the density anomalies (with respect to the climatology from 1980 to 2020). An inverse relationship between density and SSH anomalies is observed across the North Atlantic basin. At the shelf edge, a corresponding density anomaly change is observed, with density shifting from a positive anomaly phase before 1997 to a mostly negative density anomaly phase 1997 onwards. Geostrophic eastward (zonal) transport from 30 °W has decreased since 1997, and the resultant mean transport has shifted to a warmer (>11 °C) phase. Calculations of eastward geostrophic transport at 30 °W, 45 - 60 °N (Fig. 3.5), chosen to represent the region with the strongest density gradients, closely resemble the time series of total northward volume transport calculations at various transects at the shelf edge (Fig. 3.8). Combining the observed hydrographic variability and zonal transport calculations with analysis of two 4-year Lagrangian particle tracking hindcast experiments, we find that geostrophic inflow to the shelf edge provides the majority of the water residing in the Slope Current. The basin-scale warming of the sub-polar North Atlantic (including the SPG) has decreased the volume flux of Atlantic water into the Slope Current by approximately 5 Sv. The Lagrangian analysis shows a general southward shift to the inflow, as well as a slowdown of the transport, a shallowing by 20m and a warming of 1 °C. The southward shift and warming of the flow is indicative of a southward shift of the Gulf Stream, which in the Lagrangian difference plot (Fig. 3.11) is visible in panels a

(particle distribution) and b (particle age). Although not tested in this study, there may also be a link with the observed reduction in AMOC, which has been seen to cool the subpolar gyre and increase recirculation, providing less heat transport in the Gulf Stream Bryden et al. (2019). It is also possible that the AMV pattern has influenced this, though it is impossible to confirm this with the data used here due to the relatively short time period of data available.

We have shown that variations to sub-polar North Atlantic density gradients (predominantly driven by changes in temperature distribution) is the main source of variability in inflow to the Slope Current. This answers the first part of research question 1, that hydrographic changes do indeed exert a strong influence on shelf edge transport. Density in the SPG region is controlled predominantly by temperature fluctuations, and the corresponding baroclinic geostrophic flow towards the shelf is an important heat flux to the European shelf seas. This may have implications on the weather and climate of the UK and European countries, by altering the air-sea heat flux in the region. During the the recent sub-polar gyre cold temperature anomalies of 2014-16 ("The Cold Blob" or "Big Blue Blob"), enhanced cold water upwelling and extreme surface heat loss combined to create the observed effects (Josey et al., 2018). A corresponding heatwave was seen across the European continent and the UK, linked to the cooling of the North Atlantic affecting the state of the North Atlantic Oscillation (Josey et al., 2018). This highlights the importance of air-sea interaction in the wider North Atlantic basin. As mentioned in Ch. 3.4, the negative phase of the North Atlantic Oscillation (NAO) has been linked to enhancing Slope Current transport (Pingree, 2002). The NAO has previously been linked to changing Atlantic inputs to the North Sea and subsequent marine ecosystem response (eg: Edwards et al. (2013); Beaugrand and Reid (2003); Reid et al. (2001a)), something that will be discussed later in section 6.3. Therefore, future studies that aim to assess or simulate the impacts of the slowdown of the Slope Current should also look further at atmospheric forcing, something which has only been indirectly analysed in this work.

6.2 Changing inputs to northeastern shelf seas and the North Sea

In Chapter 4, it was shown that the destination of the Slope Current had changed, which can be directly related to the geostrophic Atlantic inflow as discussed in Ch. 3. 22 further Lagrangian experiments were performed forward in time, using the same release strategy as in Ch. 3. These experiments revealed the point at which Slope Current water crosses onto the shelf has shifted to the southwest. This cross shelf exchange remains strongly seasonal: with a greater number and proportion of released particles making it onto the shelf occurring in the winter months (Fig. 4.3).

This seasonal pattern was expected, due to the way cross shelf exchange is controlled in this region, and similar regions around the world. Cross shelf/slope exchange can be driven in a number of ways. In the case of the SC and the European Shelf edge, there are two main forcing mechanisms. The first is the steep and irregular bathymetry can create enhanced eddy flow, enhancing turbulent mixing and exchange of Atlantic water onto the shelf (Porter et al., 2016a, 2018). The Slope Current is prone to this at approximately 55 °N along the shelf edge (Porter et al., 2018; Hill, 1995), where the slope gradient is very steep at 70m km^{-1} (Hill, 1995). Eddying should increase with the strength of the flow. The second mechanism is through the slope gradient helping to generate stronger localised internal tides, which again aid mixing and upwelling of the core Slope Current waters (Porter et al., 2018; Huthnance, 1984). Since ORCA12 does not include tidal forcing, this pathway will be missing from the Ariane results. Re-running with a shelf sea model that includes tides would better capture this. In more southern regions of the slope, the ADCP, satellite altimetry data and drouged drifters have shown that the SC exhibits a seasonal summer equatorward-flowing phase (Porter et al., 2018; Xu et al., 2015), which further limits the amount of water onto the shelf from the SC. The latitude of mean Atlantic inflow to the shelf still remains well north of this region (at a mean of 56.5 °N as of 2009, see Fig. 4.8). Cross shelf exchange is not correlated with eastward Ekman transport (showing a statistically insignificant relationship with an $r^2 = 0.02$, Fig. 4.7). Whilst there is great seasonality in Ekman transport, there is no observable long term trend (Fig. 4.6). We conclude that Ekman transport is therefore not a strong influence on variable cross shelf exchange of Slope Current waters.

Salinity of the inflow to the shelf, and eventually the North Sea, has been shown to be declining (Fig. 4.8), despite Atlantic salinity appearing to increase slightly in the TS analysis (Fig. 3.7). This can be explained in two ways. We have shown that the Atlantic inflow to the Slope Current is declining, resulting in less higher-salinity Atlantic water being entrained in the Slope Current and being deposited into the North Sea. Secondly, with less Atlantic inflow to the North Sea, estuarine inflow becomes a more significant contribution and may act to freshen the North Sea. Estuarine inflow may also have been augmented by different rainfall patterns. The effect of estuarine input being mixed with Atlantic-origin waters conveyed through the Slope Current directly into the North Sea (or associated mixing processes along the slope that allows Atlantic water onto the shelf) has not been quantified in this study. However, this should be of research significance in future studies. Moving further onto the shelf, the salinity of these waters is expected to decrease over time as the influence of river outflow becomes more significant. The influence of Slope Current and Atlantic water on the shelf seas is therefore dependant on the strength of the Slope Current and the mixing processes that help bring the Atlantic water onto the shelf.

As Slope Current transport has reduced, we have shown how residence time on the

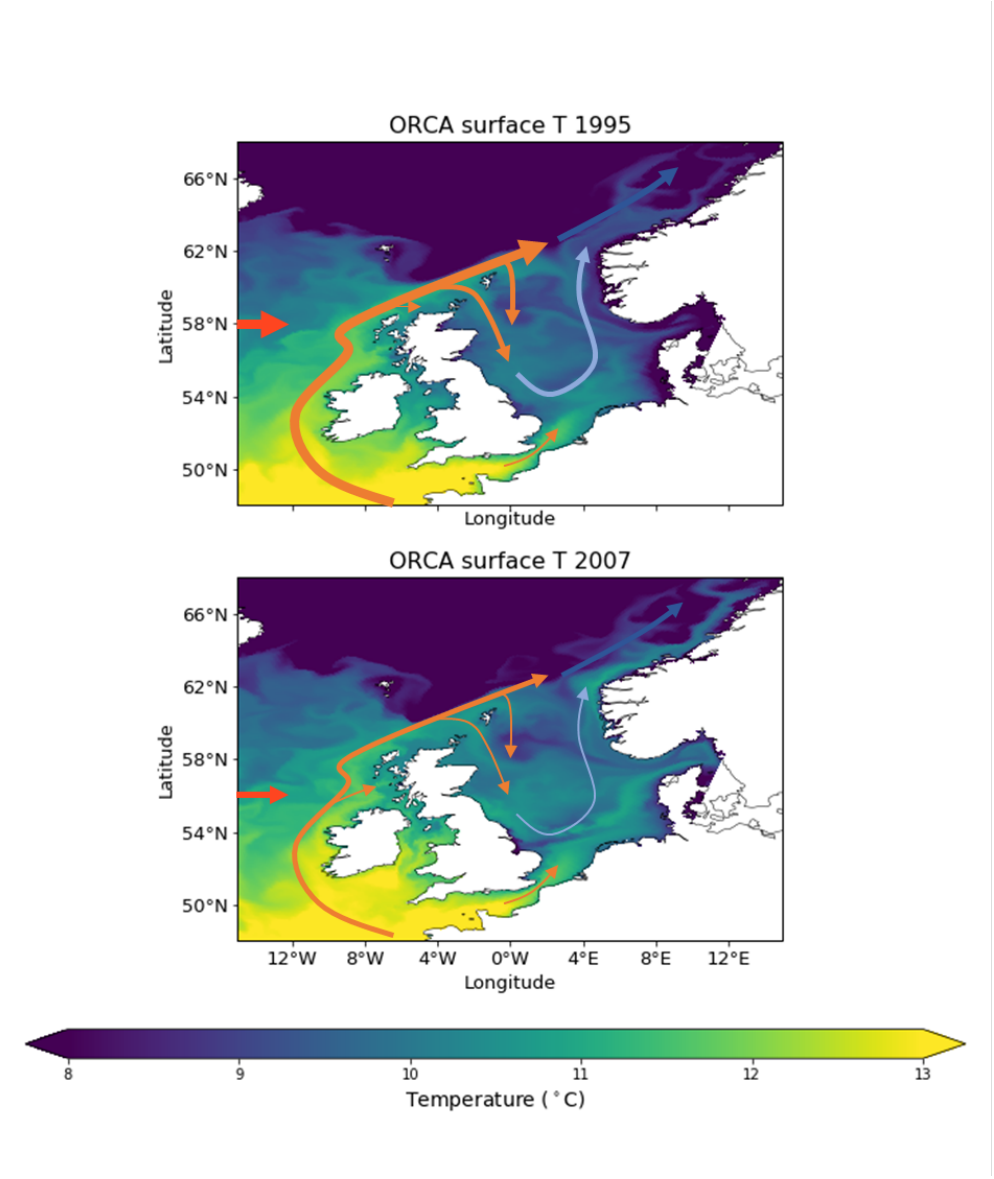

FIGURE 6.1: A schematic diagram showing the changing Slope Current (SC) provenance and inputs to the North Sea after the warming of the North Atlantic in the late 1990s. The top panel shows the SC pre-1997, the right panel shows the SC post-1997. The thickness of the arrows represents the approximate flow (transport) of the Slope Current and associated inflow to the North Sea. The colour of the arrows represents the relative temperature of each flux. The red horizontal arrow represents the mean position and strength of the subpolar Atlantic inflow to the Slope Current. The background colour is surface temperature (from ORCA12) on 10th January of each respective year (1995 and 2007).

shelf has increased by 60 days, with considerable interannual variability (Fig. 4.4). We have shown that the the residence time of the particles that make it onto the shelf is somewhat negatively correlated, with an r^2 of 0.29. This suggests that circulation in the North Sea is also slowing down, which means Atlantic water is not being flushed back out as quickly. Circulation in the North Sea is cyclonic. Inflow to the northern North Sea is drawn southwards past the eastern UK shores, before turning

northwards once again and crossing the central and eastern North Sea. Any inflow from the English Channel combines with the flow, though this is considered minimal compared to other inflow sources, and is on the order of 0.1 Sv (Marzocchi et al., 2015), compared to 2.7 $\pm$ 0.5 Sv in the Faroe-Shetland channel (Berx et al., 2013). The flow continues northward and is exported back into the Atlantic via the Norwegian Trench with the Norwegian Current. Figure 6.1 summarises the weakening of flows and associated January SST pre-1997 and post-1997.

The results presented and discussed here have answered the first and second research questions: a reduction of shelfward geostrophic transport from the subpolar region is responsible for up to 50 percent decline in northward transport of the Slope Current and a reduction in inflow to the North Sea. This has led to a slowdown of cross shelf exchange and subsequently longer on-shelf residence times.

This work has not attempted to project how the Slope Current or North Sea inputs will change in the future. Clearly, establishing the likelihood of continued inflow reduction and assessing the impacts remains a significant gap in current research in shelf sea dynamics. The trends in eastward inflow (both the majority geostrophic component and the total volume transport) to the Slope Current and indeed the northward transport of the Slope Current itself suggests a continuing decline. Whether or not there is a possibility of a 'shutdown' of the Slope Current remains to be seen, yet if the trend continues it may happen. There is also the potential for a more permanent flow reversal: a seasonal southward flow is already observed at times near the Goban Spur in the summer months (Pingree et al., 1999; Porter et al., 2016b). A model study would be a good opportunity to assess the impacts of changing Slope Current inputs, and the influence of the wider changes to North Atlantic circulation and hydrography, on the North Sea circulation and biogeochemistry. Holt et al. (2018) used the AMM7 model of the northwest European continental shelf to assess the bio-physical impacts due to changing inflow to the North Sea. They suggest a continued slowdown or eventual shutdown of North Atlantic inflow to the North Sea will lead to a riverine-dominated environment and reduction of wintertime DIN availability (Holt et al., 2018). As already mentioned, a better understanding of the shelf edge mixing processes that allows Atlantic water onto the shelf, whether or not through the Slope Current, is also needed.

6.3 Impacts on shelf sea biochemistry from a weakening European Slope Current

A shelf sea coupled physics-biogeochemistry (S2P3) model was used in Chapter 5 to assess how changing Atlantic inflow to the North Sea, via the Slope Current, would influence primary production. This study aimed to investigate the third research

question. Slope Current transport, the number of Ariane Lagrangian particles making it onto the shelf and the Atlantic salinity signature in the northern North Sea were used in creating 3 proxies for DIN flux into the North Sea. These proxies were used to force the biogeochemistry model. The model study indicated that the decreasing Atlantic inflow (and associated reduction in DIN flux) leads to a decrease in primary production. The phytoplankton spring bloom is identified as a sudden increase of NPP and chl-α at a mean of day 150. The timing or magnitude of the main bloom does not vary much over the 22 simulation years or different proxies, as high DIN concentrations in spring are due to strong vertical mixing during winter months, hence lateral influx is not limiting. However, the second peak is much more variable in both the timing of the peak and the magnitude because DIN is otherwise used up during the spring bloom but replenished via the Slope Current inflow. The magnitude of the NPP and chl-α is decreasing over time (Fig. 5.13), strongly emulating the decreases previously observed in Slope Current transport and the number of particles making it onto the shelf.

Chapter 5 already discusses some of the implications of the reduced flux of nutrients from the Atlantic coming into the northern North Sea. The Slope Current provides a pathway for nutrients from the sub-polar Atlantic and upwelling regions further south along the eastern Atlantic boundary to be brought northwards and eventually into the North Sea. With the trend going towards a potential shutdown of the Slope Current, this would mean that the nutrients used in primary production of phytoplankton would not be as quickly replenished, with the seabed flux and any estuarine inputs becoming the main nutrient sources. This would result in reduced net primary production, particularly in the autumn bloom where decreasing NPP is already observed (Fig. 5.13). Not only will this impact the phytoplankton, but it has the potential to limit the productivity of any higher trophic levels. Although not directly related in this study, it is highly likely that the Slope Current assists in the distribution of species and their larvae. Variations in North Sea inflow patterns have previously been linked to changing distributions of plankton species (Gao et al., 2021; Reid et al., 2003). Subtropicalization of the shelf seas was also introduced in Chapter 1.3. A shutdown of the Slope Current will reduce warm subtropical Atlantic water (as well as subpolar water) inflow to the North Sea, thus reducing the potential for warmer-water species of plankton and fish to be conveyed there, as previously documented (Beaugrand et al., 2009; Montero-Serra et al., 2015).

The carbon and nutrient budgets of the North Sea from previous studies may be changing. Atlantic inflow, particularly from the Shetland and Fair Isle channels, has previously been the main flux of DIN into the North Sea (Thomas et al., 2005). With the reduction of the Slope Current and shelf edge exchange, inputs from terrestrial sources could have greater significance on the nutrient budgets. This however depends on over-land rainfall levels, which determine river fluxes. Reduced primary

production in the North Sea will also reduce the amount of carbon that can be sequestered from the atmosphere, potentially having local and global effects on atmospheric and oceanic warming. This remains an open avenue for future research.

6.4 Conclusions and future research opportunities

The North Atlantic Ocean is changing, and that change has many influences and implications on the circulation and ecology of the northwest European shelf seas. This research has shown that basin-scale warming of the sub-polar North Atlantic Ocean, locally by up to 2 °C over recent decades, has reduced the meridional density gradients in the sub-polar gyre region. The warming and freshening of the subpolar North Atlantic is responsible for a reduction in eastward geostrophic volume transport towards the shelf by nearly 10 Sv. This in turn has decreased the northward transport of the European Slope Current. Warmer water is still being pushed onto the shelf and entering the North Sea via the Slope Current. However, with the decrease in Slope Current transport, less Atlantic water reaches the shelf resides for up to 60 days longer. In addition to the salinity and temperature signals, we have shown that the Slope Current continues to act as a pathway for nutrients entering the shelf seas, including the northern North Sea. This reaffirms previous work by Beaugrand et al. (2009) by providing the physical mechanism of how warmer water species of zooplankton and fish are entering the northwest European shelf seas.

My work leaves many open avenues for further research, either by myself or other researchers, and has identified gaps in the current data available for research. I was limited to an version of ORCA12 that spanned 1988 to 2010. This meant any more recent changes to the Slope Current and corresponding fluxes to the North Sea were not analysed with Lagrangian tools. More recent ORCA12 simulations now exist, but time and computational limitations meant that analysis of more up-to-date data has not been possible. In terms of remaining research questions, this Thesis (particularly the work in Ch. 5) has highlighted the lack of a complete picture of nutrient fluxes in the northern North Sea. Given the ecological and potentially economic significance of changes to the ecology of the North Sea as a result of Atlantic inflow, there is a possibility of further observational and more targeted model studies of the region to identify and better quantify the changing Atlantic nutrient flux.

References

A. Akimova, I. Núñez-Riboni, A. Kempf, and M. H. Taylor. Spatially-Resolved Influence of Temperature and Salinity on Stock and Recruitment Variability of Commercially Important Fishes in the North Sea. *PLoS ONE*, 11(9):e0161917, 2016. doi: 10.1371/journal.pone.0161917.

M. B. Association. CPR Survey | Sir Alister Hardy. Accessed 25/08/2022, Aug. 2022. URL https://www.cprsurvey.org.

M. Baatsen, R. J. Haarsma, A. J. Aarnout J. Van Delden, and H. de Vries. Severe Autumn storms in future Western Europe with a warmer Atlantic Ocean. *Climate Dynamics*, 45(3):949–964, 2015. doi: 10.1007/s00382-014-2329-8.

A. Bakun. Global climate change and the intensification of coastal upwelling. *Science*, 247(4939):198–201, Jan. 1990. doi: 10.1126/science.247.4939.198.

A. Bakun, B. A. Black, S. J. Bograd, M. Garcia-Reyes, A. J. Miller, R. R. Rykaczewski, and W. J. Sydeman. Anticipated Effects of Climate Change on Coastal Upwelling Ecosystems. *Current Climate Change Reports*, 1(2):85–93, 2015. doi: 10.1007/s40641-015-0008-4.

S. D. Batten, R. Clark, J. Flinkman, G. C. Hays, E. John, A. W. G. John, T. Jonas, J. A. Lindley, D. P. Stevens, and A. Walne. CPR sampling: the technical background, materials and methods, consistency and comparability. *Progress in Oceanography*, 58 (2-4):193–215, 2003. ISSN 0079-6611. doi: 10.1016/j.pocean.2003.08.004.

D. J. Beare, F. Burns, A. Greig, E. G. Jones, K. Peach, M. Kienzle, E. McKenzie, and D. G. Reid. Long-term increases in prevalence of North Sea fishes having southern biogeographic affinities. *Marine Ecology Progress Series*, 284:269–278, 2004. ISSN 0171-8630. doi: DOI10.3354/meps284269.

G. Beaugrand. The North Sea regime shift: evidence, causes, mechanisms and consequences. *Progress in Oceanography*, 60(2-4):245–262, 2004. doi: 10.1016/j.pocean.2004.02.018.

G. Beaugrand and P. C. Reid. Long-term changes in phytoplankton, zooplankton and salmon related to climate. *Global Change Biology*, 9(6):801–817, 2003. ISSN 1365-2486.

doi: 10.1046/j.1365-2486.2003.00632.x. URL https://onlinelibrary.wiley.com/doi/abs/10.1046/j.1365-2486.2003.00632.x. _eprint: https://onlinelibrary.wiley.com/doi/pdf/10.1046/j.1365-2486.2003.00632.x.

G. Beaugrand, P. C. Reid, F. Ibanez, J. A. Lindley, and M. Edwards. Reorganization of North Atlantic marine copepod biodiversity and climate. *Science*, 296(5573): 1692–1694, May 2002. ISSN 0036-8075. doi: DOI10.1126/science.1071329.

G. Beaugrand, M. Edwards, K. Brander, C. Luczak, and F. Ibanez. Causes and projections of abrupt climate-driven ecosystem shifts in the North Atlantic. *Ecology Letters*, 11:1157–1168, 2008. doi: 10.1111/j.1461-0248.2008.01218.x.

G. Beaugrand, C. Luczak, and M. Edwards. Rapid biogeographical plankton shifts in the North Atlantic Ocean. *Global Change Biology*, 15(7):1790–1803, July 2009. ISSN 1354-1013. doi: 10.1111/j.1365-2486.2009.01848.x.

D. Behringer and Y. Xue. Evaluation of the global ocean data assimilation system at NCEP: The Pacific Ocean. In *Eighth Symposium on Integrated Observing and Assimilation Systems for Atmosphere, Oceans and Land Surface, AMS 84th Annual Meeting*, pages 1–6, Washington State Convention and Trade Center, Seattle, Washington, Jan. 2004. Americal Meteorological Society. URL https://origin.cpc.ncep.noaa.gov/products/people/yxue/pub/13.pdf.

A. Benazzouz, S. Mordane, A. Orbi, M. Chagdali, K. Hilmi, A. Atillah, J. L. Pelegri, and H. Demarcq. An improved coastal upwelling index from sea surface temperature using satellite-based approach - The case of the Canary Current upwelling system. *Continental Shelf Research*, 81:38–54, June 2014. ISSN 0278-4343. doi: 10.1016/j.csr.2014.03.012.

M. Bersch, I. Yashayaev, and K. P. Koltermann. Recent changes of the thermohaline circulation in the subpolar North Atlantic. *Ocean Dynamics*, 57(3):223–235, June 2007. ISSN 1616-7228. doi: 10.1007/s10236-007-0104-7. URL https://doi.org/10.1007/s10236-007-0104-7.

B. Berx and S. Hughes. Climatology of Surface and Near-bed Temperature and Salinity on the North-West European Continental Shelf for 1971–2000. *Continental Shelf Research*, 29(19):2286–2292, 2009.

B. Berx, B. Hansen, S. Osterhus, K. M. Larsen, T. Sherwin, and K. Jochumsen. Combining in situ measurements and altimetry to estimate volume, heat and salt transport variability through the Faroe-Shetland Channel. *Ocean Science*, 9(4): 639–654, 2013. ISSN 1812-0784. doi: 10.5194/os-9-639-2013.

B. Blanke and S. Raynaud. Kinematics of the Pacific Equatorial Undercurrent: An Eulerian and Lagrangian approach from GCM results. *Journal of Physical*

Oceanography, 27(6):1038–1053, June 1997. ISSN 0022-3670. doi: 10.1175/1520-0485(1997)027<1038:Kotpeu>2.0.Co;2.

J. A. Bonachela, M. Raghib, and S. A. Levin. Dynamic model of flexible phytoplankton nutrient uptake. *Proceedings of the National Academy of Sciences*, 108(51):20633–20638, Dec. 2011. doi: 10.1073/pnas.1118012108. URL https://www.pnas.org/doi/full/10.1073/pnas.1118012108. Publisher: Proceedings of the National Academy of Sciences.

N. Brion, W. Baeyens, S. De Galan, M. Elskens, and R. W. Laane. The North Sea: source or sink for nitrogen and phosphorus to the Atlantic Ocean? *Biogeochemistry*, 68:277–296, Apr. 2004. doi: 10.1023/B:BIOG.0000031041.38663.aa. URL https://link.springer.com/article/10.1023/B:BIOG.0000031041.38663.aa.

H. L. Bryden, W. E. Johns, B. A. King, G. McCarthy, E. L. McDonagh, B. I. Moat, and D. A. Smeed. Reduction in ocean heat transport at 26°N since 2008 cools the eastern subpolar gyre of the North Atlantic Ocean. *Journal of Climate*, 0(0):null, 2019. doi: 10.1175/jcli-d-19-0323.1.

M. W. Buckley and J. Marshall. Observations, inferences, and mechanisms of the Atlantic Meridional Overturning Circulation: A review. *Reviews of Geophysics*, 54(1): 5–63, 2016. ISSN 1944-9208. doi: 10.1002/2015RG000493. URL https://onlinelibrary.wiley.com/doi/abs/10.1002/2015RG000493. _eprint: https://onlinelibrary.wiley.com/doi/pdf/10.1002/2015RG000493.

X. Chen and K.-K. Tung. Global surface warming enhanced by weak Atlantic overturning circulation. *Nature*, 559:387–400, 2018. doi: 10.1038/s41586-018-0320-y.

M. Clark, R. Marsh, and J. Harle. Code for "Weakening and warming of the European Slope Current since the late 1990s attributed to basin-scale density changes", Apr. 2022a. URL https://zenodo.org/record/6415360.

M. Clark, R. Marsh, and J. Harle. Weakening and warming of the European Slope Current since the late 1990s attributed to basin-scale density changes. *Ocean Science*, 18(2):549–564, May 2022b. ISSN 1812-0784. doi: 10.5194/os-18-549-2022. URL https://os.copernicus.org/articles/18/549/2022/. Publisher: Copernicus GmbH.

A. Clement, K. Bellomo, L. N. Murphy, M. A. Cane, T. Mauritsen, G. Rädel, and B. Stevens. The Atlantic Multidecadal Oscillation without a role for ocean circulation. *Science*, 350(6258):320–324, Oct. 2015. doi: 10.1126/science.aab3980. URL https://www.science.org/doi/full/10.1126/science.aab3980. Publisher: American Association for the Advancement of Science.

R. M. Cook, A. Sinclair, and G. Stefánsson. Potential collapse of North Sea cod stocks. *Nature*, 385(6616):521–522, Feb. 1997. ISSN 1476-4687. doi: 10.1038/385521a0. URL

https://www.nature.com/articles/385521a0. Number: 6616 Publisher: Nature Publishing Group.

A. Drews and R. J. Greatbatch. Atlantic Multidecadal Variability in a model with an improved North Atlantic Current. *Geophysical Research Letters*, 43(15):8199–8206, 2016. ISSN 1944-8007. doi: 10.1002/2016GL069815. URL https://onlinelibrary.wiley.com/doi/abs/10.1002/2016GL069815. _eprint: https://onlinelibrary.wiley.com/doi/pdf/10.1002/2016GL069815.

A. Duchez, E. Frajka-Williams, S. A. Josey, D. G. Evans, J. P. Grist, R. Marsh, G. D. McCarthy, B. Sinha, D. I. Berry, and J. J.-M. Hirschi. Drivers of exceptionally cold North Atlantic Ocean temperatures and their link to the 2015 European heat wave. *Environmental Research Letters*, 11(074004):1–19, 2016. doi: 10.1088/1748-9326/11/7/074004.

M. Edwards, G. Beaugrand, P. Helaouet, J. Alheit, and S. Coombs. Marine Ecosystem Response to the Atlantic Multidecadal Oscillation. *PLoS ONE*, 8(2), Feb. 2013. ISSN 1932-6203. doi: ARTNe5721210.1371/journal.pone.0057212.

M. Edwards, P. Hélaouët, E. Goberville, A. Lindley, G. A. Tarling, M. T. Burrows, and A. Atkinson. North Atlantic warming over six decades drives decreases in krill abundance with no associated range shift. *Communications Biology*, 4(1):644, May 2021. ISSN 2399-3642. doi: 10.1038/s42003-021-02159-1.

G. H. Engelhard, D. A. Righton, and J. K. Pinnegar. Climate change and fishing: a century of shifting distribution in North Sea cod. *Global Change Biology*, 20(8): 2473–2483, 2014. ISSN 1365-2486. doi: 10.1111/gcb.12513. URL https://onlinelibrary.wiley.com/doi/abs/10.1111/gcb.12513. _eprint: https://onlinelibrary.wiley.com/doi/pdf/10.1111/gcb.12513.

J. M. Foster and G. B. Shimmield. 234Th as a tracer of particle flux and POC export in the northern North Sea during a coccolithophore bloom. *Deep Sea Research Part II: Topical Studies in Oceanography*, 49(15):2965–2977, Jan. 2002. ISSN 0967-0645. doi: 10.1016/S0967-0645(02)00066-8. URL https://www.sciencedirect.com/science/article/pii/S0967064502000668.

P. S. Fratantoni and M. S. McCartney. Freshwater export from the Labrador Current to the North Atlantic Current at the Tail of the Grand Banks of Newfoundland. *Deep-Sea Research I*, 57(2):258–283, Feb. 2010. ISSN 0967-0637. doi: 10.1016/j.dsr.2009.11.006.

S. Gao, S. S. Hjøllo, T. Falkenhaug, E. Strand, M. Edwards, and M. D. Skogen. Overwintering distribution, inflow patterns and sustainability of Calanus finmarchicus in the North Sea. *Progress in Oceanography*, 194:102567, June 2021. ISSN 0079-6611. doi: 10.1016/j.pocean.2021.102567. URL https://www.sciencedirect.com/science/article/pii/S0079661121000549.

C. Garcia-Soto, R. D. Pingree, and L. Valdes. Navidad development in the southern Bay of Biscay: Climate change and swoddy structure from remote sensing and in situ measurements. *Journal of Geophysical Research-Oceans*, 107(C8), Aug. 2002. ISSN 2169-9275. doi: Artn311810.1029/2001jc001012.

S. A. Good, M. J. Martin, and N. A. Rayner. EN4: Quality controlled ocean temperature and salinity profiles and monthly objective analyses with uncertainty estimates. *Journal of Geophysical Research-Oceans*, 118(12):6704–6716, Dec. 2013. ISSN 2169-9275. doi: 10.1002/2013jc009067.

J. M. Gregory, K. W. Dixon, R. J. Stouffer, A. J. Weaver, E. Driesschaert, M. Eby, T. Fichefet, H. Hasumi, A. Hu, J. H. Jungclaus, I. V. Kamenkovich, A. Levermann, M. Montoya, S. Murakami, S. Nawrath, A. Oka, A. P. Sokolov, and R. B. Thorpe. A model intercomparison of changes in the Atlantic thermohaline circulation in response to increasing atmospheric CO2 concentration. *Geophysical Research Letters*, 32(12), June 2005. ISSN 0094-8276. doi: 10.1029/2005gl023209.

S. Hallam, R. Marsh, S. A. Josey, P. Hyder, B. Moat, and J. J.-M. Hirschi. Ocean precursors to the extreme Atlantic 2017 hurricane season. *Nature Communications*, 10 (1):896, Feb. 2019. ISSN 2041-1723. doi: 10.1038/s41467-019-08496-4. URL https://www.nature.com/articles/s41467-019-08496-4. Number: 1 Publisher: Nature Publishing Group.

G. C. Hays and A. J. Warner. Consistency of Towing Speed and Sampling Depth for the Continuous Plankton Recorder. *Journal of the Marine Biological Association of the United Kingdom*, 73(4):967–970, Nov. 1993. ISSN 1469-7769, 0025-3154. doi: 10.1017/S0025315400034846. URL https://www.cambridge.org/core/journals/journal-of-the-marine-biological-association-of-the-united-kingdom/article/consistency-of-towing-speed-and-sampling-depth-for-the-continuous-plankton-recorder/2AD4E78F97EDE17B720CCB2F296386CD. Publisher: Cambridge University Press.

G. C. Hays, A. J. Richardson, and C. Robinson. Climate change and marine plankton. *TRENDS in ecology and evolution*, 20(6):337–344, 2005. doi: 10.1016/j.tree.2005.03.004.

M. R. Heath. Changes in the structure and function of the North Sea fish foodweb, 1973–2000, and the impacts of fishing and climate. *ICES Journal of Marine Science*, 62 (5):847–868, Jan. 2005. ISSN 1054-3139. doi: 10.1016/j.icesjms.2005.01.023. URL https://doi.org/10.1016/j.icesjms.2005.01.023.

A. E. Hill. Leakage of Barotropic Slope Currents onto the Continental Shelf. *Journal of Physical Oceanography*, 25(7):1617–1621, July 1995. ISSN 0022-3670, 1520-0485. doi: 10.1175/1520-0485(1995)025<1617:LOBSCO>2.0.CO;2. URL https://journals.ametsoc.org/view/journals/phoc/25/7/1520-0485_1995_

025_1617_lobsco_2_0_co_2.xml. Publisher: American Meteorological Society Section: Journal of Physical Oceanography.

A. E. Hill and E. G. Mitchelson-Jacob. Observations of a Poleward-Flowing Saline Core on the Continental-Slope West of Scotland. *Deep-Sea Research Part I-Oceanographic Research Papers*, 40(7):1521–1527, July 1993. ISSN 0967-0637. doi: 10.1016/0967-0637(93)90127-O.

R. t. Hofstede, J. G. Hiddink, and A. D. Rijnsdorp. Regional warming changes fish species richness in the eastern North Atlantic Ocean. *Marine Ecology Progress Series*, 414:1–9, 2010. doi: 10.3354/meps08753.

N. P. Holliday and P. C. Reid. Is there a connection between high transport of water through the Rockall Trough and ecological changes in the North Sea? *Ices Journal of Marine Science*, 58(1):270–274, Feb. 2001. ISSN 1054-3139. doi: 10.1006/jmsc.2000.1008.

N. P. Holliday, S. Bacon, S. A. Cunningham, S. F. Gary, J. Karstensen, B. A. King, F. Li, and E. L. Mcdonagh. Subpolar North Atlantic Overturning and Gyre-Scale Circulation in the Summers of 2014 and 2016. *Journal of Geophysical Research-Oceans*, 123(7):4538–4559, July 2018. ISSN 2169-9275. doi: 10.1029/2018jc013841.

N. P. Holliday, M. Bersch, B. Berx, L. Chafik, S. Cunningham, C. Florindo-López, H. Hátún, W. Johns, S. A. Josey, K. M. H. Larsen, S. Mulet, M. Oltmanns, G. Reverdin, T. Rossby, V. Thierry, H. Valdimarsson, and I. Yashayaev. Ocean circulation causes the largest freshening event for 120 years in eastern subpolar North Atlantic. *Nature Communications*, 11(1):585, Jan. 2020. ISSN 2041-1723. doi: 10.1038/s41467-020-14474-y.

J. Holt, S. Wakelin, and J. Huthnance. Down-welling circulation of the northwest European continental shelf: A driving mechanism for the continental shelf carbon pump. *Geophysical Research Letters*, 36(14), 2009. ISSN 0094-8276. doi: 10.1029/2009GL038997.

J. Holt, J. Polton, J. Huthnance, S. Wakelin, E. O'Dea, J. Harle, A. Yool, Y. Artioli, J. Blackford, J. Siddorn, and M. Inall. Climate-Driven Change in the North Atlantic and Arctic Oceans Can Greatly Reduce the Circulation of the North Sea. *Geophysical Research Letters*, 45(21):11827–11836, Nov. 2018. ISSN 0094-8276. doi: 10.1029/2018gl078878.

R. Hu and J. Zhao. Sea surface salinity variability in the western subpolar North Atlantic based on satellite observations. *Remote Sensing of Environment*, 281:113257, Nov. 2022. ISSN 0034-4257. doi: 10.1016/j.rse.2022.113257. URL https://www.sciencedirect.com/science/article/pii/S0034425722003637.

J. Huthnance. The Rockall slope current and shelf-edge processes. *Proceedings of the Royal Society of Edinburgh, Section B: Biological Sciences*, 88:83–101, 1984. doi: https://doi.org/10.1017/S0269727000004486.

J. M. Huthnance, J. T. Holt, and S. L. Wakelin. Deep ocean exchange with west-European shelf seas. *Ocean Sci.*, 5(4):621–634, 2009. ISSN 1812-0792. doi: 10.5194/os-5-621-2009.

H. Hátún and L. Chafik. On the Recent Ambiguity of the North Atlantic Subpolar Gyre Index. *Journal of Geophysical Research-Oceans*, 123(8):5072–5076, Aug. 2018. ISSN 2169-9275. doi: 10.1029/2018jc014101.

H. Hátún, A. B. Sandø, H. Drange, B. Hansen, and H. Valdimarsson. Influence of the Atlantic Subpolar Gyre on the Thermohaline Circulation. *Science*, 309(5742): 1841–1844, 2005. doi: 10.1126/science.1114777.

H. Hátún, M. R. Payne, G. Beaugrand, P. C. Reid, A. B. Sando, H. Drange, B. Hansen, J. A. Jacobsen, and D. Bloch. Large bio-geographical shifts in the north-eastern Atlantic Ocean: From the subpolar gyre, via plankton, to blue whiting and pilot whales. *Progress in Oceanography*, 80(3-4):149–162, Mar. 2009. ISSN 0079-6611. doi: 10.1016/j.pocean.2009.03.001.

H. Hátún, K. Lohmann, D. Matei, J. H. Jungclaus, S. Pacariz, M. Bersch, A. Gislason, J. Olafsson, and P. C. Reid. An inflated subpolar gyre blows life toward the northeastern Atlantic. *Progress in Oceanography*, 147:49–66, Sept. 2016. ISSN 0079-6611. doi: 10.1016/j.pocean.2016.07.009.

H. Hátún, B. Olsen, and S. Pacariz. The Dynamics of the North Atlantic Subpolar Gyre Introduces Predictability to the Breeding Success of Kittiwakes. *Frontiers in Marine Science*, 4(123), May 2017. ISSN 2296-7745. doi: 10.3389/fmars.2017.00123.

H. Hátún, K. M. H. Larsen, S. K. Eliasen, and M. Mathis. Major Nutrient Fronts in the Northeastern Atlantic: From the Subpolar Gyre to Adjacent Shelves. In *The Handbook of Environmental Chemistry*, pages 1–45. Springer Berlin Heidelberg, Berlin, Heidelberg, 2021. URL https://doi.org/10.1007/698_2021_794.

IOC, SCOR, and IAPSO. *The international thermodynamic equation of seawater - 2010: Calculation and use of thermodynamic properties [includes corrections up to 31st October 2015].* Intergovernmental Oceanographic Commission, Manuals and Guides no. 56. UNESCO, Paris, France, 2015. URL https://doi.org/10.25607/OBP-1338.

S. Jacobsen, E. Gaard, H. Hátún, P. Steingrund, K. M. H. Larsen, J. Reinert, S. R. Ólafsdóttir, M. Poulsen, and H. B. M. Vang. Environmentally Driven Ecological Fluctuations on the Faroe Shelf Revealed by Fish Juvenile Surveys. *Frontiers in Marine Science*, 6(559), Sept. 2019. ISSN 2296-7745. doi: 10.3389/fmars.2019.00559.

S. R. Jayne, D. Roemmich, N. Zilberman, S. C. Riser, K. S. Johnson, G. C. Johnson, and S. R. Piotrowicz. The Argo Program: Present and Future. *Oceanography*, 30(2):18–28, 2017. ISSN 1042-8275. URL https://www.jstor.org/stable/26201840. Publisher: Oceanography Society.

C. Johnson, M. Inall, and S. Hakkinen. Declining nutrient concentrations in the northeast Atlantic as a result of a weakening Subpolar Gyre. *Deep-Sea Research I*, 82: 95–107, Dec. 2013. ISSN 0967-0637. doi: 10.1016/j.dsr.2013.08.007.

S. A. Josey, J. J. M. Hirschi, B. Sinha, A. Duchez, J. P. Grist, and R. Marsh. The Recent Atlantic Cold Anomaly: Causes, Consequences, and Related Phenomena. *Annual Review of Marine Science, Vol 10*, 10:475–501, 2018. ISSN 1941-1405. doi: 10.1146/annurev-marine-121916-063102.

E. Kalnay, M. Kanamitsu, R. Kistler, W. Collins, D. Deaven, L. Gandin, M. Iredell, S. Saha, G. White, J. Woollen, Y. Zhu, M. Chelliah, W. Ebisuzaki, W. Higgins, J. Janowiak, K. C. Mo, C. Ropelewski, J. Wang, A. Leetmaa, R. Reynolds, R. Jenne, and D. Joseph. The NCEP/NCAR 40-Year Reanalysis Project. *Bulletin of the American Meteorological Society*, 77(3):437–472, Mar. 1996. ISSN 0003-0007. doi: 10.1175/1520-0477(1996)077<0437:Tnyrp>2.0.Co;2.

N. S. Keenlyside, M. Latif, J. Jungclaus, L. Kornblueh, and E. Roeckner. Advancing decadal-scale climate prediction in the North Atlantic sector. *Nature*, 453(7191): 84–88, May 2008. ISSN 1476-4687. doi: 10.1038/nature06921. URL https://www.nature.com/articles/nature06921. Number: 7191 Publisher: Nature Publishing Group.

T. K. Kerby, W. W. L. Cheung, and G. H. Engelhard. The United Kingdom's role in North Sea demersal fisheries: a hundred year perspective. *Reviews in Fish Biology and Fisheries*, 22(3):621–634, Sept. 2012. ISSN 1573-5184. doi: 10.1007/s11160-012-9261-y. URL https://doi.org/10.1007/s11160-012-9261-y.

J. R. Knight, C. K. Folland, and A. A. Scaife. Climate impacts of the Atlantic Multidecadal Oscillation. *Geophysical Research Letters*, 33(17), 2006. ISSN 1944-8007. doi: 10.1029/2006GL026242. URL https://onlinelibrary.wiley.com/doi/abs/10.1029/2006GL026242. _eprint: https://onlinelibrary.wiley.com/doi/pdf/10.1029/2006GL026242.

V. Koul, C. Schrum, A. Düsterhus, and J. Baehr. Atlantic Inflow to the North Sea Modulated by the Subpolar Gyre in a Historical Simulation With MPI-ESM. *Journal of Geophysical Research: Oceans*, 124:1–20, 2019. doi: 10.1029/2018JC014738.

M. S. Lozier, F. Li, S. Bacon, F. Bahr, A. S. Bower, S. A. Cunningham, M. F. de Jong, L. de Steur, B. Deyoung, J. Fischer, S. F. Gary, B. J. W. Greenan, N. P. Holliday, A. Houk, L. Houpert, M. E. Inall, W. E. Johns, H. L. Johnson, C. Johnson,

J. Karstensen, G. Koman, I. A. Le Bras, X. Lin, N. Mackay, D. P. Marshall, H. Mercier, M. Oltmanns, R. S. Pickart, A. L. Ramsey, D. Rayner, F. Straneo, V. Thierry, D. J. Torres, R. G. Williams, C. Wilson, J. Yang, I. Yashayaev, and J. Zhao. A sea change in our view of overturning in the subpolar North Atlantic. *Science*, 363(6426):516–+, Feb. 2019. ISSN 0036-8075. doi: 10.1126/science.aau6592.

I. Ma. The influence of variable shelf edge exchange on carbon sequestration in the northern North Sea. Masters dissertation, University of Southampton, Sept. 2022.

G. Madec. NEMO ocean engine, Note du Pole de modélisation, Institut Pierre-Simon Laplace (IPSL), France. *Technical ReportTech. Rep.*, 2015.

R. Marsh, I. D. Haigh, S. A. Cunningham, M. E. Inall, M. Porter, and B. I. Moat. Large-scale forcing of the European Slope Current and associated inflows to the North Sea. *Ocean Science*, 13:315–335, 2017. doi: 10.5194/os-13-315-2017.

J. Marshall, H. Johnson, and J. Goodman. A Study of the Interaction of the North Atlantic Oscillation with Ocean Circulation. *Journal of Climate*, 14(7):1399–1421, Apr. 2001. ISSN 0894-8755. doi: 10.1175/1520-0442(2001)014<1399:Asotio>2.0.Co;2.

A. Marzocchi, J. J.-M. Hirschi, N. P. Holliday, S. A. Cunningham, A. T. Blaker, and A. C. Coward. The North Atlantic subpolar circulation in an eddy-resolving global ocean model. *Journal of Marine Systems*, 142:126–143, Feb. 2015. ISSN 0924-7963. doi: 10.1016/j.jmarsys.2014.10.007.

M. Mathis, A. Elizalde, and U. Mikolajewicz. The future regime of Atlantic nutrient supply to the Northwest European Shelf. *Journal of Marine Systems*, 189:98–115, Jan. 2019. ISSN 0924-7963. doi: 10.1016/j.jmarsys.2018.10.002.

G. D. McCarthy, D. A. Smeed, W. E. Johns, E. Frajka-Williams, B. I. Moat, D. Rayner, M. O. Baringer, C. S. Meinen, J. Collins, and H. L. Bryden. Measuring the Atlantic Meridional Overturning Circulation at 26 N. *Progress in Oceanography*, 130:91–111, Jan. 2015. ISSN 0079-6611. doi: 10.1016/j.pocean.2014.10.006.

G. D. McCarthy, T. M. Joyce, and S. A. Josey. Gulf Stream Variability in the Context of Quasi-Decadal and Multidecadal Atlantic Climate Variability. *Geophysical Research Letters*, 45(20):11,257–11,264, 2018. ISSN 1944-8007. doi: 10.1029/2018GL079336. URL https://onlinelibrary.wiley.com/doi/abs/10.1029/2018GL079336. _eprint: https://onlinelibrary.wiley.com/doi/pdf/10.1029/2018GL079336.

G. D. McCarthy, P. J. Brown, C. N. Flagg, G. Goni, L. Houpert, C. W. Hughes, R. Hummels, M. Inall, K. Jochumsen, K. M. H. Larsen, P. Lherminier, C. S. Meinen, B. I. Moat, D. Rayner, M. Rhein, A. Roessler, C. Schmid, and D. A. Smeed. Sustainable Observations of the AMOC: Methodology and Technology. *Reviews of Geophysics*, 58(1):e2019RG000654, 2020. ISSN 1944-9208. doi: 10.1029/2019RG000654. URL

https://onlinelibrary.wiley.com/doi/abs/10.1029/2019RG000654. _eprint: https://onlinelibrary.wiley.com/doi/pdf/10.1029/2019RG000654.

M. S. McCartney and L. D. Talley. The Subpolar Mode Water of the North Atlantic Ocean. *Journal of Physical Oceanography*, 12(11):1169–1188, Nov. 1982. ISSN 0022-3670. doi: 10.1175/1520-0485(1982)012<1169:Tsmwot>2.0.Co;2.

A. McQuatters-Gollop, D. E. Raitsos, M. Edwards, Y. Pradhan, L. D. Mee, S. J. Lavender, and M. J. Attrill. A long-term chlorophyll dataset reveals regime shift in North Sea phytoplankton biomass unconnected to nutrient levels. *Limnology and Oceanography*, 52(2):635–648, 2007. ISSN 0024-3590. doi: 10.4319/lo.2007.52.2.0635.

B. I. Moat, S. A. Josey, B. Sinha, A. T. Blaker, D. A. Smeed, G. D. McCarthy, W. E. Johns, J. J. M. Hirschi, E. Frajka-Williams, D. Rayner, A. Duchez, and A. C. Coward. Major variations in subtropical North Atlantic heat transport at short (5 day) timescales and their causes. *Journal of Geophysical Research-Oceans*, 121(5):3237–3249, May 2016. ISSN 2169-9275. doi: 10.1002/2016jc011660.

I. Montero-Serra, M. Edwards, and M. J. Genner. Warming shelf seas drive the subtropicalization of European pelagic fish communities. *Global Change Biology*, 21 (1):144–153, 2015. ISSN 1365-2486. doi: 10.1111/gcb.12747.

C. Mooney. Why some scientists are worried about a surprisingly cold 'blob' in the North Atlantic Ocean, 2015.

T. Nishida, T. Kitakado, H. Matsuura, and S.-P. Wang. Validation of the Global Ocean Data Assimilation System (GODAS) data in the NOAA National Centre for Environmental System (NCEP) by theory, comparative studies, applications and sea truth. In *IOTC 9th WPB meeting*, volume IOTC-2011-WPTT13-INF05, pages 1–18, Victoria, Seychelles, 2011.

E. S. R. L. NOAA. NCEP Global Ocean Data Assimilation System (GODAS) at NOAA ESRL/PSD. Technical report, NOAA, 2019. URL https://www.esrl.noaa.gov/psd/data/gridded/data.godas.html.

M. I. O'Connor, J. F. Bruno, S. D. Gaines, B. S. Halpern, S. E. Lester, B. P. Kinlan, and J. M. Weiss. Temperature control of larval dispersal and the implications for marine ecology, evolution, and conservation. *Proceedings of the National Academy of Sciences*, 104(4):1266–1271, Jan. 2007. doi: 10.1073/pnas.0603422104. URL https://www.pnas.org/doi/abs/10.1073/pnas.0603422104. Publisher: Proceedings of the National Academy of Sciences.

P. Ortega. An update on the North Atlantic cold blob (January 2017) | Weather and Climate @ Reading, 2017. URL https://blogs.reading.ac.uk/weather-and-climate-at-reading/2017/an-update-on-the-north-atlantic-cold-blob-january-2017/.

P. Ortega, J. Robson, R. T. Sutton, and M. B. Andrews. Mechanisms of decadal variability in the Labrador Sea and the wider North Atlantic in a high-resolution climate model. *Climate Dynamics*, online(10.1007/s00382-016-3467-y):1–23, 2016.

A. L. Perry, P. J. Low, J. R. Ellis, and J. D. Reynolds. Climate Change and Distribution Shifts in Marine Fishes. *Science*, 308:1912–1915, 2005. doi: 10.1126/science.1111322.

R. Pingree. Ocean structure and climate (Eastern North Atlantic): in situ measurement and remote sensing (altimeter). *Journal of the Marine Biological Association of the United Kingdom*, 82(5):681–707, 2002. ISSN 0025-3154. doi: 10.1017/S0025315402006082.

R. D. Pingree, B. Sinha, and C. R. Griffiths. Seasonality of the European slope current (Goban Spur) and ocean margin exchange. *Continental Shelf Research*, 19(7):929–975, June 1999. ISSN 0278-4343. doi: 10.1016/S0278-4343(98)00116-2.

M. Porter, M. E. Inall, J. A. M. Green, J. H. Simpson, A. C. Dale, and P. I. Miller. Drifter observations in the summer time Bay of Biscay slope current. *Journal of Marine Systems*, 157:65–74, May 2016a. ISSN 0924-7963. doi: 10.1016/j.jmarsys.2016.01.002. URL https://www.sciencedirect.com/science/article/pii/S092479631600004X.

M. Porter, M. E. Inall, J. Hopkins, M. R. Palmer, A. C. Dale, D. Aleynik, J. A. Barth, C. Mahaffey, and D. A. Smeed. Glider observations of enhanced deep water upwelling at a shelf break canyon: A mechanism for cross-slope carbon and nutrient exchange. *Journal of Geophysical Research: Oceans*, 121(10):7575–7588, 2016b. ISSN 2169-9275. doi: 10.1002/2016JC012087.

M. Porter, A. C. Dale, S. Jones, B. Siemering, and M. E. Inall. Cross-slope flow in the Atlantic Inflow Current driven by the on-shelf deflection of a slope current. *Deep-Sea Research Part I-Oceanographic Research Papers*, 140:173–185, Oct. 2018. ISSN 0967-0637. doi: 10.1016/j.dsr.2018.09.002.

J. Pätsch, V. Gouretski, I. Hinrichs, and V. Koul. Distinct Mechanisms Underlying Interannual to Decadal Variability of Observed Salinity and Nutrient Concentration in the Northern North Sea. *Journal of Geophysical Research: Oceans*, 125(5): e2019JC015825, 2020. ISSN 2169-9275. doi: https://doi.org/10.1029/2019JC015825.

P. C. Reid, M. D. Borges, and E. Svendsen. A regime shift in the North Sea circa 1988 linked to changes in the North Sea horse mackerel fishery. *Fisheries Research*, 50(1-2): 163–171, Feb. 2001a. ISSN 0165-7836. doi: Doi10.1016/S0165-7836(00)00249-6.

P. C. Reid, N. P. Holliday, and T. J. Smyth. Pulses in the eastern margin current and warmer water off the north west European shelf linked to North Sea ecosystem changes. *Marine Ecology Progress Series*, 215:283–287, 2001b. doi: doi:10.3354/meps215283.

P. C. Reid, M. Edwards, G. Beaugrand, M. Skogen, and D. Stevens. Periodic changes in the zooplankton of the North Sea during the twentieth century linked to oceanic inflow. *Fisheries Oceanography*, 12(4/5):260–269, Sept. 2003. ISSN 1054-6006. doi: 10.1046/j.1365-2419.2003.00252.x.

A. Sarafanov. On the effect of the North Atlantic Oscillation on temperature and salinity of the subpolar North Atlantic intermediate and deep waters. *ICES Journal of Marine Science*, 66(7):1448–1454, Aug. 2009. ISSN 1054-3139. doi: 10.1093/icesjms/fsp094. URL https://doi.org/10.1093/icesjms/fsp094.

A. Schmittner. Decline of the marine ecosystem caused by a reduction in the Atlantic overturning circulation. *Nature*, 434(7033):628–633, Mar. 2005. ISSN 0028-0836. doi: 10.1038/nature03476.

W. J. Schmitz and M. S. McCartney. On the North Atlantic circulation. *Reviews of Geophysics*, 31:29–49, Feb. 1993. ISSN 8755-1209. doi: 10.1029/92RG02583.

J. Sharples. Investigating the seasonal vertical structure of phytoplankton in shelf seas. *Marine Models*, 1(1):3–38, Dec. 1999. ISSN 1369-9350. doi: 10.1016/S0079-6611(99)00002-6. URL https://www.sciencedirect.com/science/article/pii/S0079661199000026.

J. H. Simpson and J. Sharples. *Introduction to the Physical and Biological Oceanography of Shelf Seas*. Cambridge University Press, Cambridge, 2012. ISBN 978-0-521-87762-6. doi: 10.1017/CBO9781139034098. URL https://www.cambridge.org/core/books/introduction-to-the-physical-and-biological-oceanography-of-shelf-seas/D28A42640D9F3D5BADB6D9533D663ECD.

A. R. D. Stebbing, S. M. D. Turk, A. Wheeler, and K. R. Clarke. Immigration of southern fish species to south-west England linked to warming of the North Atlantic (1960-2001). *Journal of the Marine Biological Association of the United Kingdom*, 82:177–180, 2002. doi: 10.1017/S0025315402005325.

S. Sundby. Recruitment of Atlantic cod stocks in relation to temperature and advectlon of copepod populations. *Sarsia*, 85(4):277–298, Nov. 2000. ISSN 0036-4827. doi: 10.1080/00364827.2000.10414580. URL https://doi.org/10.1080/00364827.2000.10414580.

A. D. Tappin, J. R. W. Harris, R. J. Uncles, and D. Boorman. Potential modification of the fluxes of nitrogen from the Humber Estuary catchment (U.K.) to the North Sea in response to changing agricultural inputs and climate patterns. In E. Orive, M. Elliott, and V. N. de Jonge, editors, *Nutrients and Eutrophication in Estuaries and Coastal Waters: Proceedings of the 31st Symposium of the Estuarine and Coastal Sciences Association (ECSA), held in Bilbao, Spain, 3–7 July 2000*, Developments in Hydrobiology, pages 65–77. Springer Netherlands, Dordrecht, 2002. ISBN

978-94-017-2464-7. doi: 10.1007/978-94-017-2464-7_5. URL https://doi.org/10.1007/978-94-017-2464-7_5.

H. Thomas, Y. Bozec, H. J. W. de Baar, K. Elkalay, M. Frankignoulle, L.-S. Schiettecatte, G. Kattner, and A. V. Borges. The carbon budget of the North Sea. *Biogeosciences*, 2 (1):87–96, Mar. 2005. ISSN 1726-4170. doi: 10.5194/bg-2-87-2005. URL https://bg.copernicus.org/articles/2/87/2005/. Publisher: Copernicus GmbH.

M. Ting, Y. Kushnir, R. Seager, and C. Li. Robust features of Atlantic multi-decadal variability and its climate impacts. *Geophysical Research Letters*, 38(17), 2011. ISSN 1944-8007. doi: 10.1029/2011GL048712. URL https://onlinelibrary.wiley.com/doi/abs/10.1029/2011GL048712. _eprint: https://onlinelibrary.wiley.com/doi/pdf/10.1029/2011GL048712.

J. van der Kooij, G. H. Engelhard, and D. A. Righton. Climate change and squid range expansion in the North Sea. *Journal of Biogeography*, 43(11):2285–2298, 2016. ISSN 0305-0270. doi: 10.1111/jbi.12847.

H. van Haren. Properties of vertical current shear across stratification in the North Sea. *Journal of Marine Research*, 58(3):465–491, May 2000. doi: 10.1357/002224000321511115.

R. Varela, F. P. Lima, R. Seabra, C. Meneghesso, and M. Gomez-Gesteira. Coastal warming and wind-driven upwelling: A global analysis. *Science of the Total Environment*, 639:1501–1511, Oct. 2018. ISSN 0048-9697. doi: 10.1016/j.scitotenv.2018.05.273.

J. E. Vermaat, A. McQuatters-Gollop, M. A. Eleveld, and A. J. Gilbert. Past, present and future nutrient loads of the North Sea: Causes and consequences. *Estuarine, Coastal and Shelf Science*, 80(1):53–59, Oct. 2008. ISSN 0272-7714. doi: 10.1016/j.ecss.2008.07.005. URL https://www.sciencedirect.com/science/article/pii/S0272771408002692.

A. J. Warner and G. C. Hays. Sampling by the Continuous Plankton Recorder Survey. *Progress in Oceanography*, 34(2-3):237–256, 1994. ISSN 0079-6611. doi: 10.1016/0079-6611(94)90011-6.

R. G. Williams, V. Roussenov, D. Smith, and M. S. Lozier. Decadal Evolution of Ocean Thermal Anomalies in the North Atlantic: The Effects of Ekman, Overturning, and Horizontal Transport. *Journal of Climate*, 27(2):698–719, Jan. 2014. ISSN 0894-8755, 1520-0442. doi: 10.1175/JCLI-D-12-00234.1. URL https://journals.ametsoc.org/view/journals/clim/27/2/jcli-d-12-00234.1.xml. Publisher: American Meteorological Society Section: Journal of Climate.

N. G. Winther and J. A. Johannessen. North Sea circulation: Atlantic inflow and its destination. *Journal of Geophysical Research*, 111(C12018):1–12, 2006. doi: 10.1029/2005JC003310.

M. Winton, S. M. Griffies, B. L. Samuels, J. L. Sarmiento, and T. L. Frölicher. Connecting Changing Ocean Circulation with Changing Climate. *Journal of Climate*, 26(7):2268–2278, Apr. 2013. ISSN 0894-8755, 1520-0442. doi: 10.1175/JCLI-D-12-00296.1. URL https://journals.ametsoc.org/view/journals/clim/26/7/jcli-d-12-00296.1.xml. Publisher: American Meteorological Society Section: Journal of Climate.

E. L. Worthington, B. I. Moat, D. A. Smeed, J. V. Mecking, R. Marsh, and G. D. McCarthy. A 30-year reconstruction of the Atlantic meridional overturning circulation shows no decline. *Ocean Science*, 17(1):285–299, Feb. 2021. ISSN 1812-0784. doi: 10.5194/os-17-285-2021. URL https://os.copernicus.org/articles/17/285/2021/. Publisher: Copernicus GmbH.

W. D. Xu, P. I. Miller, G. D. Quartly, and R. D. Pingree. Seasonality and interannual variability of the European Slope Current from 20 years of altimeter data compared with in situ measurements. *Remote Sensing of Environment*, 162:196–207, 2015. ISSN 0034-4257. doi: 10.1016/j.rse.2015.02.008.

S. G. Yeager, W. M. Kim, and J. Robson. What caused the Atlantic cold blob of 2015. *US CLIVAR Variations*, 14(2):24–31, 2016.

R. Zhang, R. Sutton, G. Danabasoglu, Y.-O. Kwon, R. Marsh, S. G. Yeager, D. E. Amrhein, and C. M. Little. A Review of the Role of the Atlantic Meridional Overturning Circulation in Atlantic Multidecadal Variability and Associated Climate Impacts. *Reviews of Geophysics*, 57(2):316–375, 2019. ISSN 1944-9208. doi: 10.1029/2019RG000644. URL https://onlinelibrary.wiley.com/doi/abs/10.1029/2019RG000644. _eprint: https://onlinelibrary.wiley.com/doi/pdf/10.1029/2019RG000644.